Cosmic re-ionization

Gianfranco De Zotti
INAF – Osservatorio Astronomico di Padova

- Cosmological reionization is the last major phase change of our Universe, when ionizing radiation stripped electrons from almost every atom in our Universe, ending the ``dark ages'' and allowing visible light to finally spread throughout space.
- The epoch or reionization (EoR) corresponds to the transition between the relative simplicity of the early Universe and the complexity of the present-day one, 13 billion years later.

Outline

- Overview of the IGM history
- The Gunn-Peterson effect
- The Lyman-α forest and its evolution
- The detection of the Gunn-Peterson effect
- Other probes of the re-ionization history
- Cosmic reionization and the CMB
- Re-ionization and 21cm HI line
- Evolution of the photo-ionization rate
- AGN contribution to re-ionization
- Ionizing photons from star-forming galaxies
- Conclusions

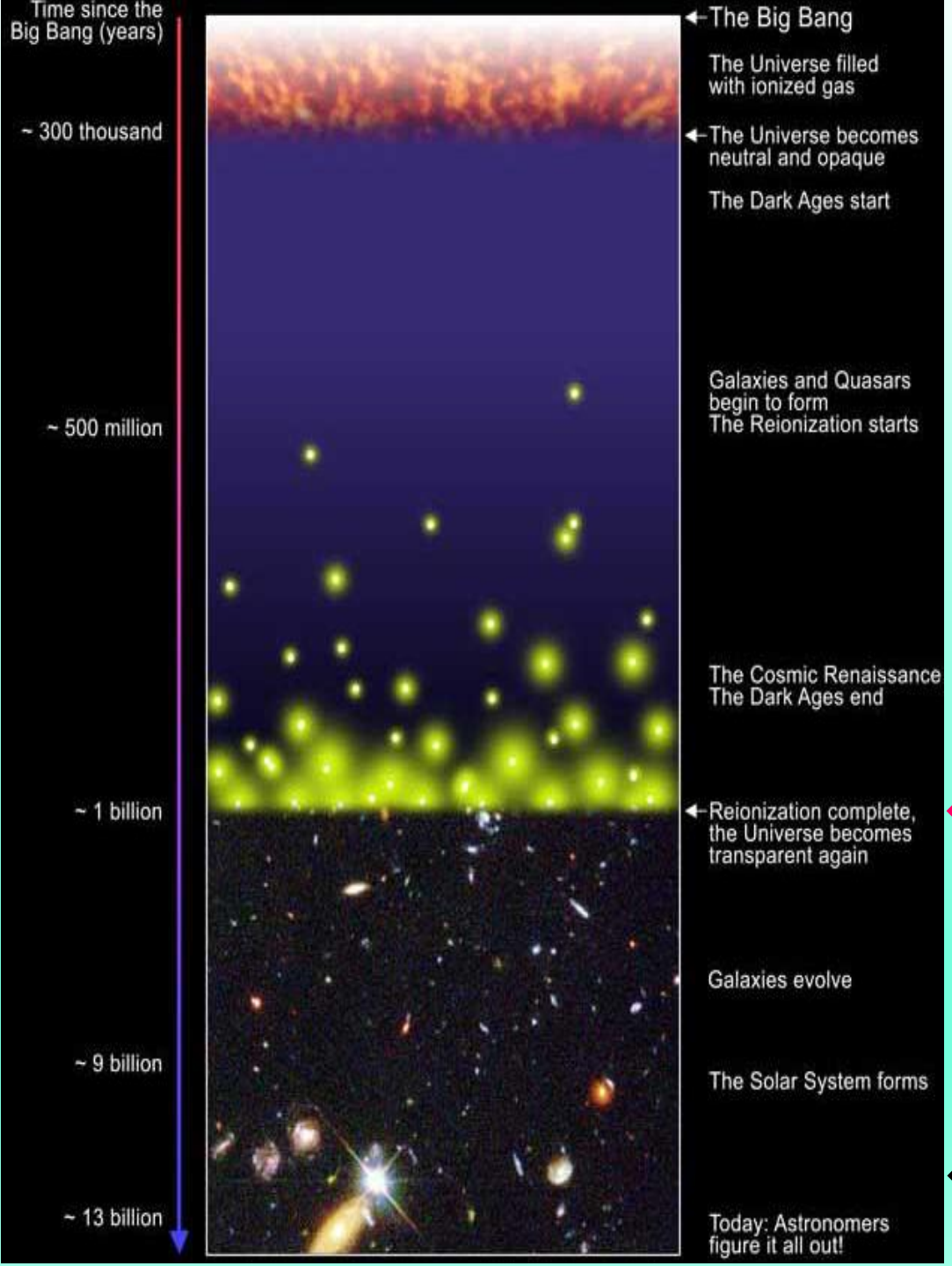

← Hot Big Bang

← Cosmic Dark Ages: no light
no star, no quasar, universe dark;
IGM atomic (neutral) and opaque to UV

← First light: the first galaxies and quasars in the universe

← End of cosmic dark ages:
Universe lit up and heated up
Dark --> light
Neutral --> ionized (***reionization***)

← today

Courtesy: G. Djorgovski

The IGM history in a nutshell

- H recombines at z ~ 1000: free electron fraction x_e=0.5 (half H recombines) by z= 1210, x_e=0.1 by z = 980, x_e=0.01 by z = 820; x_e will not go to 0 as z ⇒ 0, but freezes at ~ 5×10^{-4} (e.g., Seager et al. 2000).
- However, it has long been known that the IGM is almost completely ionized ($x_e \approx 1$) at low redshifts.
- He recombines earlier because of its higher ionization energies (54.4 eV for the transition He+ ⇒ He++, 24.6 eV for He ⇒ He+, to be compared with 13.6 eV for H). Hence the He recombination proceeds in 2 stages. Half of the He++ recombines to He+ by z=5800 and half of He+ recombines to He by z=2000 (e.g. Switzer & Hirata 2007).

The Gunn-Peterson effect - 1

- Shortly after the discovery of quasars (Schmidt 1963) it became clear that some of them are at substantial redshifts, so that their resonant H Lyα line (at 1215.7 Å) can be redshifted to the optical making it observable from the ground (the atmosphere is opaque to UV radiation shortward of about 3000 Å, so that the line becomes visible for z > 2).
- It was than independently suggested by Shklovski (1964), Scheuer (1965), Gunn & Peterson (1965) that the attenuation of the UV radiation due to Lyα resonance scattering in atomic H is an extremely sensitive probe of the density of the neutral IGM.

The Gunn-Peterson effect - 3

- Gunn & Peterson had the good fortune to have made the suggestion at the right time and place, at Caltech, when Schmidt had just obtained the spectrum of 3C9 (z=2.0199) in which for the first time one could see the Lyα emission line.

  Thus they were able to apply the test and make people pay attention to it. This is why it is called the Gunn-Peterson effect.
- Searches for neutral H in the IGM were carried out in the context of efforts to determine the mean mass density of the universe, ρ_m, believed to be in the form of baryons.
- The only known contribution to ρ_m was that provided by galaxies but: i) it was unable to account for the dynamics of groups and clusters of galaxies; ii) it is hardly conceivable that the galaxy formation process has a 100% efficiency.

Gunn & Peterson 1965, ApJ, 142, 507

NOTES

ON THE DENSITY OF NEUTRAL HYDROGEN IN INTERGALACTIC SPACE

Recent spectroscopic observations by Schmidt (1965) of the quasi-stellar source 3C 9, which is reported by him to have a redshift of 2.01, and for which Lyman-α is in the visible spectrum, make possible the determination of a new very low value for the density of neutral hydrogen in intergalactic space. It is observed that the continuum of the source continues (though perhaps somewhat weakened) to the blue of Ly-α; the line as seen on the plates has some structure but no obvious asymmetry. Consider, however, the fate of photons emitted to the blue of Ly-α. As we move away from the source along the line of sight, the source becomes redshifted to observers locally at rest in the expansion, and for one such observer, the frequency of any such photon coincides with the rest frequency of Ly-α in his frame and can be scattered by neutral hydrogen in his vicinity.

Ly α SOURCE BEFORE REIONIZATION

Loeb & Barkana (2001)

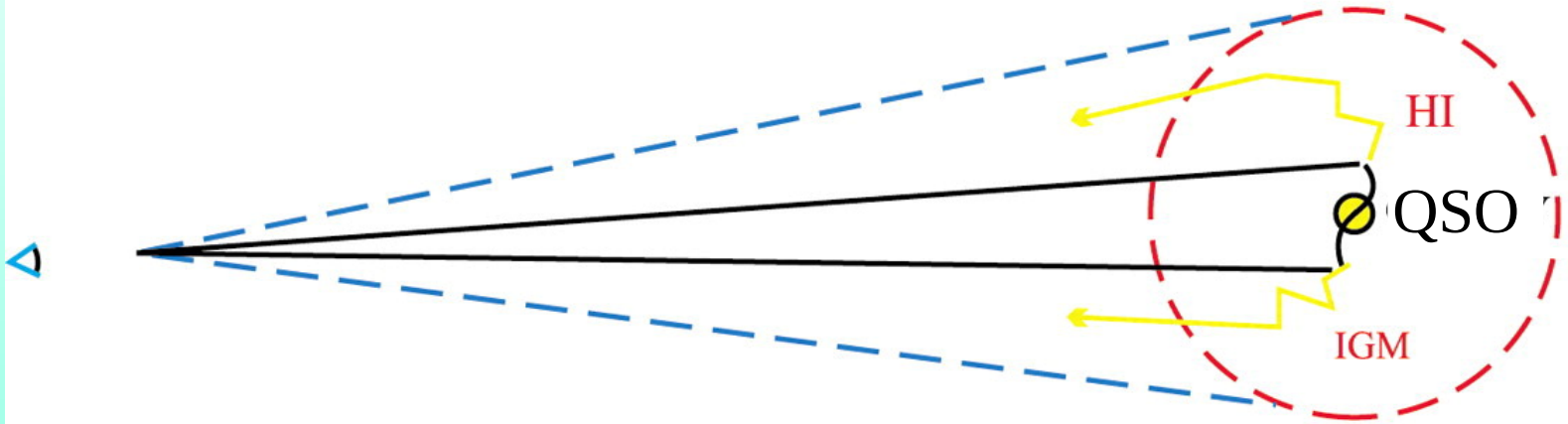

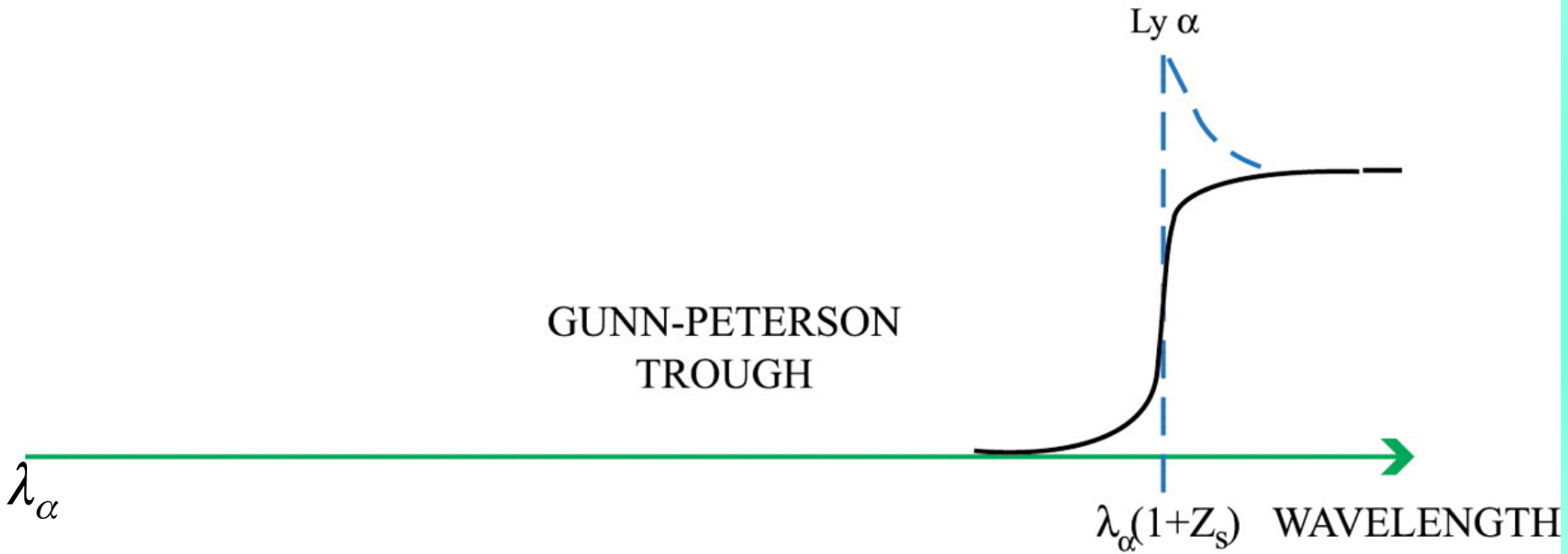

DETERMINING THE REIONIZATION REDSHIFT

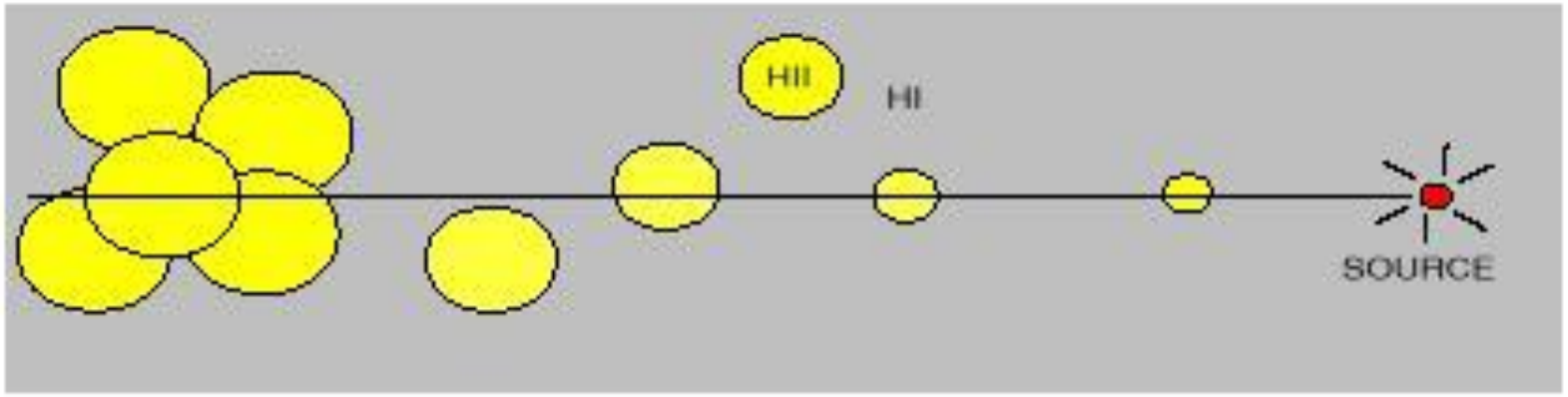

Spectrum

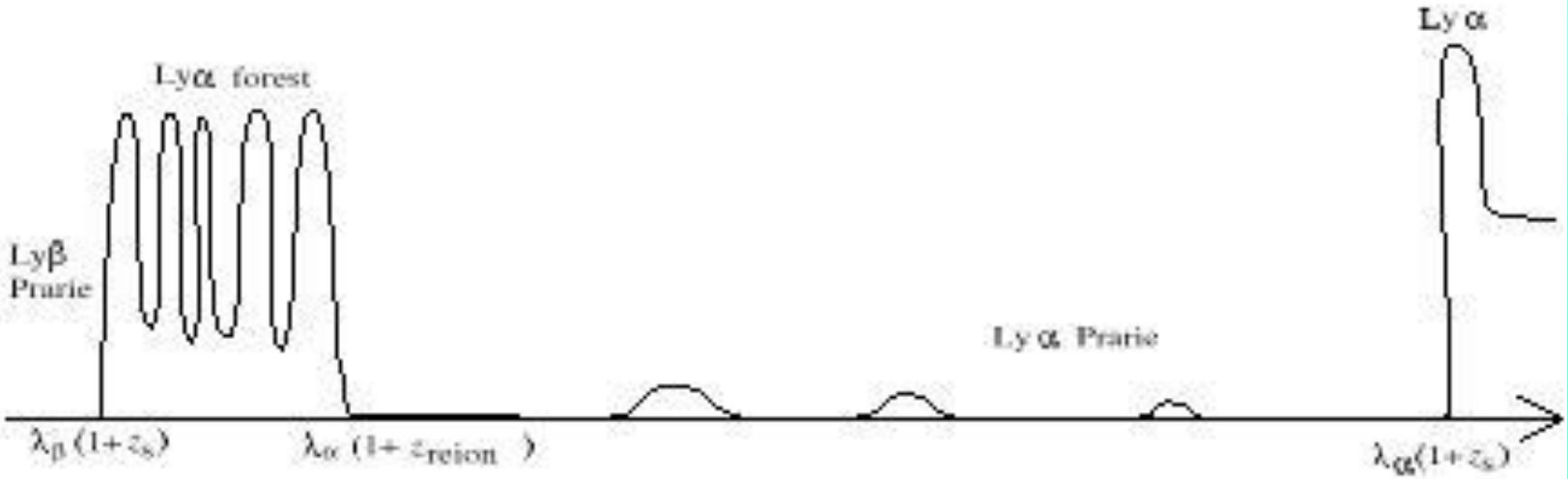

$$1 < \frac{1+z_s}{1+z_{reion}} < \frac{\lambda_\alpha}{\lambda_\beta} = 1.18$$

The Gunn-Peterson effect - 4

When the UV light travels across a region with neutral H gas it suffers attenuation due to Lyα absorption (i.e. by the 1s–2p transition in H):

$$F = F_0 e^{-\tau},$$

where F_0 is the unattenuated flux and τ is the optical depth

$$\tau(z) = \int n_{\rm HI}(z')\sigma dl\,,$$

$n_{\rm HI}(z)$ being the number density of atomic H and σ the absorption cross section.

Note that this is not the general solution of the transport equation. We have neglected the spontaneous emission (because we are considering neutral gas) and the correction for stimulated emission because $h\nu_\alpha/kT_s \gg 1$, T_s being the H equivalent spin temperature. Otherwise a substantial fraction of the atoms would be in the 2p state, which is hard to arrange because the half life is $\sim 10^{-9}$ s (recall that the energy associated to the Lyα transition is 10.6 eV, corresponding to a temperature of 1.18×10^5 K).

The Gunn-Peterson effect - 5

The cross section σ for absorption at a resonance line, where the absorption cross section is sharply peaked, can be written as

$$\sigma(\nu) = \frac{\pi e^2}{m_e c} f \phi(\nu) ,$$

where $\phi(\nu)$ is the line profile and f is the oscillator strength of the line ($f = 0.416$ for Lyα).

Approximating $\phi(\nu)$ with a $\delta_D(\nu - \nu_\alpha)$ we get

$$\sigma(\nu) \simeq \sigma_0 \nu_\alpha \delta_D(\nu - \nu_\alpha),$$

with $\sigma_0 \simeq 4.5 \times 10^{-18}\,\mathrm{cm}^2$, which is 7 orders of magnitude larger than the Thomson cross section ($\sigma_T \simeq 6.55 \times 10^{-25}\,\mathrm{cm}^2$).

The Gunn-Peterson effect - 6

Taking into account that:

$$dl = c\,dt = -c\frac{dt}{dz}dz = -\frac{c}{H(z)}\frac{dz}{1+z},$$

and that, from $\nu = \nu_{\rm obs}(1+z)$

$$\frac{dz}{1+z} = \frac{d\nu}{\nu},$$

we get

$$\begin{aligned}\tau(\nu_{\rm obs}) &= \int n_{\rm HI}(z')\sigma dl = \sigma_0\nu_\alpha\int n_{\rm HI}(z')\delta_D(\nu-\nu_\alpha)\left|\frac{c}{H(z)}\right|\frac{d\nu}{\nu}\\ &= \sigma_0 n_{\rm HI}(z')(z)\frac{c}{H(z)},\end{aligned}$$

where z is given by $1+z = \nu_{\rm obs}/\nu_\alpha$ and
$H(z) = H_0\sqrt{\Omega_m(1+z)^3 + \Omega_k(1+z)^2 + \Omega_\Lambda}$.

The Gunn-Peterson effect - 7

The *average* H number density

$$\bar{n}_{\rm H} = \frac{X}{m_p}\Omega_b\rho_{\rm crit}(1+z)^3 \simeq 1.2\times10^{-5}\frac{X}{0.75}\,\frac{h^2\Omega_b}{0.0223}\left(\frac{1+z}{4}\right)^3\ {\rm cm}^{-3},$$

where X is the H mass fraction and Ω_b is the mass density in baryons relative to the critical density $\rho_{\rm crit}$. Hence:

$$\tau(\nu_{\rm obs}) \simeq 5.2\times10^5 h^{-1}\,\frac{n_{\rm HI}}{n_{\rm H}}\,\frac{n_{\rm H}}{\bar{n}_{\rm H}}\,\frac{H_0}{H(z)}\,\frac{X}{0.75}\,\frac{h^2\Omega_b}{0.0223}\left(\frac{1+z}{4}\right)^3,$$

where $n_{\rm HI}/n_{\rm H}$ quantifies the neutral H fraction and $n_{\rm H}/\bar{n}_{\rm H} \simeq 1$ is a measure of the over/under-density.

If $\Omega_k \simeq 0$ and we focus on the high-z universe, so that $\Omega_\Lambda \ll \Omega_m(1+z)^3$ we have

$$H(z) \simeq H_0\Omega_m^{1/2}(1+z)^{3/2}.$$

The Gunn-Peterson effect - 8

Hence:

$$\tau(\nu_{\rm obs}) \simeq 1.7\times10^5 \frac{n_{\rm HI}}{n_{\rm H}} \frac{n_{\rm H}}{\bar{n}_{\rm H}} \frac{h^2\Omega_m}{0.142} \frac{X}{0.75} \frac{h^2\Omega_b}{0.0223} \left(\frac{1+z}{4}\right)^{3/2} ,$$

implying that a very small amount of neutral H is sufficient to absorb very efficiently the light at and shortwards of Lyα. For example, an attenuation of the signal by a factor of 100 ($\tau \simeq 4.6$) would be produced by a neutral fraction of $n_{\rm HI}/n_{\rm H} \simeq 2.7\times10^{-5}$.

Thus, the detection of the Lyα provides very strong constraints on the abundance on neutral H. On the other hand, it is "too sensitive" to reconstruct the re-ionization history: the detection of the Gunn-Peterson effect is just telling us about the end of it. It is possible to make some progress using higher order Lyman lines. This is because τ is proportional to the oscillator strength times the wavelength .

The Gunn-Peterson effect - 9

Table 1: Absorption oscillator strengths fu hydrogen (Allen's Astrophysical quantities).

Line	Transition	Wavelength (Å)	f
Lyα	1s-2p	1215.67	0.41620
Lyβ	1s-3p	1025,72	0.07910
Lyγ	1s-4p	972.54	0.02899

Thus by going to Lyγ it is possible to measure $n_{\rm HI}/n_{\rm H}$ ratios about a factor of 14 larger, but still very small.

Higher order lines are extremely hard to measure accurately because they become blended with lower z Lyα absorption.

By measuring the Gunn-Peterson effect in distant quasars, we can nevertheless get some insight into the properties of the IGM at those redshifts. There is a complication, however...

The Lyman-α forest

At z < 6 the neutral H is in discrete structures yielding Lyα absorption lines (Lyα forest) which attenuate the continuum but not absorb it completely.

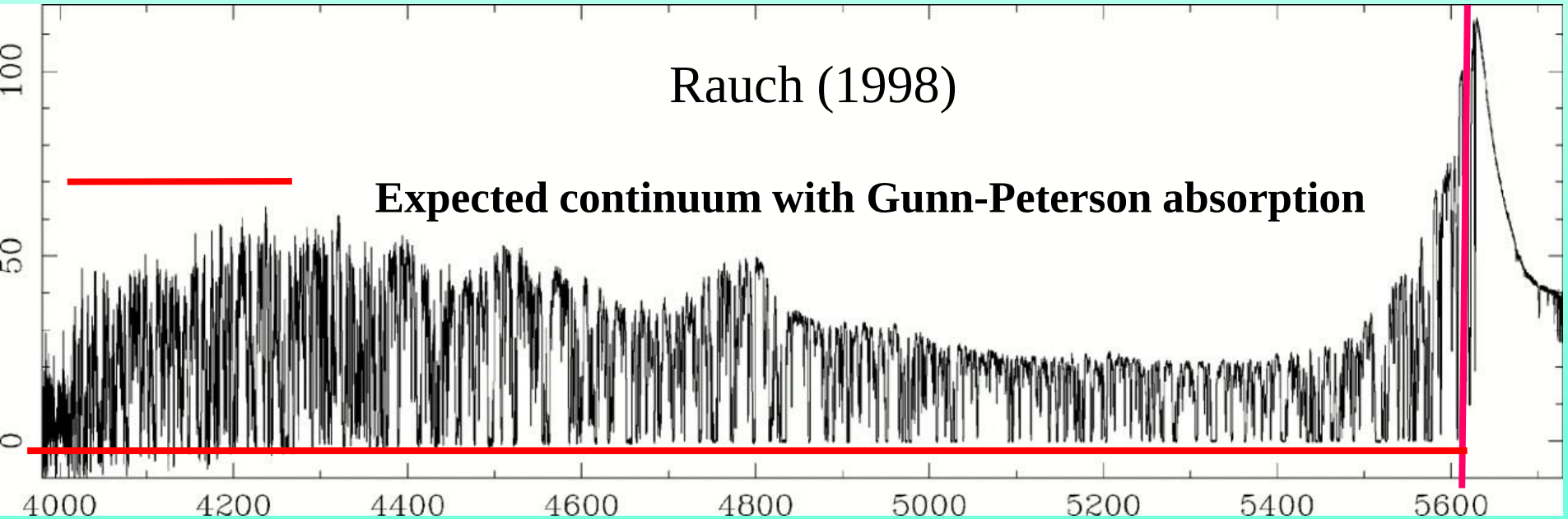

High resolution [full width at half maximum (FWHM) ≈ 6.6 km s^{-1}] spectrum of the z_{em} = 3.62 QSO1422+23 taken with the Keck High Resolution Spectrograph (HIRES).

The number density of Lyα forest lines increases strongly with z.

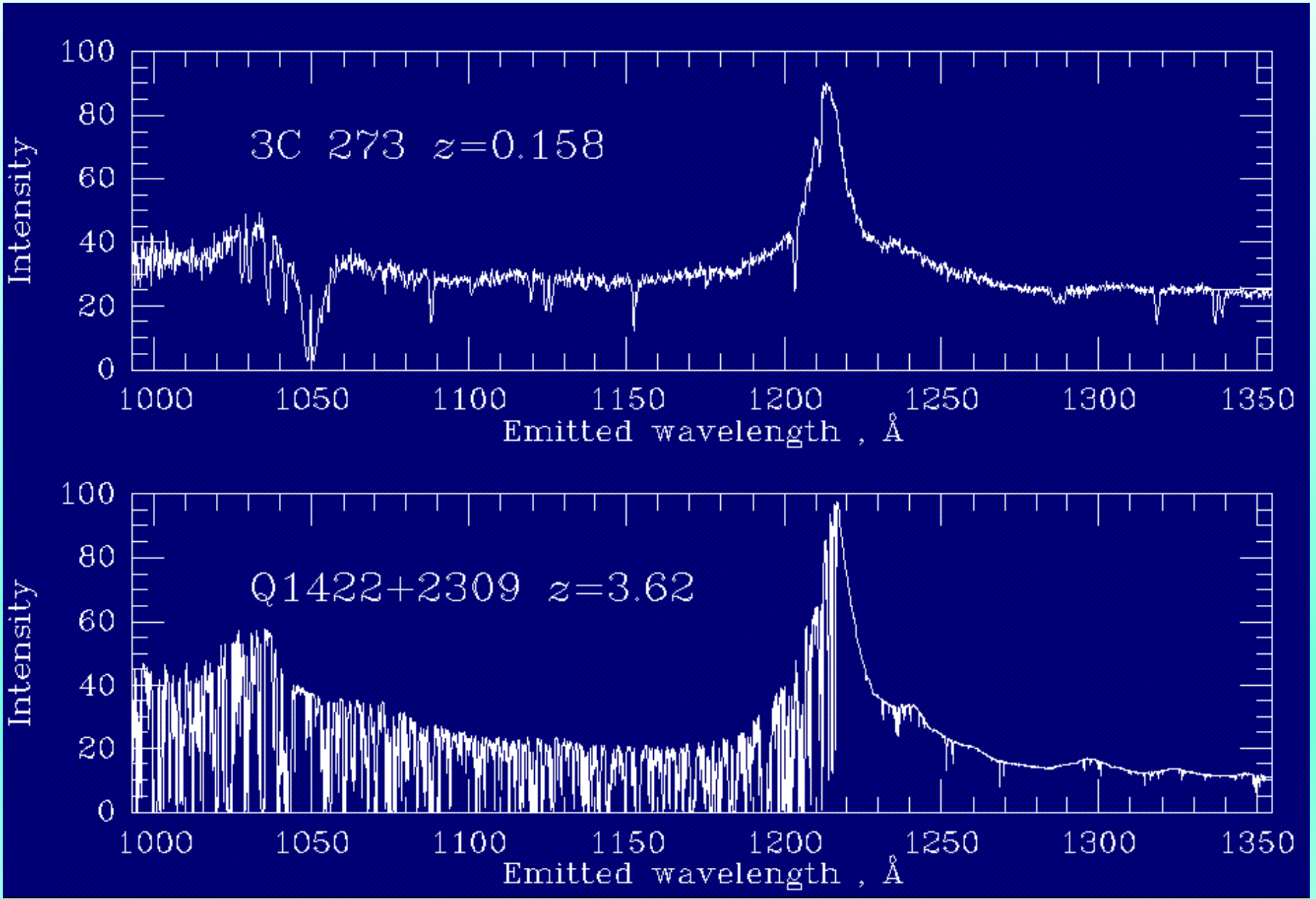

Evolution of the Lyα forest

- This implies a substantial absorption at high-z. even in the absence of the Gunn-Peterson effect.
- It is standard practice to define the fraction of QSO continuum absorbed as

$$D_A = \langle 1 - \frac{f_{\rm obs}}{f_{\rm cont}} \rangle = \langle 1 - e^{-\tau} \rangle = 1 - e^{-\tau_{\rm eff}}$$

Measurements of D_A yield information on the evolution of the Lyα forest, which is usually described as $dN/dz \propto (1+z)^{\gamma}$, with $1.7 < \gamma < 3$ for $2<z<4$, with the evolution increasing to $\gamma = 5.5$ at $z > 4$ (Rauch 1998)

Evolution of Lyα optical depth (Songaila 2004)

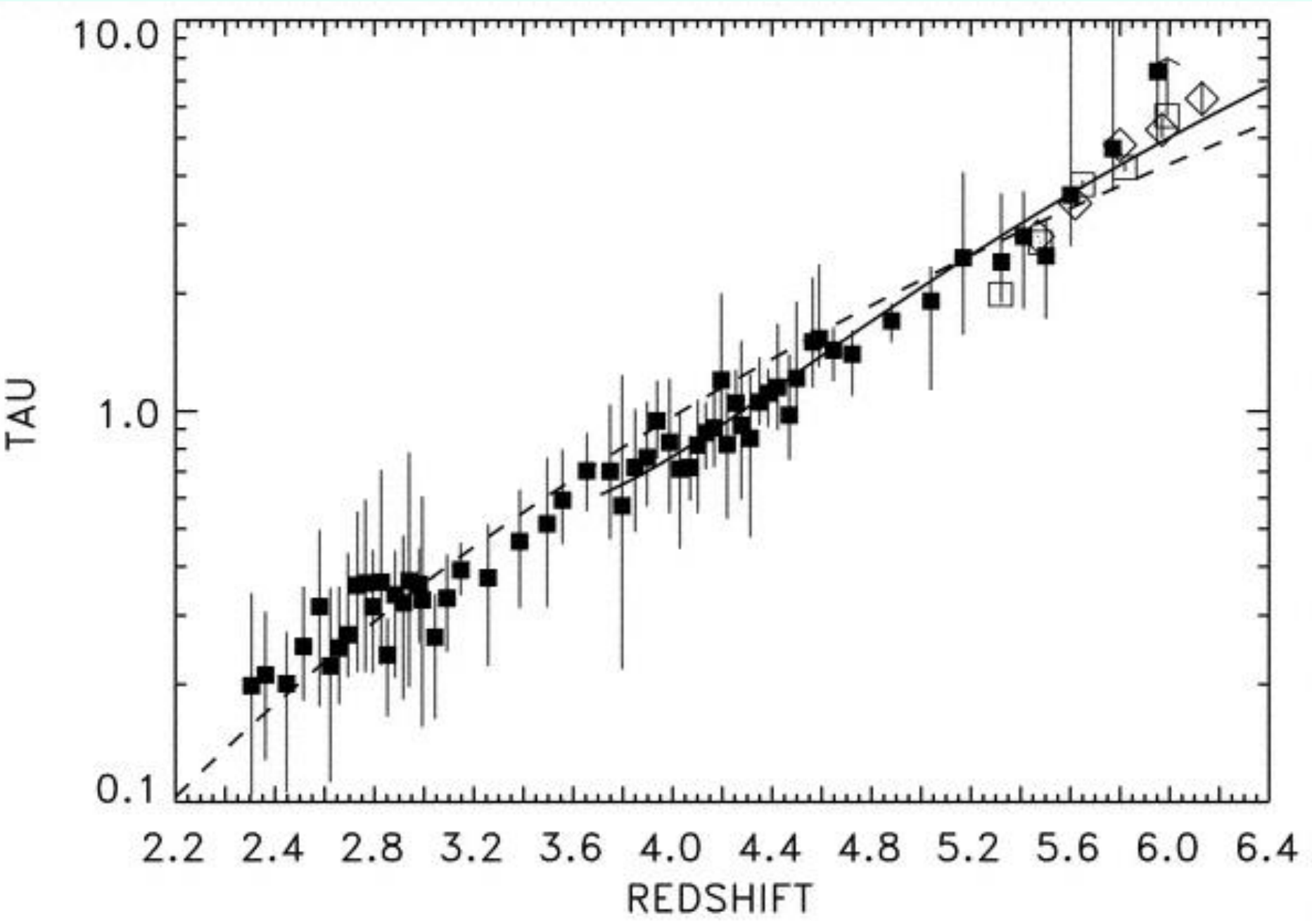

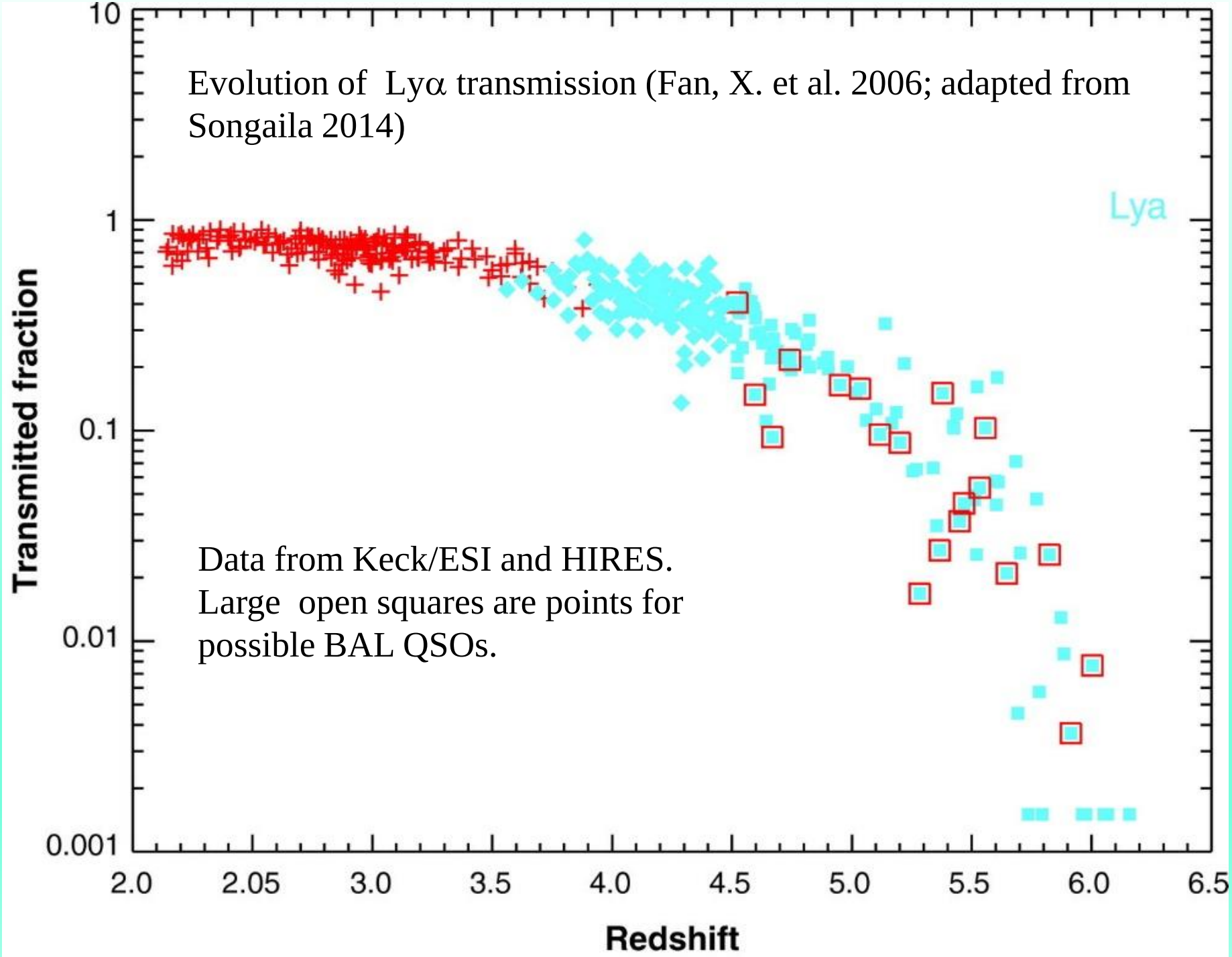
Evolution of Lyα transmission (Fan, X. et al. 2006; adapted from Songaila 2014)
Lya
Data from Keck/ESI and HIRES.
Large open squares are points for possible BAL QSOs.
Transmitted fraction
10
1
0.1
0.01
0.001
2.0
2.05
3.0
3.5
4.0
4.5
5.0
5.5
6.0
6.5
Redshift

Evolution of Lyβ transmission (Songaila 2004)

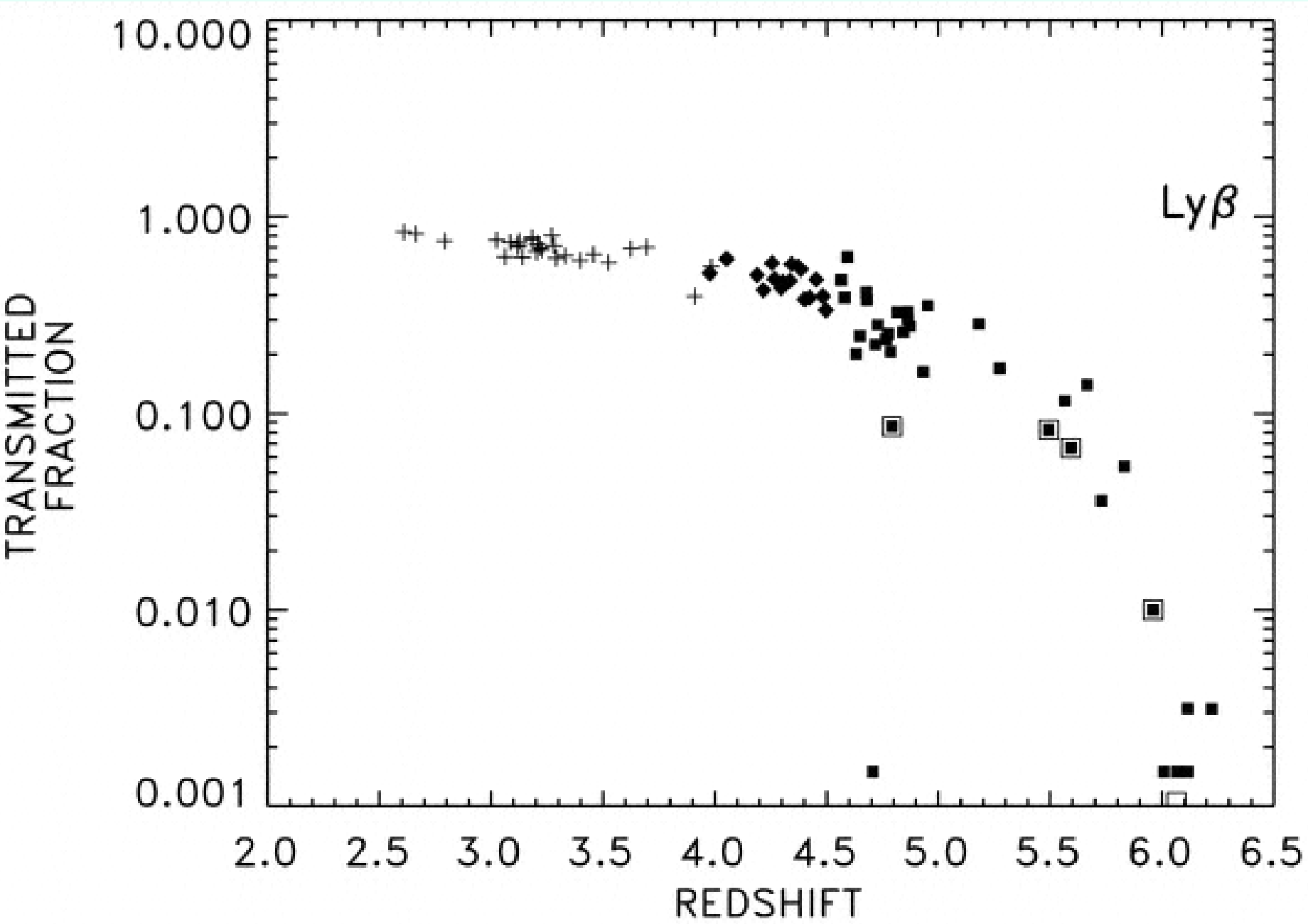

First detection of Gunn-Peterson Effect (Fan et al. 2001)

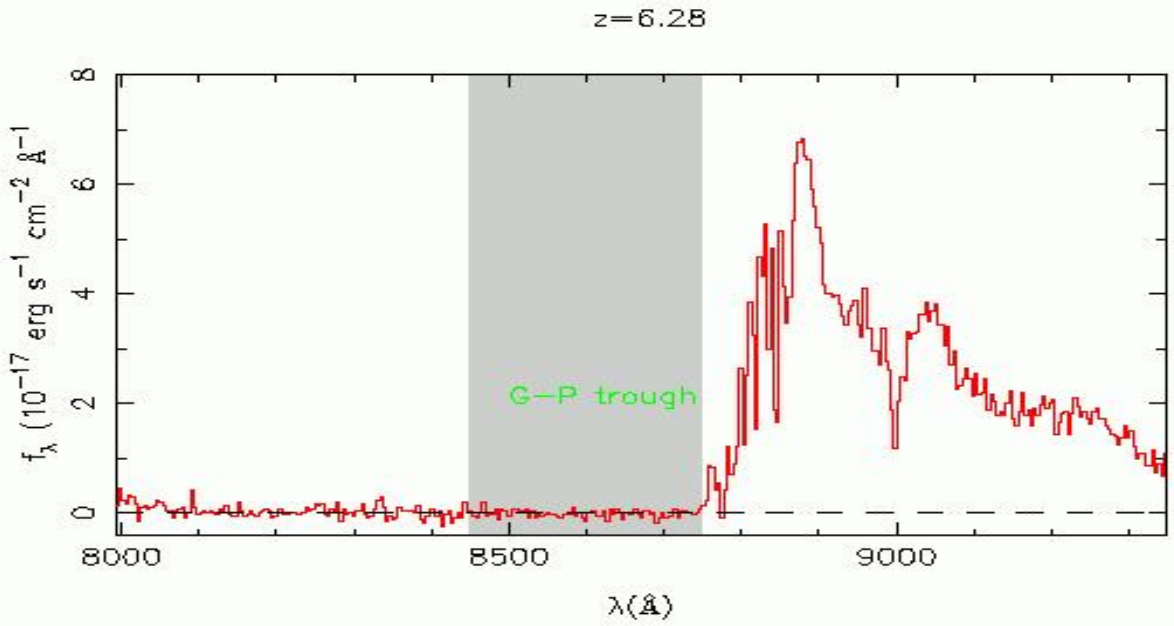

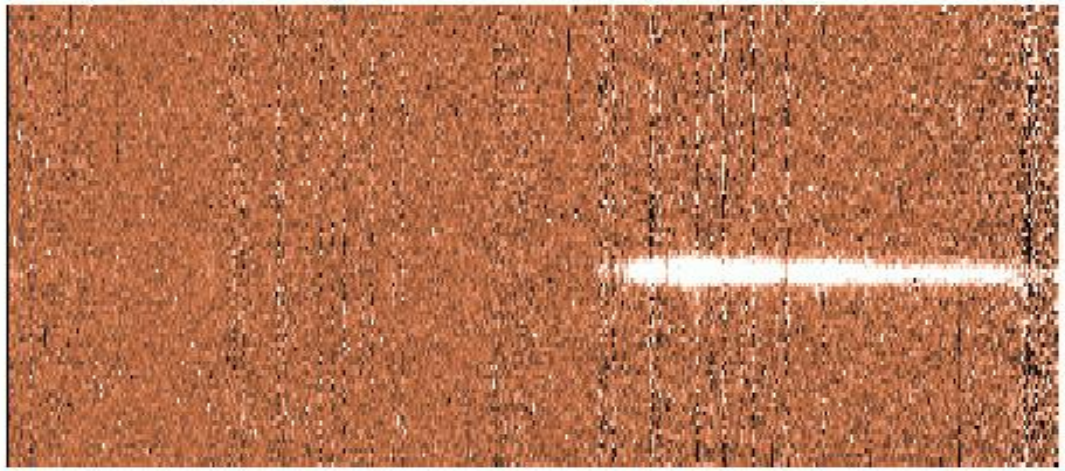

High-z quasar spectra (Fan et al. 2006)

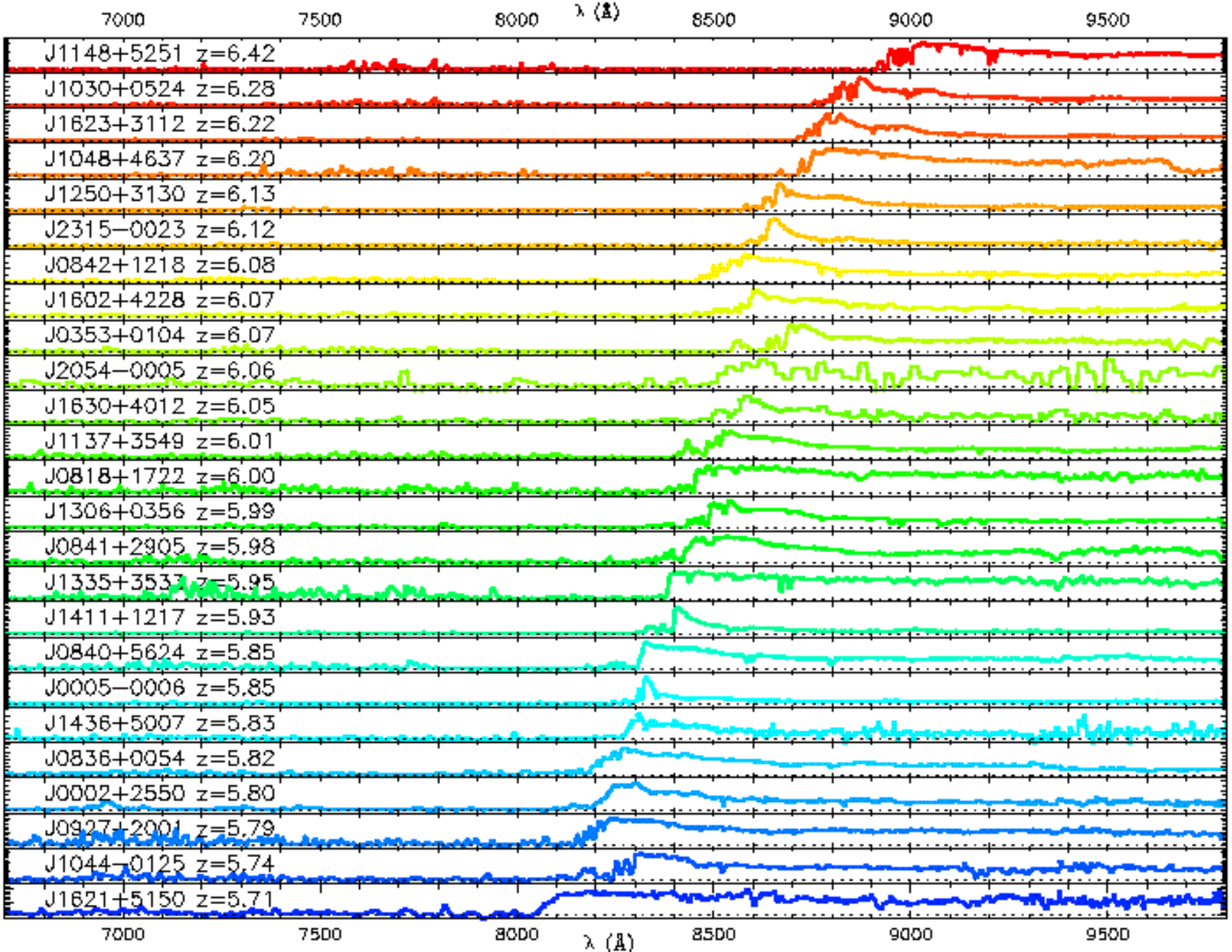

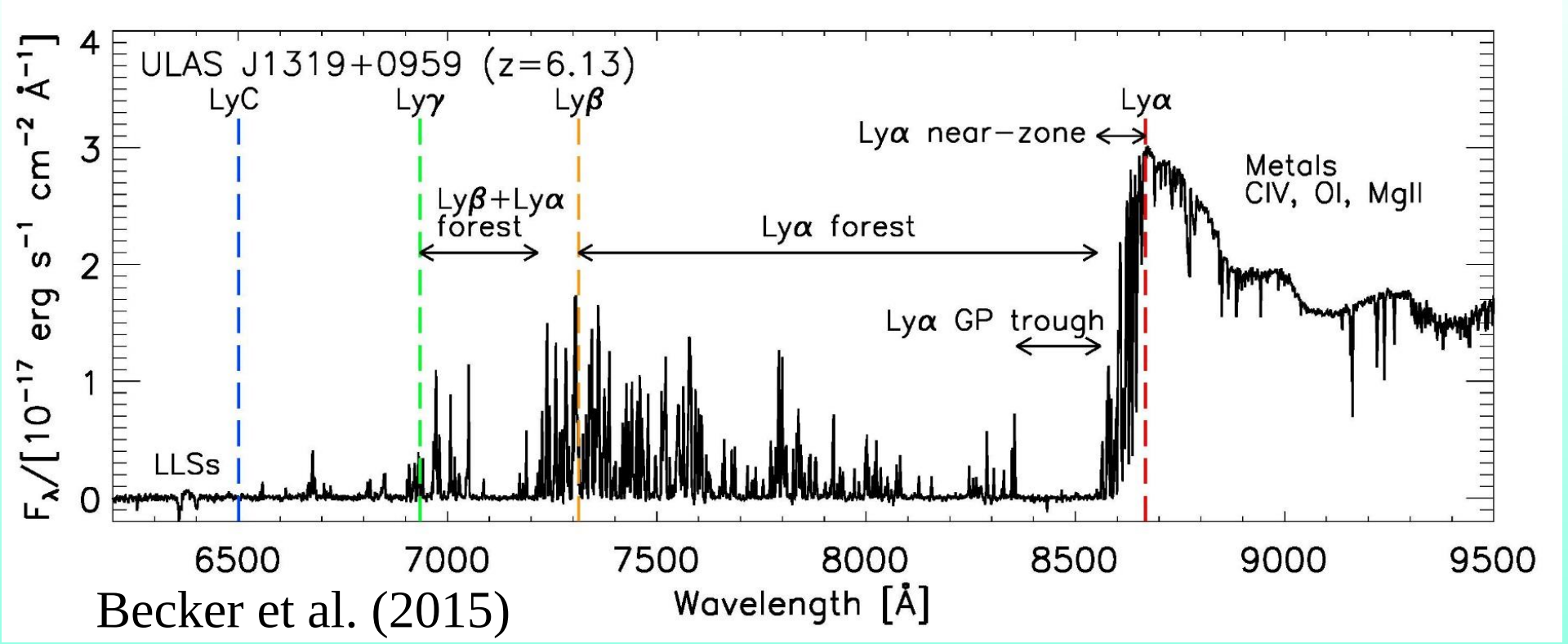

Redward of the Lyα emission from the QSO (red-dashed line): a series of metal absorption lines. Close to the QSO redshift: Lyα proximity zone, where the quasar contributes significantly to ionising the hydrogen. At shorter wavelengths: Gunn–Peterson absorption trough above 8400 Å, from hydrogen at $z \geq 5.9$ absorbing in the Lyα line. Next: Lyα absorption forest from intervening neutral hydrogen in the cosmic web. Between the green- and orange-dashed lines (wavelengths of the Lyβ and Lyγ transitions at the QSO redshift): high-redshift gas absorbs in the Lyβ line and at lower redshift, foreground gas absorbs in Lyα. At even shorter wavelengths, overlapping higher-order Lyman series transitions occur. Finally, below the line marked 'LyC' there is continuum absorption from neutral hydrogen: photons with rest frame $\lambda \leq 912$ Å are energetic enough to photoionise hydrogen. In lower-redshift quasar spectra where there is less overall absorption, Lyman-limit systems (LLSs) can be identified here.

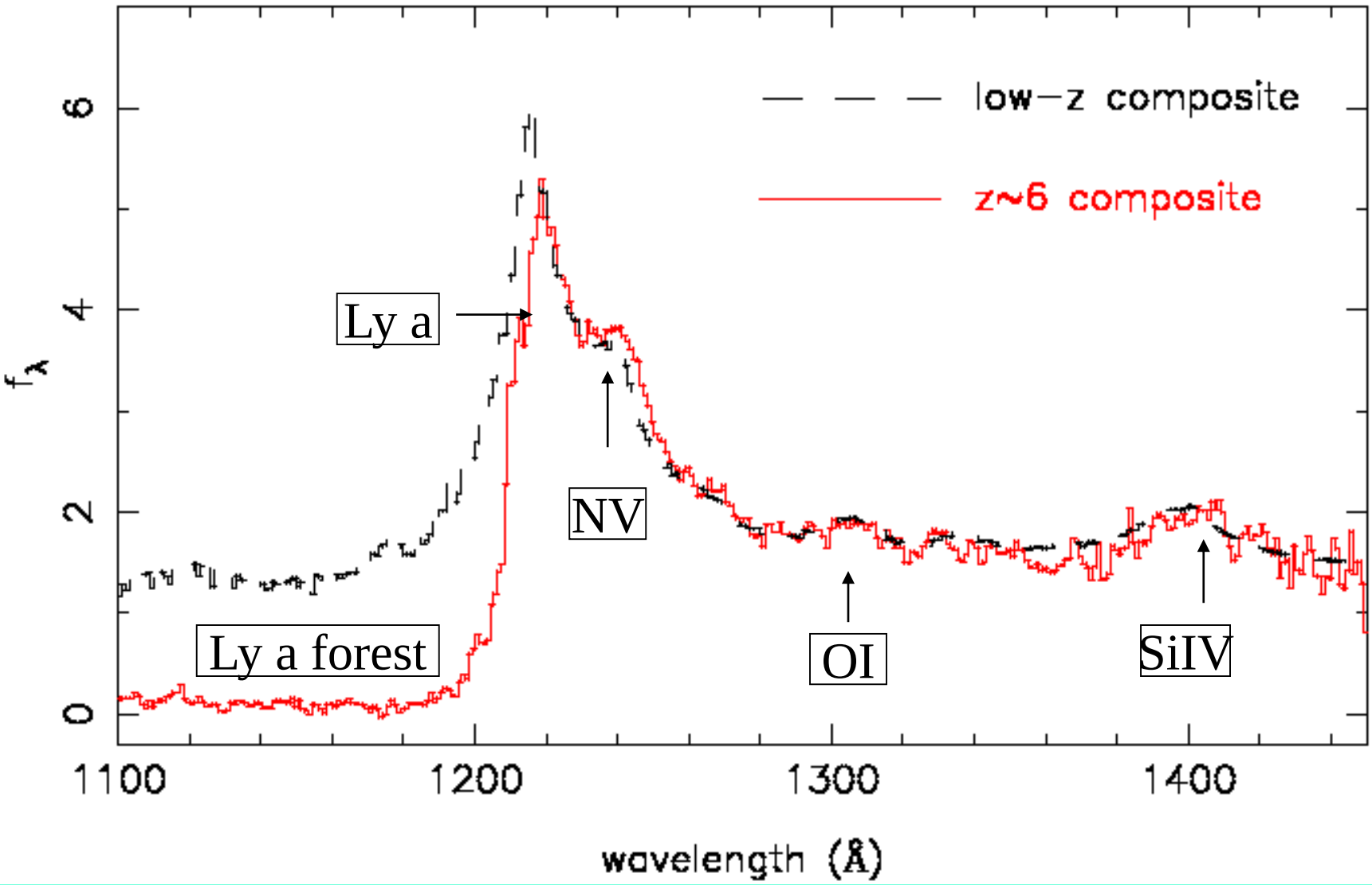

Remarkable lack of evolution in the QSO vicinity: strong metal lines, from N, C, Si etc., indicating high metallicity in the quasar envinronment: rapid chemical enrichment in quasar vicinity. *High-z quasars and their environments mature early on.*

QSO at z=7.085 (Mortlock et al. 2011)

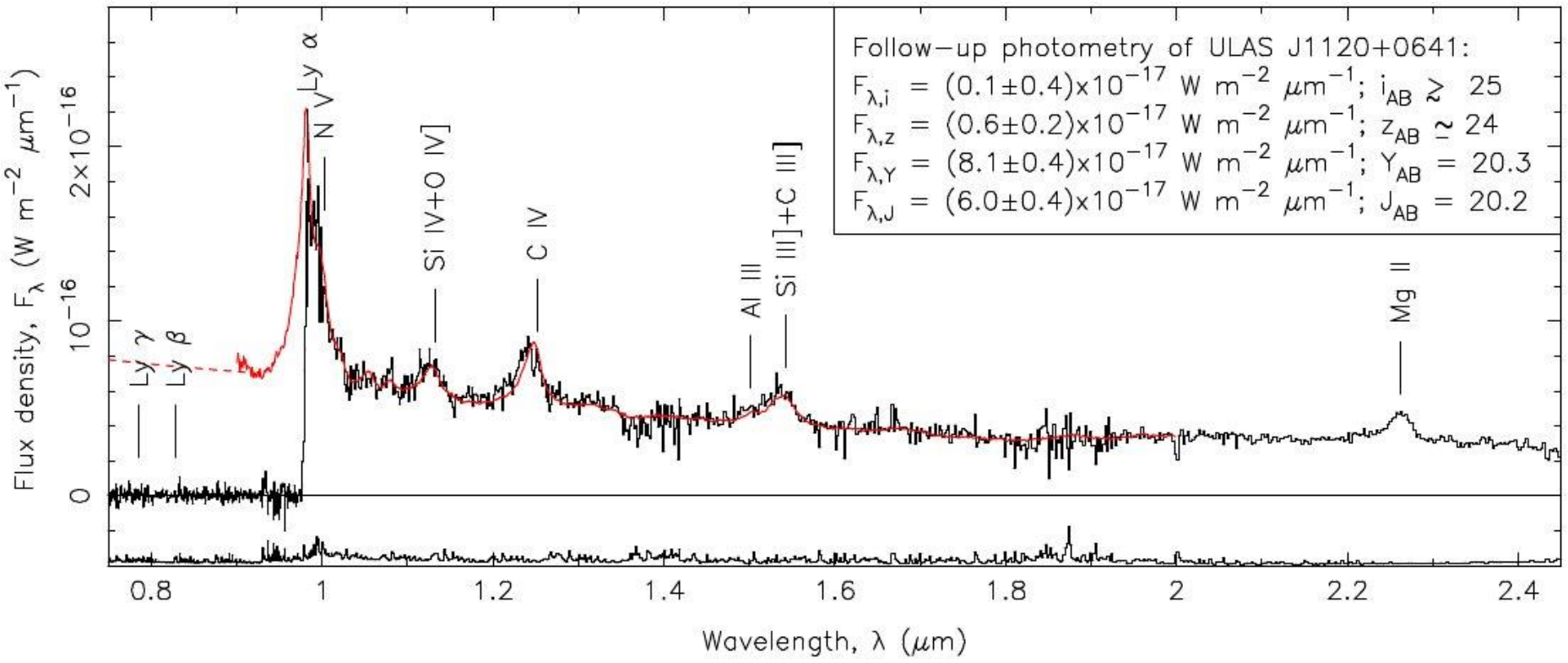

Spectrum of ULAS J112001.48+064124.3 compared to a composite spectrum derived from averaging the spectra of 169 SDSS QSO in the redshift interval $2.3 < z < 2.6$. The composite is a strikingly good fit to the spectral shape of the z=7.1 QSO and most of its emission lines, implying normal metal abundances already at a universe age of 0.77 Gyr. Aside from that, the most striking aspect is the almost complete lack of observed flux blueward of its Lyα emission line,which can be attributed to absorption by HI along the line of sight.

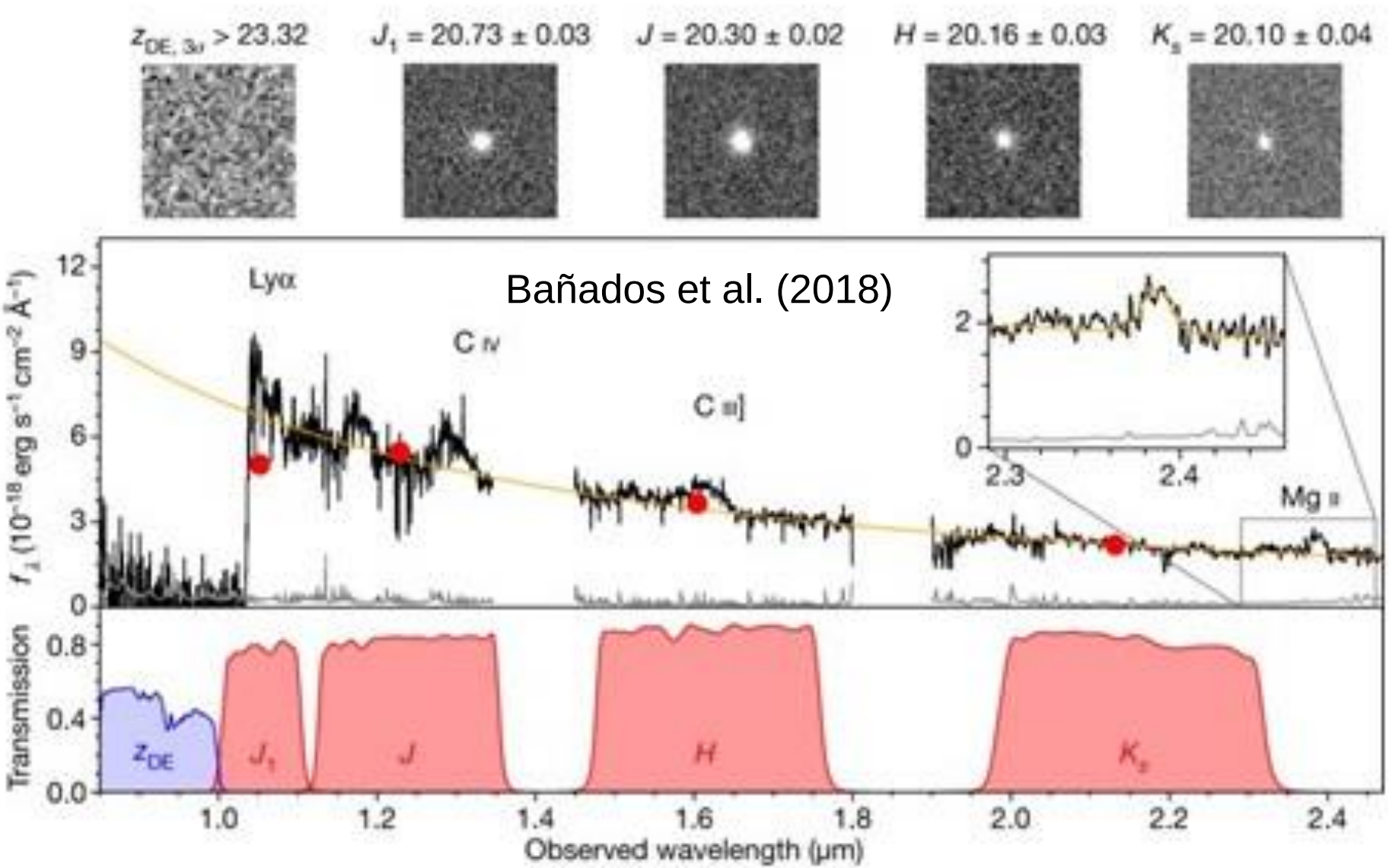

Photometry and combined Magellan/FIRE and Gemini/ GNIRS near-infrared spectrum of the quasar J1342 + 0928 at *z* = 7.54.

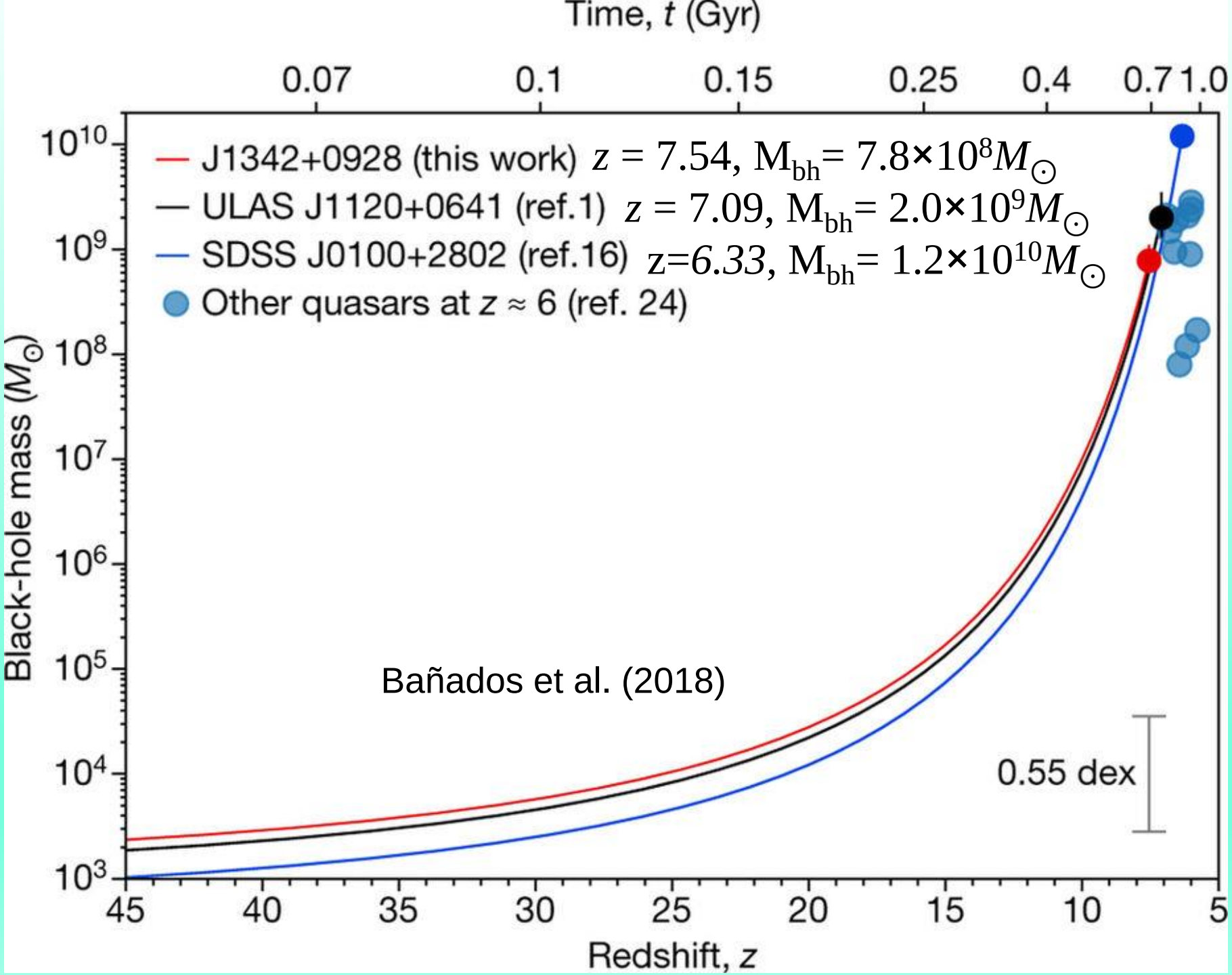
Time, t (Gyr)
0.07
0.1
0.15
0.25
0.4
0.7
1.0
J1342+0928 (this work) z = 7.54, M_bh = 7.8×10^8 M_⊙
ULAS J1120+0641 (ref.1) z = 7.09, M_bh = 2.0×10^9 M_⊙
SDSS J0100+2802 (ref.16) z=6.33, M_bh = 1.2×10^10 M_⊙
Other quasars at z ≈ 6 (ref. 24)
Black-hole mass (M_⊙)
10^10
10^9
10^8
10^7
10^6
10^5
10^4
10^3
Bañados et al. (2018)
0.55 dex
45
40
35
30
25
20
15
10
5
Redshift, z

Small aside: the black-hole growth

- The previous figure shows that, assuming Eddington limited accretion, black-hole seeds more massive than $1{,}000 M_{\odot}$ by $z = 40$ are necessary to grow the observed supermassive black holes in all three cases.
- An alternative possibility, revived by several recent investigations, is that of super-Eddington accretion. When the mass is flowing towards the BH at high rates, the matter accumulates in the vicinity of the BH and the accretion may happen via the radiatively-inefficient `slim-disk' solution (Abramowicz et al. 1988, Begelman 2012, Madau et al. 2014, Volonteri et al. 2015) that speeds up the growth of SMBHs.

Variance along different lines of sight

$\tau_{GP} = -\ln \mathcal{T}$

Do complete troughs mean reionization just ended at z=6.2?

Or is it just natural thickening of the forest as we move to higher z?

Clue: as we approach end of reionization we expect abrupt change in optical depth τ_{GP} with z

11 SDSS QSOs

Fan et al (2003)

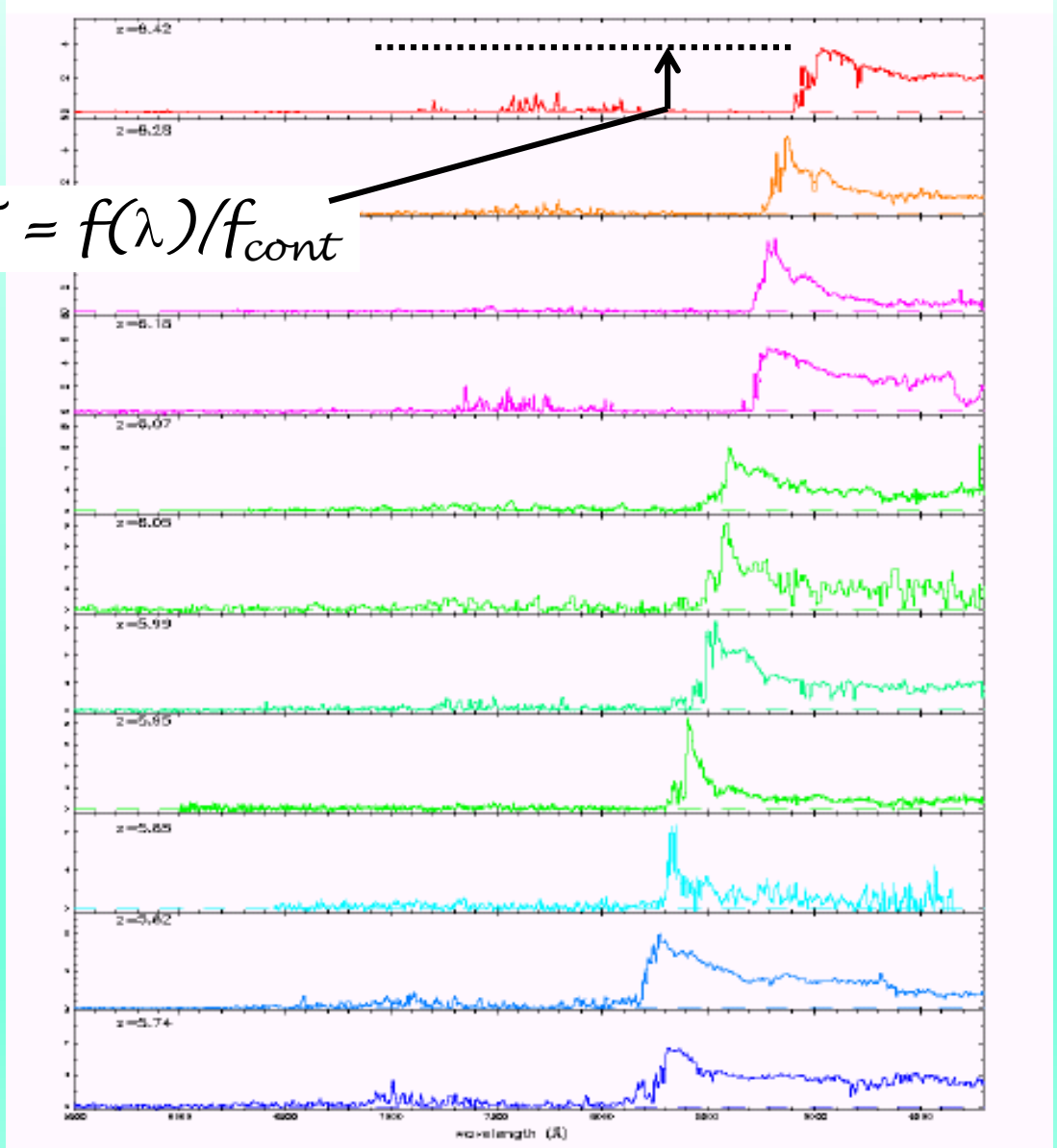

The End of Reionization

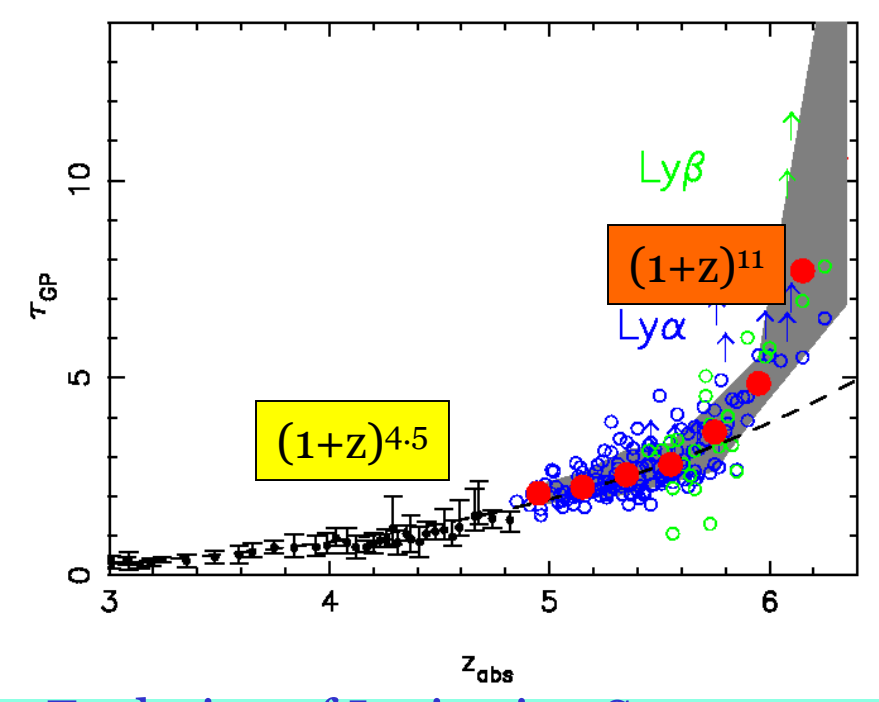

- *Optical depth evolution accelerated*
  - $z<5.7$: $\tau \sim (1+z)^{4.5}$
  - $z>5.7$: $\tau \sim (1+z)^{>11}$

Neutral fraction

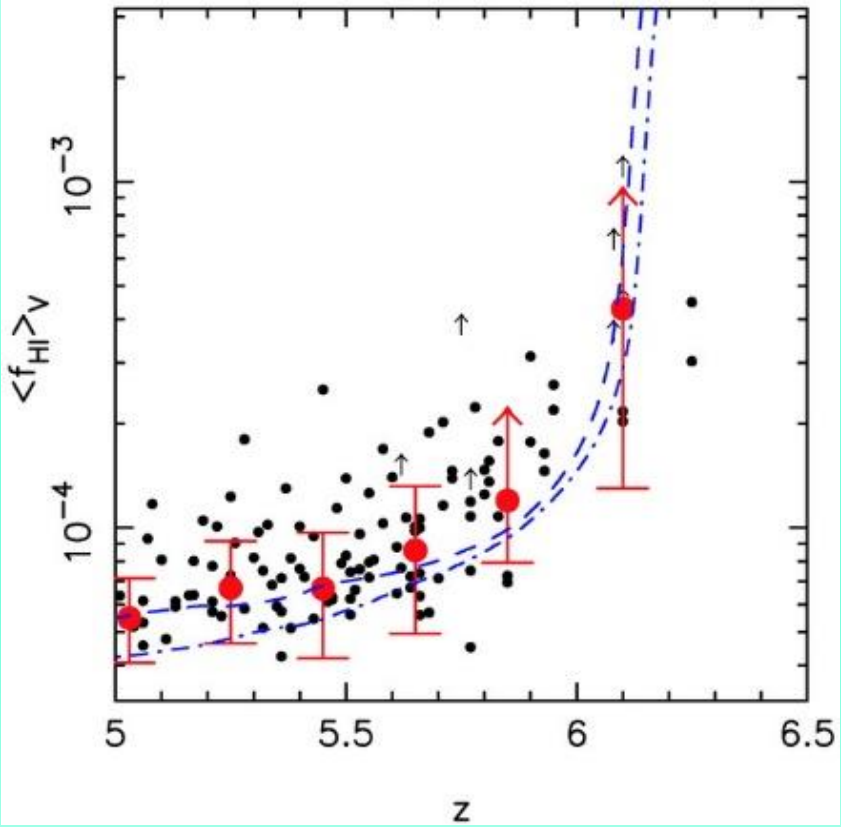

- Evolution of Ionization State:
  - Neutral fraction increases by >15
  - Mean-free-path of UV photons decreases by >10
  - Large variation in the IGM properties

  → ***z~6 marks the end of cosmic reionization***

Other probes of neutral fractions

- Other estimators, sensitive to larger neutral fractions, are needed to probe deeper into the reionization era. These include:
  - Dark gap statistics
  - Sizes of the QSO near zones
  - Damping wing of the Gunn-Peterson trough
  - Evolution of the IGM Thermal State
  - Luminosity Function and Line Profiles of Lyα Galaxies

DETERMINING THE REIONIZATION REDSHIFT

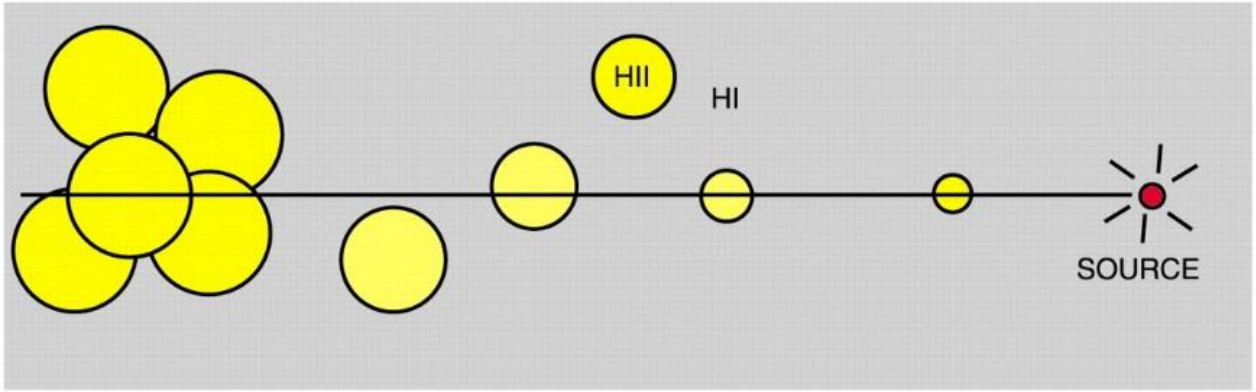

Loeb & Barkana (2001)

Spectrum

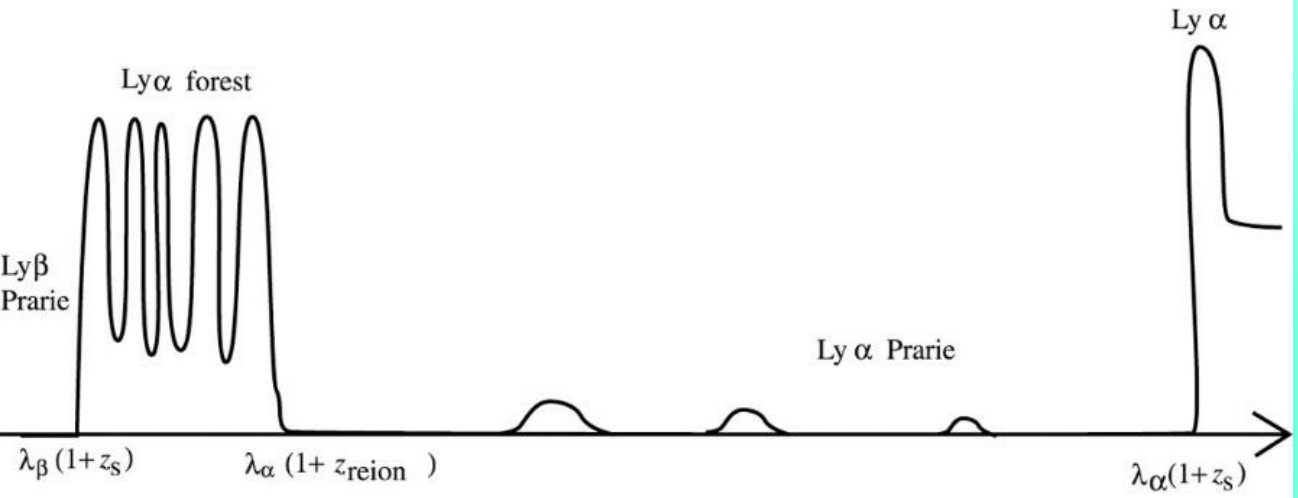

$$1 < \frac{1+z_s}{1+z_{reion}} < \frac{\lambda_\alpha}{\lambda_\beta} = 1.18$$

The reionization will be initially patchy with Lyα transmission (HII) regions intermixed with dark (HI) gaps.

Distribution of Dark Gaps

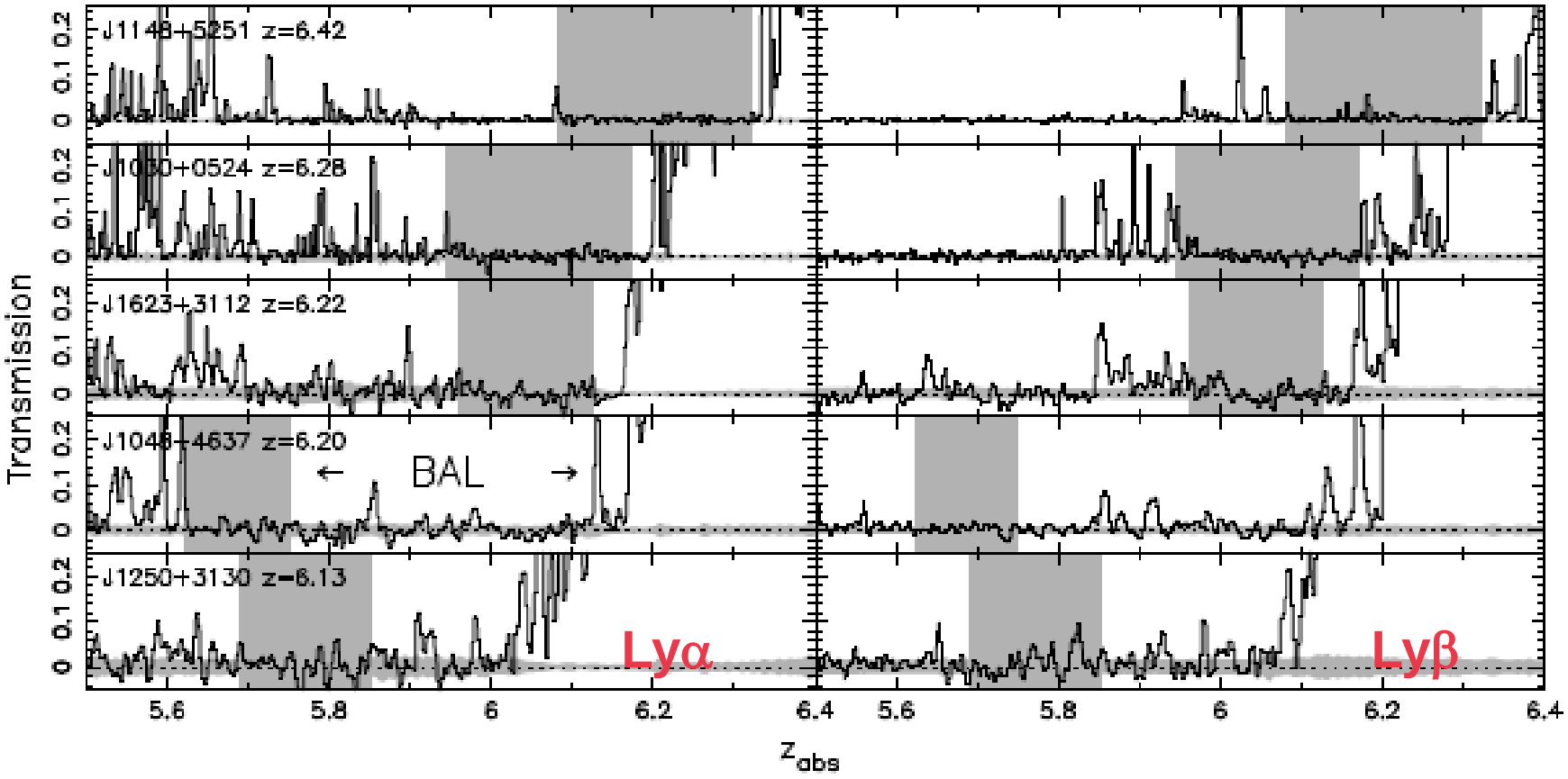

Gap or `void' statistics contain useful information on topology

Define `gap' as contiguous region where $\tau > \tau_{MIN}$ (e.g. $\tau > 2.3$, i.e. transmission < 0.1 or $\tau > 3.5$). Regions of high transmission are effectively associated with large HII regions thus their distribution acts like an indirect Lyα LF:

$\rightarrow$ probe of neutrality independent of Gunn Peterson

Dark gap statistics - 1

- McGreer et al. (2011, 2015) have demonstrated that counting the fraction of spectral pixels that are completely absorbed one can obtain a conservative, almost model-independent lower bound on the filling factor of ionised regions.
- The later study found $x_{HI} < 0.11$ at $z = 5.6$, < 0.09 at $z = 5.9$ and < 0.58 at $z = 6.1$. These results suggest that if significantly neutral diffuse gas remains at $z \leq 6$, it fills a rather small fraction of the IGM volume.
- A related diagnostic is the size distribution of contiguous saturated regions in the Lyα forest, and the redshift evolution of these so-called 'dark gaps' (e.g. Songaila & Cowie 2002; Paschos & Norman 2005; Fan et al. 2006; Gallerani et al. 2006, 2008; Mesinger 2010). As with many of the other observed properties of the $z \sim 6$ Lyα forest, the abundance of large dark gaps grows steeply near $z \sim 6$.

Dark gap statistics - 2

- However even by $z \sim 5.3$, there are some ≥ 30 Mpc contiguous regions that appear entirely absorbed, with $\tau_\alpha \geq 3.5$.
- This evolution might result in part from the presence of remaining neutral islands in the IGM, or may instead reflect the thickening of the Ly α forest owing to the increasing mean density of the Universe and the dropping intensity of the UVB, along with fluctuations in the mean free path and the IGM temperature.
- In conclusion, a conservative limit at z~5 can be $x_{HI} \leq 0.1$; the current sample of quasars is statistically insufficient to constrain x_{HI} at $z \sim 6$ to even the 10 per cent level (Mesinger 2010).

Evolution of the dark gap sizes

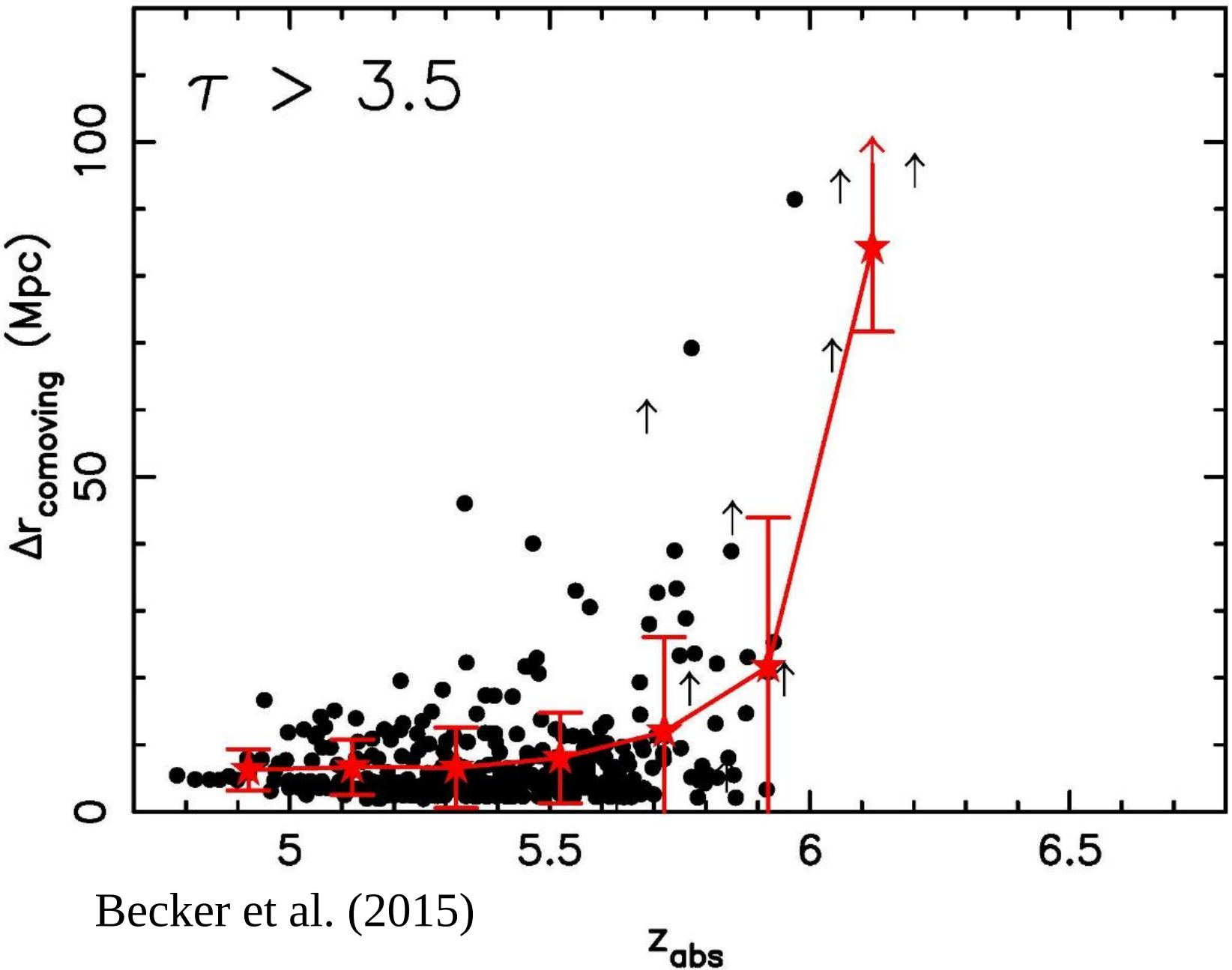

Becker et al. (2015)

Damping wing of the Gunn-Peterson trough

- The spectra of the highest-redshift QSOs presently known, at z = 7.1 and 7.5, show evidence for damping wing absorption on the red side of its Lyα line (Mortlock et al. 2011, Bañados et al. 2018).
- The comparison of the spectrum close to the Lyα emission line with damping wing models for a partly neutral IGM and a damped Lyα absorber (DLA) suggests that the damping wing could be sourced by significantly neutral material.
- For the z=7.1 QSO Bolton et al. (2011) found that either a neutral fraction of $x_{\rm HI} \geq 0.1$ is required, or a highly ionised IGM can be reconciled with the data if a DLA lies within $\sim$ 5 proper Mpc. However the DLA scenario is unlikely: DLAs of the required column density are rare and is that there is no detectable metal line absorption at the same redshift as the damping wing feature (Simcoe et al. 2012).

The z=7.085 QSO – 1

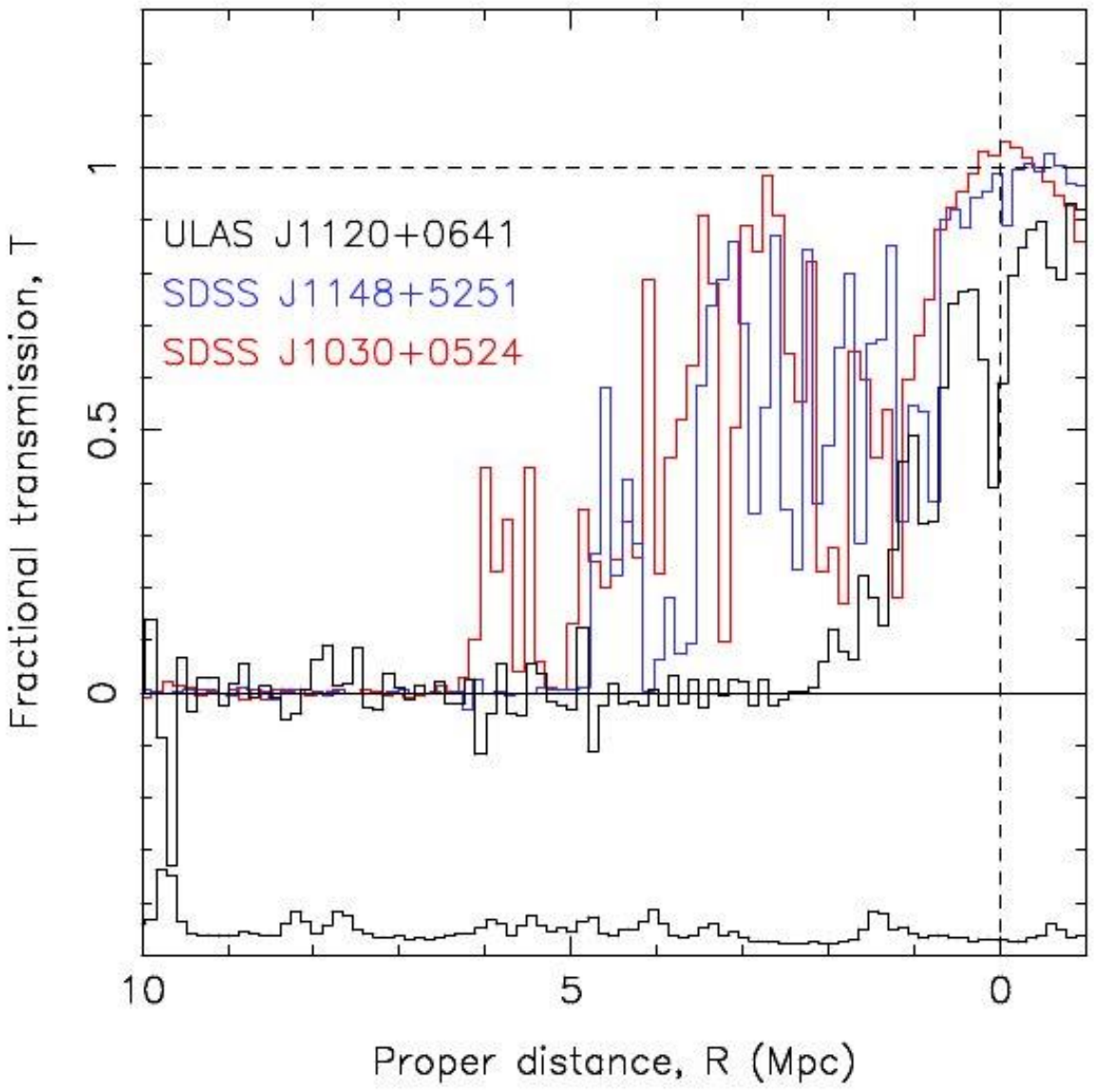

The inferred Lyα near zone transmission profile of ULAS J112001.48+064124.3 compared to those of the two lower-redshift (z=6.42 and 6.31) QSOs. The transmission profile of ULAS… is strikingly different from the others, with a measured near zone radius of ~1.9 Mpc, a factor of ~3 smaller than is typical for quasars at z between 6.0 and 6.4. The profile has also a distinct shape: whereas the profiles of SDSS J1148+5251and SDSS J1030+0524 have approximately Gaussian envelopes up to a sharp cut-off, the profile of ULAS… is much smoother and also shows absorption redward of Lyα.

The z=7.085 QSO – 2

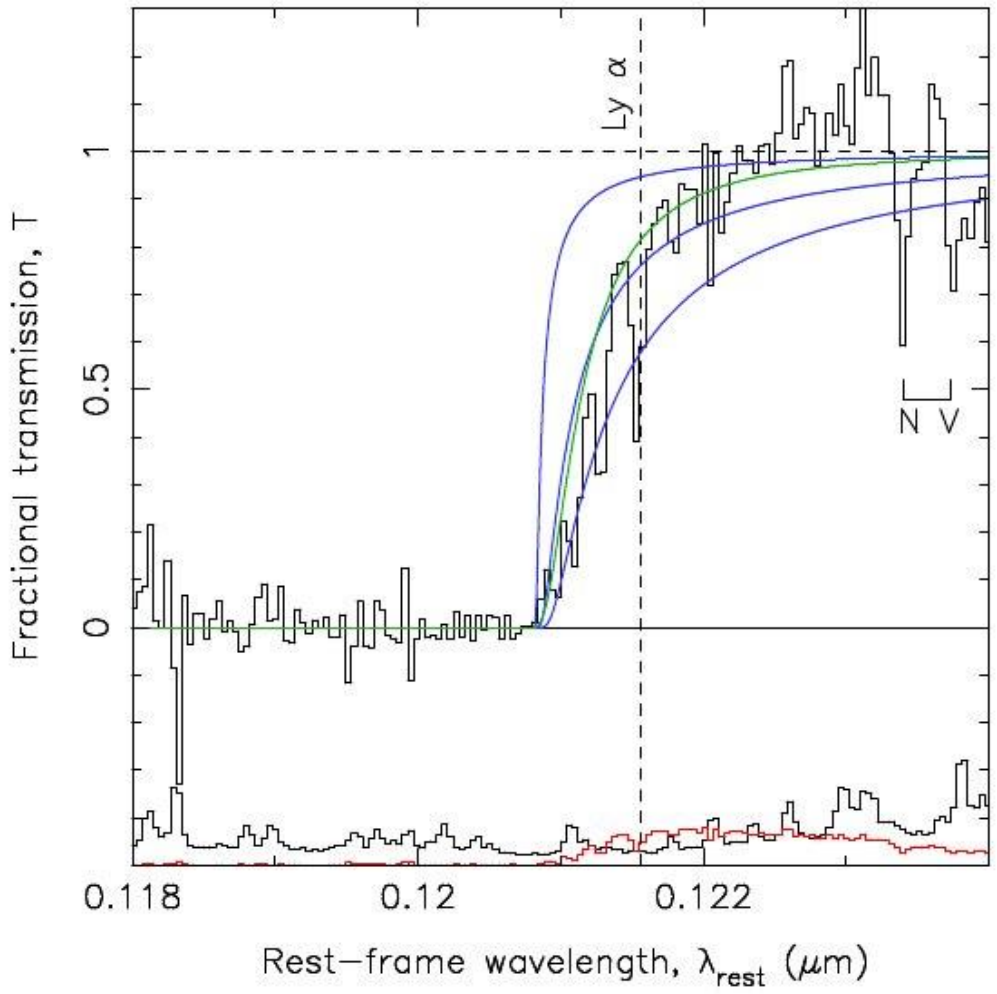

Rest-frame transmission profile of ULAS J112001.48+064124.3 in the region of the Lyα emission line. The blue curves show the Lyα damping wing of the IGM for neutral fractions of (from top to bottom) f_{HI}= 0.1, 0.5, and 1.0, assuming a sharp ionization front at 2.2 Mpc in front of the QSO. The green curve shows the absorption profile of a damped Lyα absorber of column density $N_{HI} = 4\times10^{20}$ cm^{-2} located at 2.6 Mpc in front of the quasar. If the absorption is due to the IGM, the transmission profile requires $0.1 < f_{HI} < 1$, i.e. a quite substantial HI fraction. The lower panel shows the measurement errors. There is a positive residual near 0.123μm, suggesting that the Lyα is stronger than average.

Greig et al. (2017) infer $x_{HI}=0.40^{+0.21}_{-0.19}$

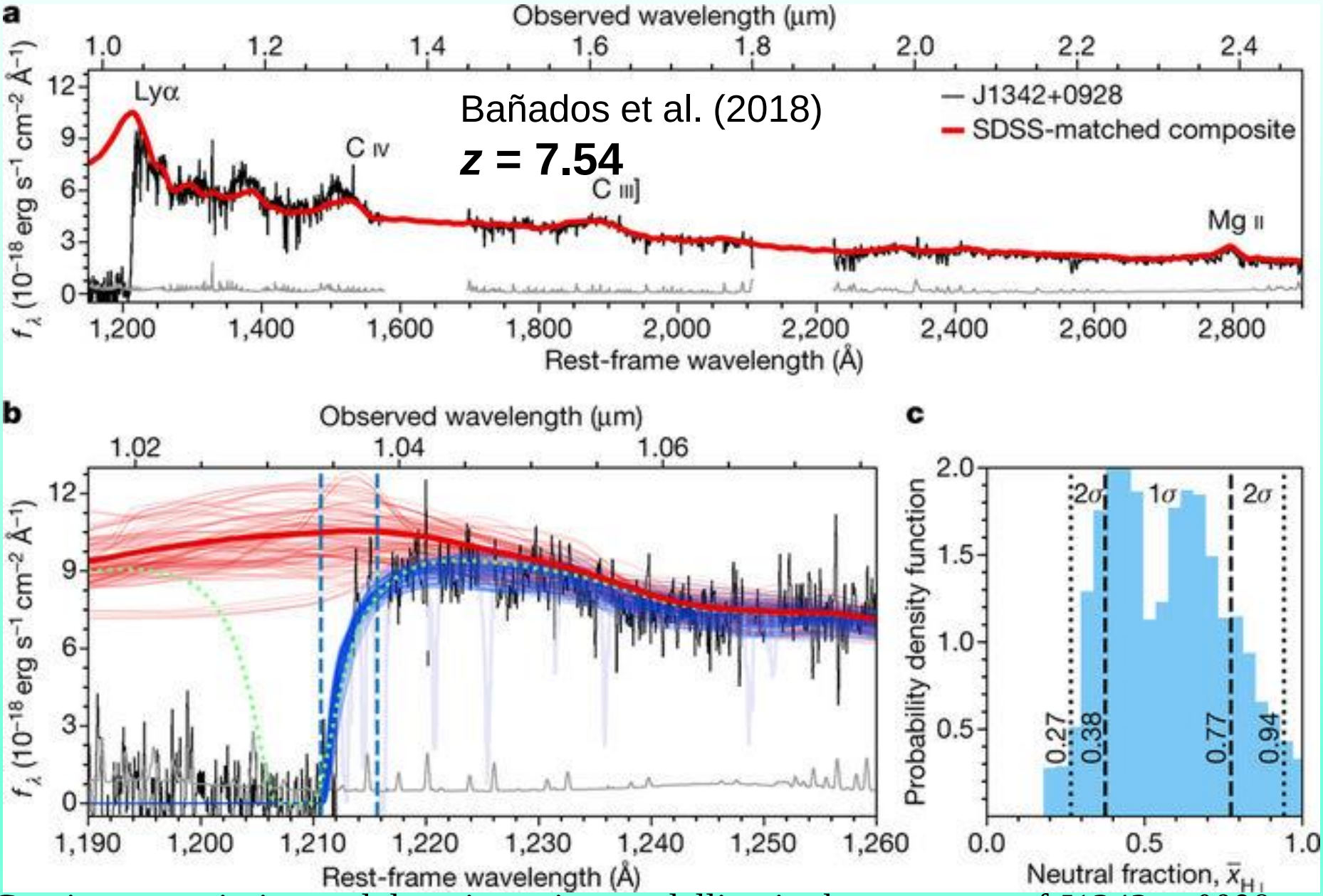

Continuum emission and damping-wing modelling in the spectrum of J1342 + 0928. The inferred mean value of the neutral fraction is x_{HI}= 0.56 (+0.21,-0.18). Somewhat lower x_{HI} estimated by Greig et al. (2018).

Lyα emitter surveys

- A highly successful approach for finding high-z galaxies uses a narrow-band selection technique to target objects with prominent Ly*α* emission lines (e.g. Dijkstra 2014).
- The visibility of these Ly*α* emitters (LAEs) is impacted by the damping wing arising from neutral gas in the IGM (Miralda-Escudè 1998). So these surveys are sensitive to the reionisation history.
- The abundance of observable LAEs will drop and their clustering will increase as one probes deeper into the EoR (Furlanetto et al. 2006; McQuinn et al. 2007; Mesinger & Furlanetto 2008).

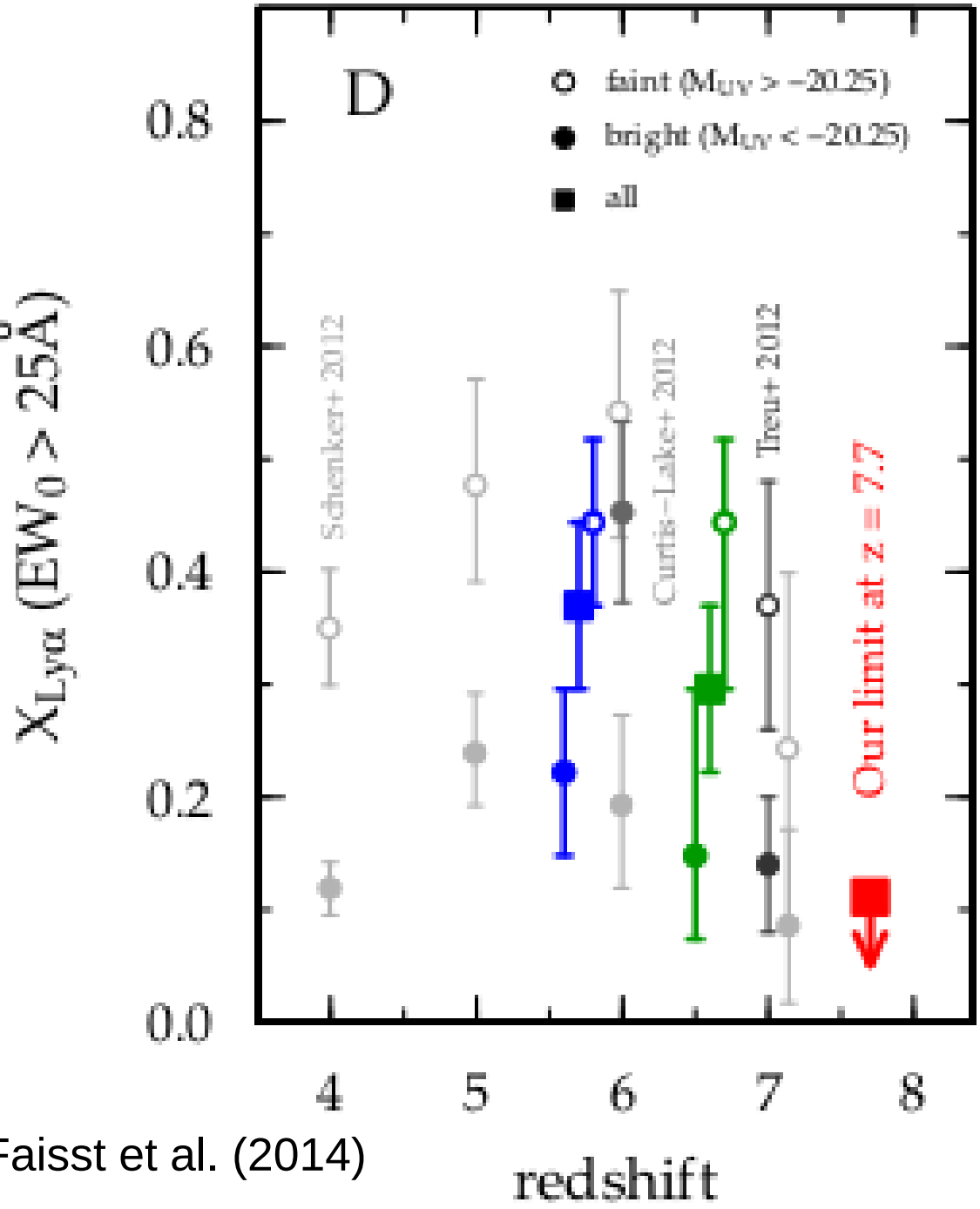

Faisst et al. (2014)

A decrease of the LAE fraction is expected when the IGM becomes partly neutral. Data indicate a drop of a factor 4 above z = 6. Faisst et al. (2014) infer lower limits of the neutral hydrogen fraction to be 50 - 70% at z ≈ 7.7. Matthee et al. (2014) did not find any LAE in a deep 10 deg^2 survey at z = 8.8 with spectroscopic follow-up.

Evolution of Lyα optical depth

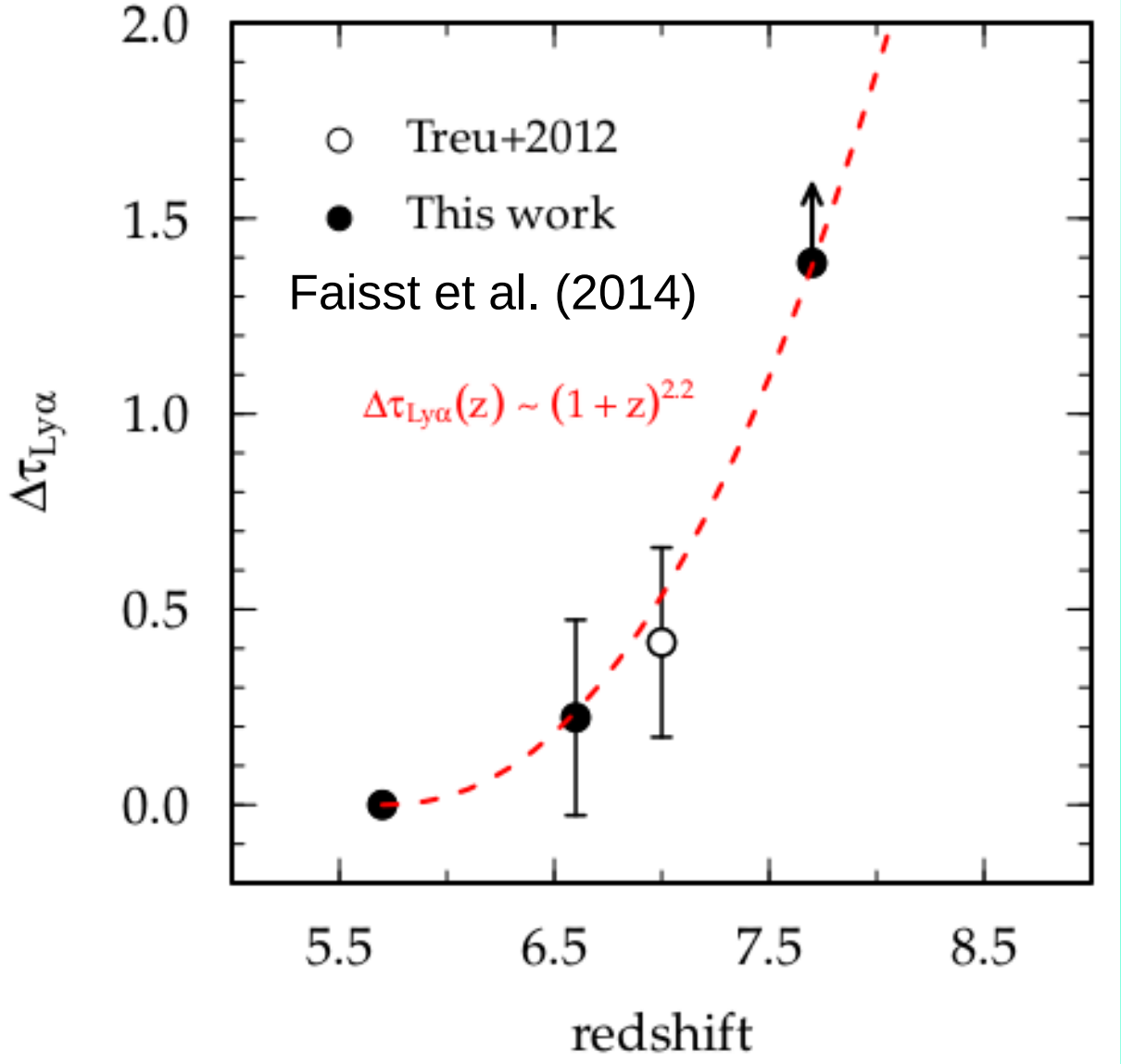

The strong evolution beyond z = 6 is apparent and could be indicative of a dramatic increase in the neutral H fraction in the IGM.

Evolution of the IGM Thermal State -1

- Constraints on the timing of the reionization also come from the temperature of the IGM at z ~6 (Bolton et al. 2010, 2012; Padmanabhan et al. 2014). The argument goes as follows.
- Reionization typically heats up the IGM to tens of thousands degrees, and the gas subsequently cools adiabatically because of the expansion of the universe and other processes (recombination & Compton cooling).
- If the universe was reionized early and has stayed highly ionized thereafter, photoionization heating of the gas cannot overcome the overall cooling, and the IGM reaches a temperature $< 10^4$ K.
- That temperature might be too low at low redshifts compared to observations.

Evolution of the IGM Thermal State -2

- The cooling time for the low-density IGM gas is long. Hence the gas temperature at a given z allows to infer the redshift when the re-ionization (Miralda-Escudè & Rees 1994; Theuns et al. 2002; Hui & Haiman 2003).
- The gas temperatures can be inferred from the line widths in near-zones observed in high-resolution quasar.
- The constraints are relaxed if there is a substantial contribution from heating by the quasar itself.
- Upper limits to z_{reion} were derived in this way by Bolton et al. (2010).
- Using measurements of the IGM temperature in the near-zones of seven quasars at z∼5.8-6.4, Raskutti et al. (2012) concluded that data were consistent with reionisation completing at $z > 6.5$ at 95% confidence. However, this inference is dependent on the assumed source spectra.

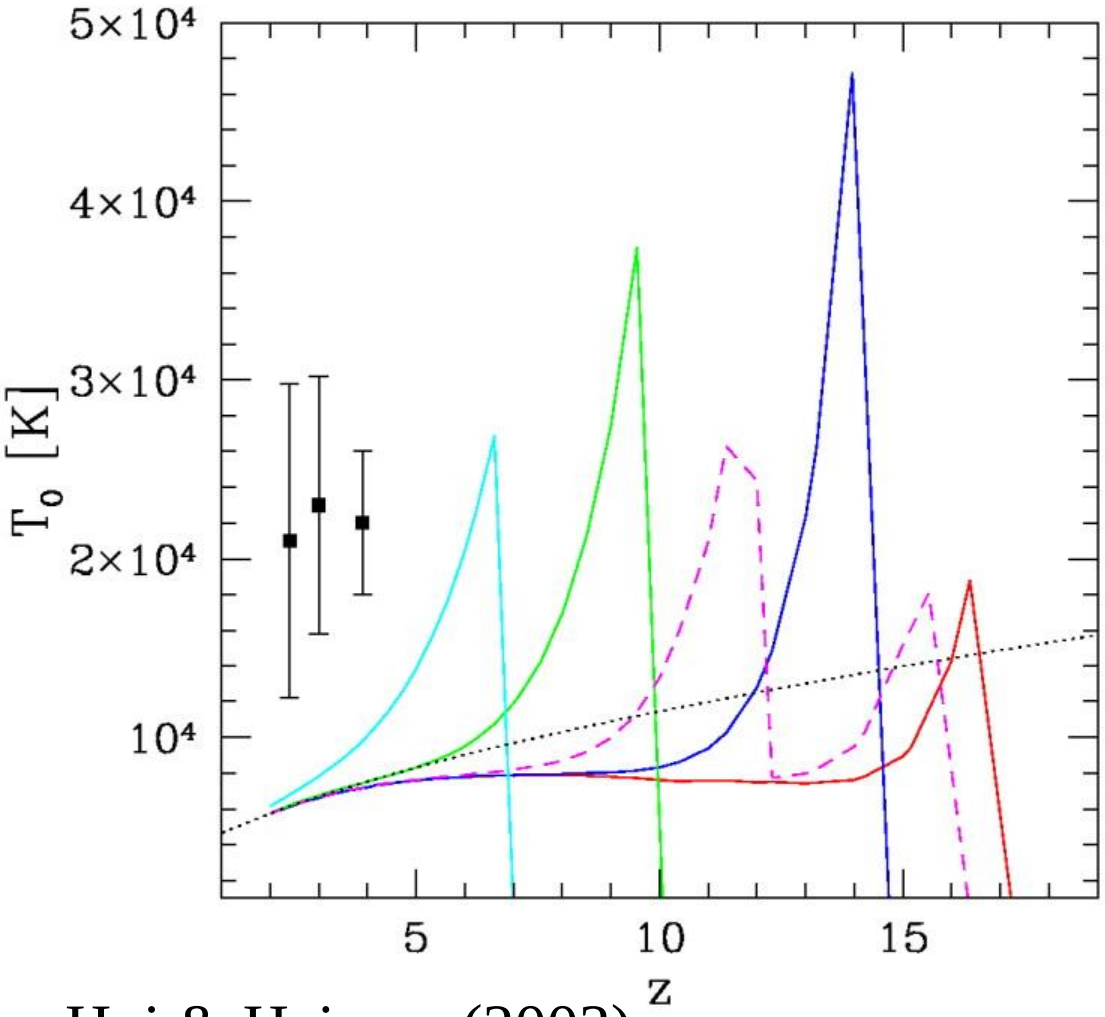

Hui & Haiman (2003)

Thermal asymptote (black dotted line), illustrating that a wide range of ionization histories results in the same IGM temp. by z = 4, unless reionization occurs late. Each colored solid line describes the evolution of the temperature for a fluid element at mean density, according to a different reionization history (and a different initial reheating temperature). The points with (2 σ) error bars on the left are measurements of T_0 from the Lyα forest.

Constraints on z_{reion} from IGM temperature - 1 (Bolton et al. 2010)

IGM temperature around a z = 6 quasar determined by analysing the Doppler widths of Ly absorption lines in the proximity zone of SDSS J0818+1722, measured with high resolution (R = 40 000) Keck/HIRES spectrum. Found T_0 = 23 600(+5000,-6900) K at 68% confidence.

If the quasar reionises the He II in its vicinity, then in the limit of instantaneous reionisation of H $z_{reion} < 9.0$ (11.0) at 68% (95%) confidence.

If the HI and He II in the IGM around the quasar are instead reionised simultaneously by a population of massive metal-free stars, characterised by very hard ionising spectra, a tighter upper limit is obtained: $z_{reion} < 8.4$ (9.4) at 68% (95%) confidence .

Constraints on z_{reion} from IGM temperature

Initiating reionisation at higher redshifts produces temperatures which are too low with respect to the measured ones. However astrophysical uncertainties in the modelling are significant especially because the exact spectrum of the ionising sources are rather uncertain at z > 6. Ionising spectra harder than typically assumed would increase these upper limits.

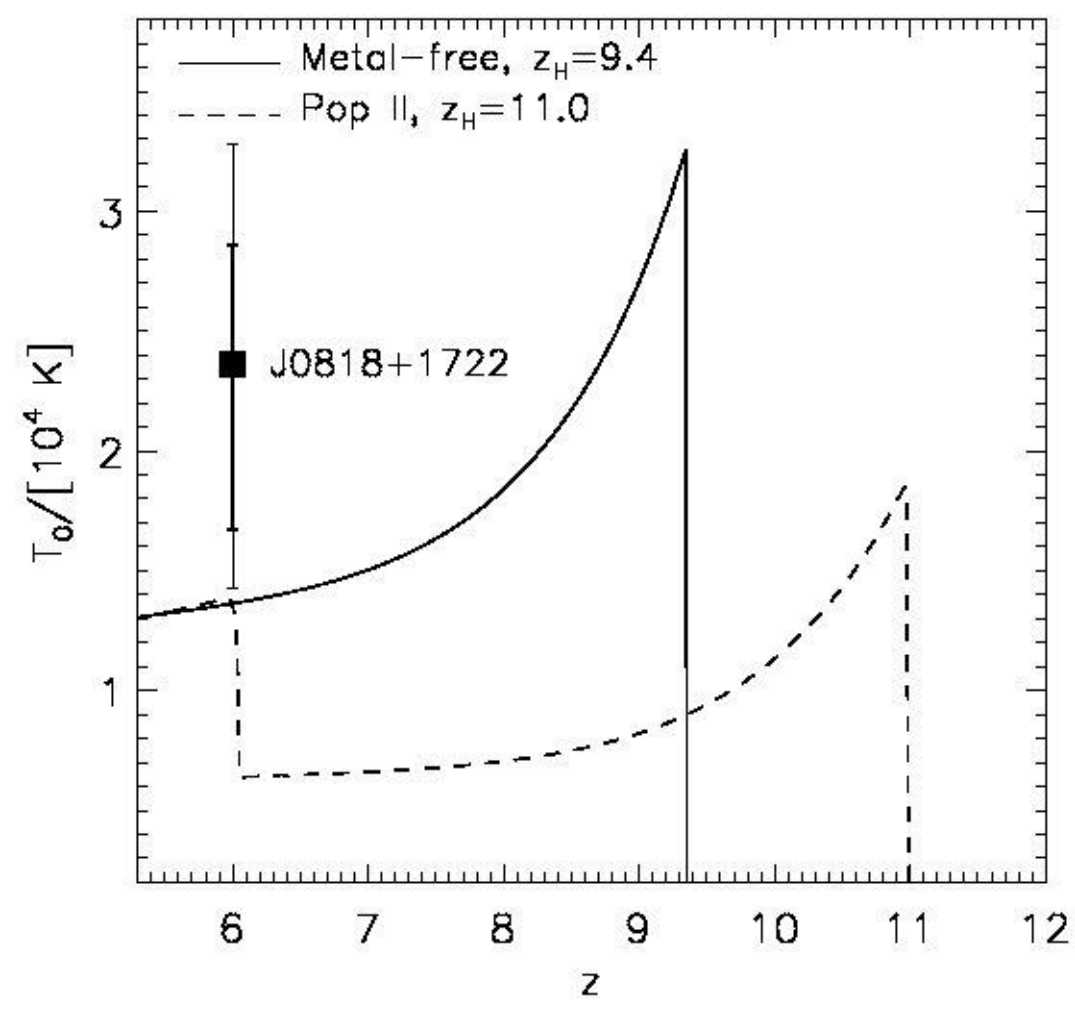

In the Pop II model (dashed), HeII is reionized by the quasar itself at z=6.05. This leads to a temperature boost by about 8000 K

Summary of information from optical data - 1

- The Gunn-Peterson effect demonstrates a rapid increase of HI at z>6. However, it only measures very low neutral fractions. Also, since reionization is highly inhomogeneous, the effect may not show up even for non-negligible values of the volume-weighted mean x_{HI}. Hence the G.P. effect does not allow us to determine the HI abundance.
- The dark-gap statistics suggests that if significantly neutral diffuse gas remains at $z \leq 6$, it fills a rather small fraction of the IGM volume. At z~5, $x_{HI} \leq 0.1$.
- A rapid increase of x_{HI} with z, above z=6, is confirmed by the evolution of the QSO near zone.

Summary of information from optical data - 2

- The Lyα damping wing of QSOs at z=7.085 and at $z = 7.54$ imply $x_{HI} \geq 0.1$ and $x_{HI} = 0.56$ (+0.21,-0.18), respectively.
- The drop of the fraction of Lyα emitters above z = 6. indicate a neutral hydrogen fraction of 50 - 70% at $z \approx 7.7$.
- The constraints in the IGM temperature around $z \approx 6$ Qsos imply $z_{reion} < 9.0$ (11.0) at 68% (95%) confidence.

Cosmic reionization and the CMB

- The Cosmic Microwave Background (CMB) offers a completely independent way to to probe the intervening IGM out to the epoch of reionisation.
- The CMB photons interact with free electrons in the IGM they pass through via Thomson scattering.
- The Thomson scattering has several effects:
  - generates a small distortion of the CMB spectrum (Sunyaev-Zeldovich effect)
  - Produces an overall damping of the CMB power spectrum
  - causes an overall polarisation of the CMB anisotropies.
- The amplitude of all these effects depends on the electron scattering optical depth, τ.

Electron scattering optical depth - 1

This can be understood as follows:

- If the optical depth is τ=0, all photons reaching us today come from the epoch of recombination.
- Correspondingly, if τ>1, then most photons that reach us would have been scattered during the period of re-ionisation.
- It turns out that the fraction of photons that were scattered at the epoch of re-ionisation is $(1-e^{-\tau}) \approx \tau$, for $\tau << 1$.
- In reality the details are a bit more complex than what we covered here; see past lectures.
- The most important effect is the generation of CMB polarization, induced by the quadrupole anisotropy.

Electron scattering optical depth - 2

If the universe is fully ionized up to the redshift z_r the electron scattering optical depth is

$$\begin{aligned}
\tau_{\rm es}(z_r) &= \int_0^{z_r} n_e\,\sigma_T\,(1+z)^{-1}\,\frac{c}{H(z)}\,{\rm d}z \\
&= 0.00123\,\frac{[\Omega_m(1+z_r)^3+\Omega_\Lambda]^{1/2}-1}{\Omega_m}+0.002 \\
&= 0.0039\{[0.315(1+z_r)^3+0.685]^{1/2}-1\}+0.002
\end{aligned}$$

where the last term (0.002) adds the extra scattering from He++ at $z \leq 3$. For $z = 6$, 6.5, 7 and 7.5 we have $\tau_{\rm es} = 0.0388$, 0.0432, 0.0478 and 0.0525, respectively.

Detection of the Gunn–Peterson effect on QSO spectra located the end of the reionization epoch at $z \simeq 6$ (Fan et al. 2006) where the neutral H fraction was found to be $f_{\rm HI} \gtrsim 10^{-2} - 10^{-3}$.

CMB and re-ionization

- As the CMB radiation possesses a primary quadrupole moment, Thomson scattering between the CMB photons and free electrons generates linear polarization. This is the case at recombination but in particular it is true at reionization.
- Re-scattering of the CMB photons at reionization generates a new polarization anisotropy at large angular scale because the horizon has grown to a much larger size by that epoch.

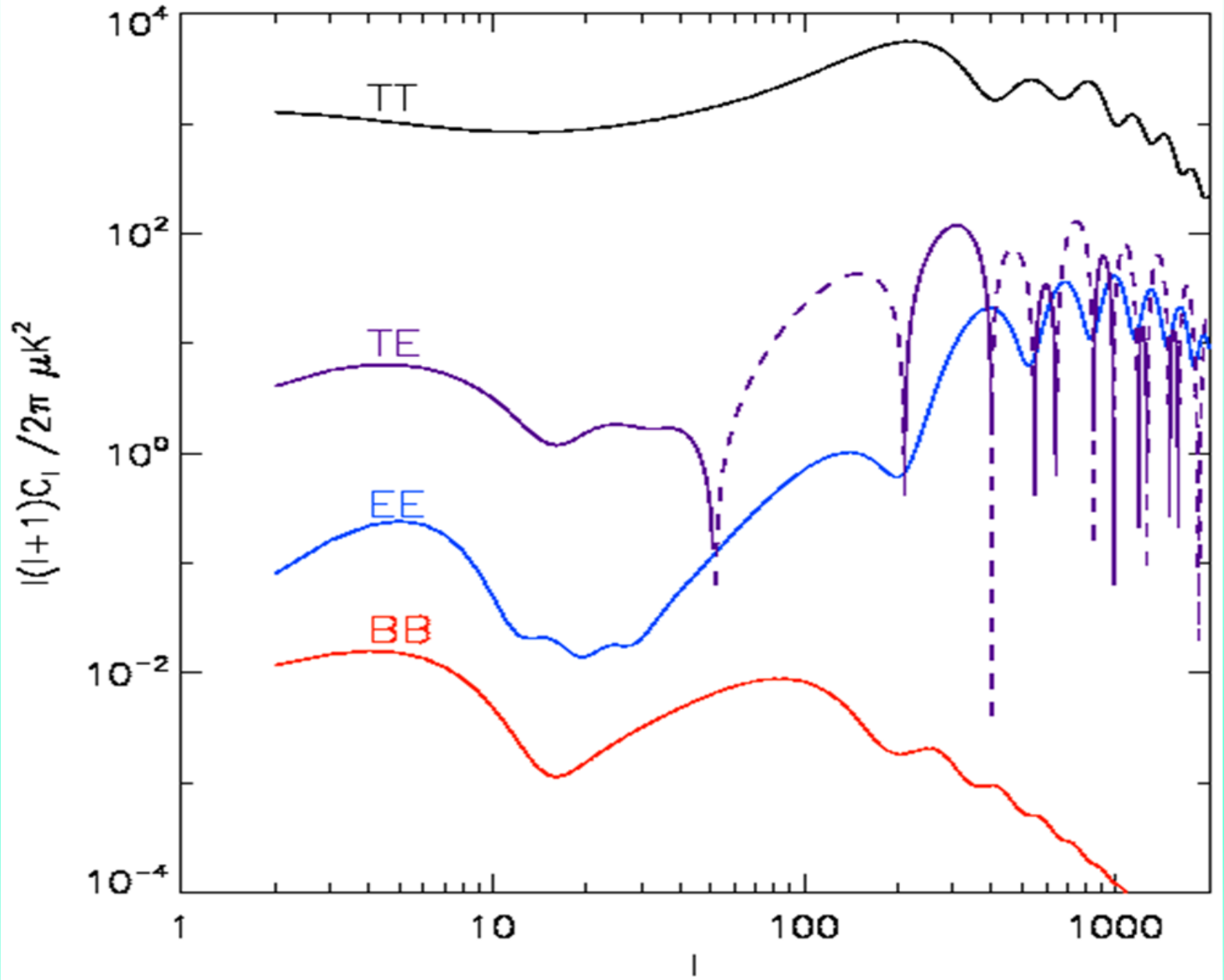
TT
TE
EE
BB
10^4
10^2
10^0
10^{-2}
10^{-4}
$l(l+1)C_l/2\pi\ \mu K^2$
1
10
100
1000
l

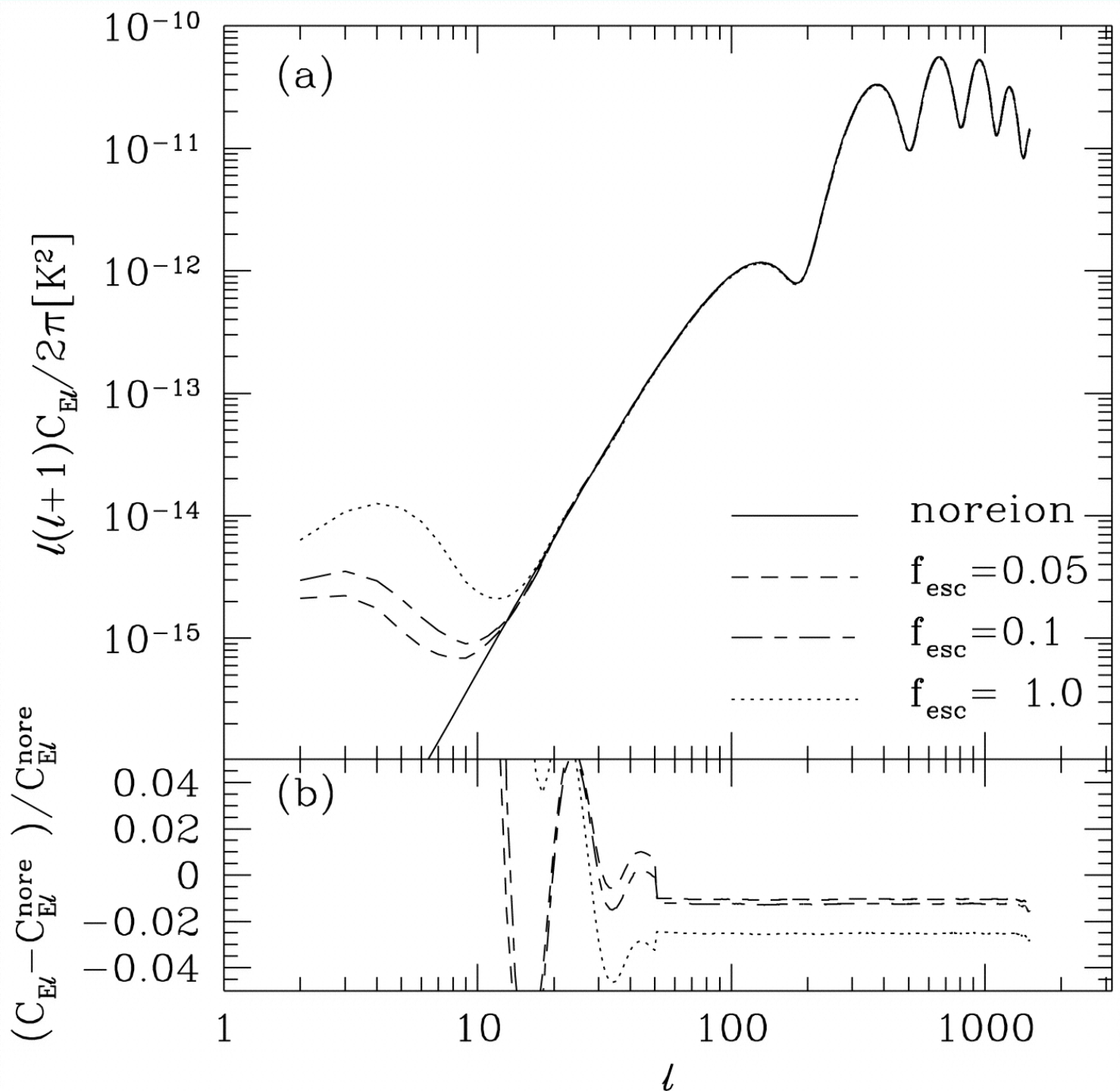

Modification of the E-mode power spectrum by reionization. (a) reionization histories with Ω_b = 0.02 and different escape fractions f_{esc}, corresponding to optical depths due to reionization τ = 0.014, 0.017, and 0.034, (*b*) The fractional change in these power spectra relative to the model with no reionization: boost on large scales and supression on small scales (Liu, G. et al. 2001)

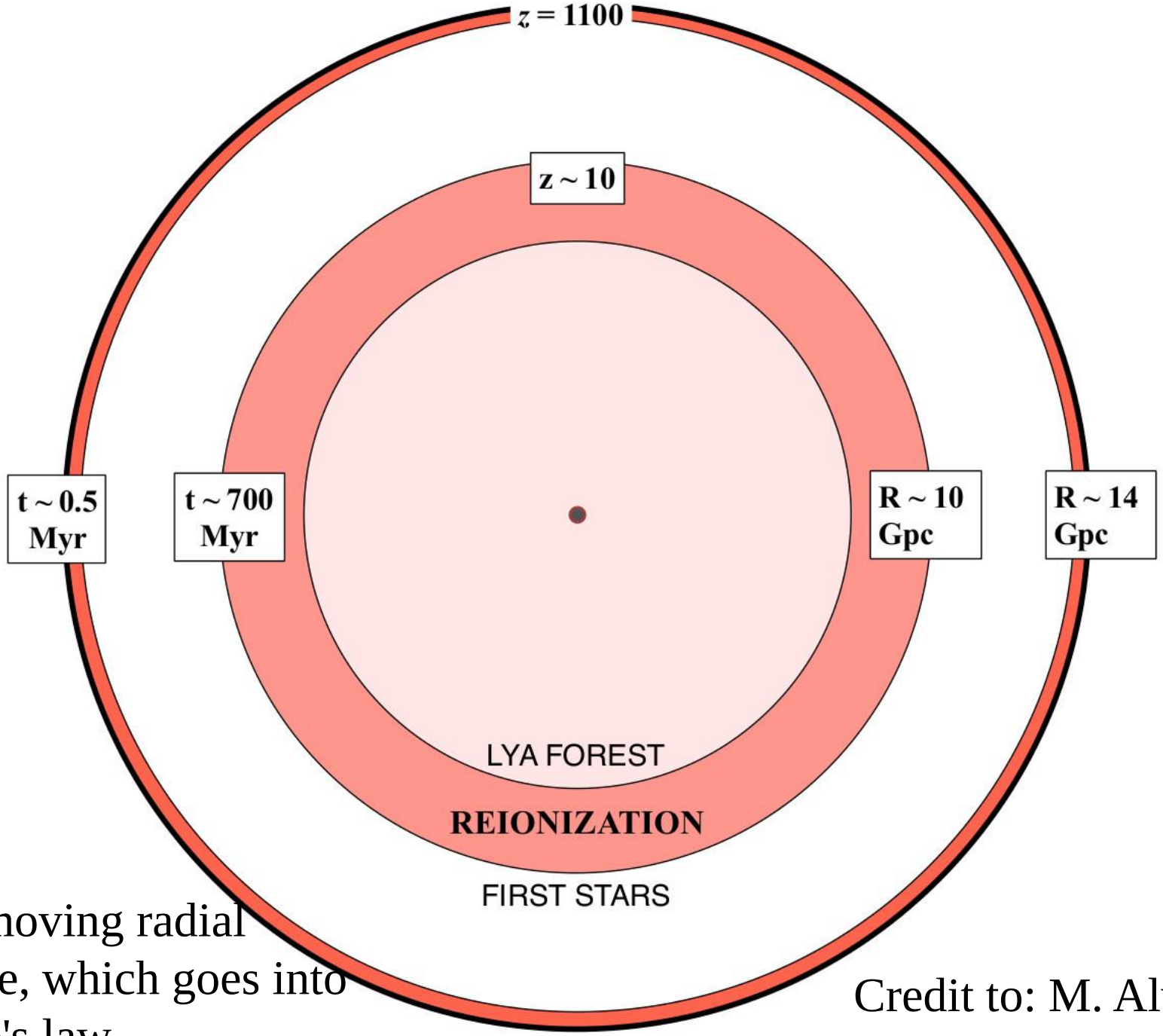

R= comoving radial distance, which goes into Hubble's law.

Credit to: M. Alvarez

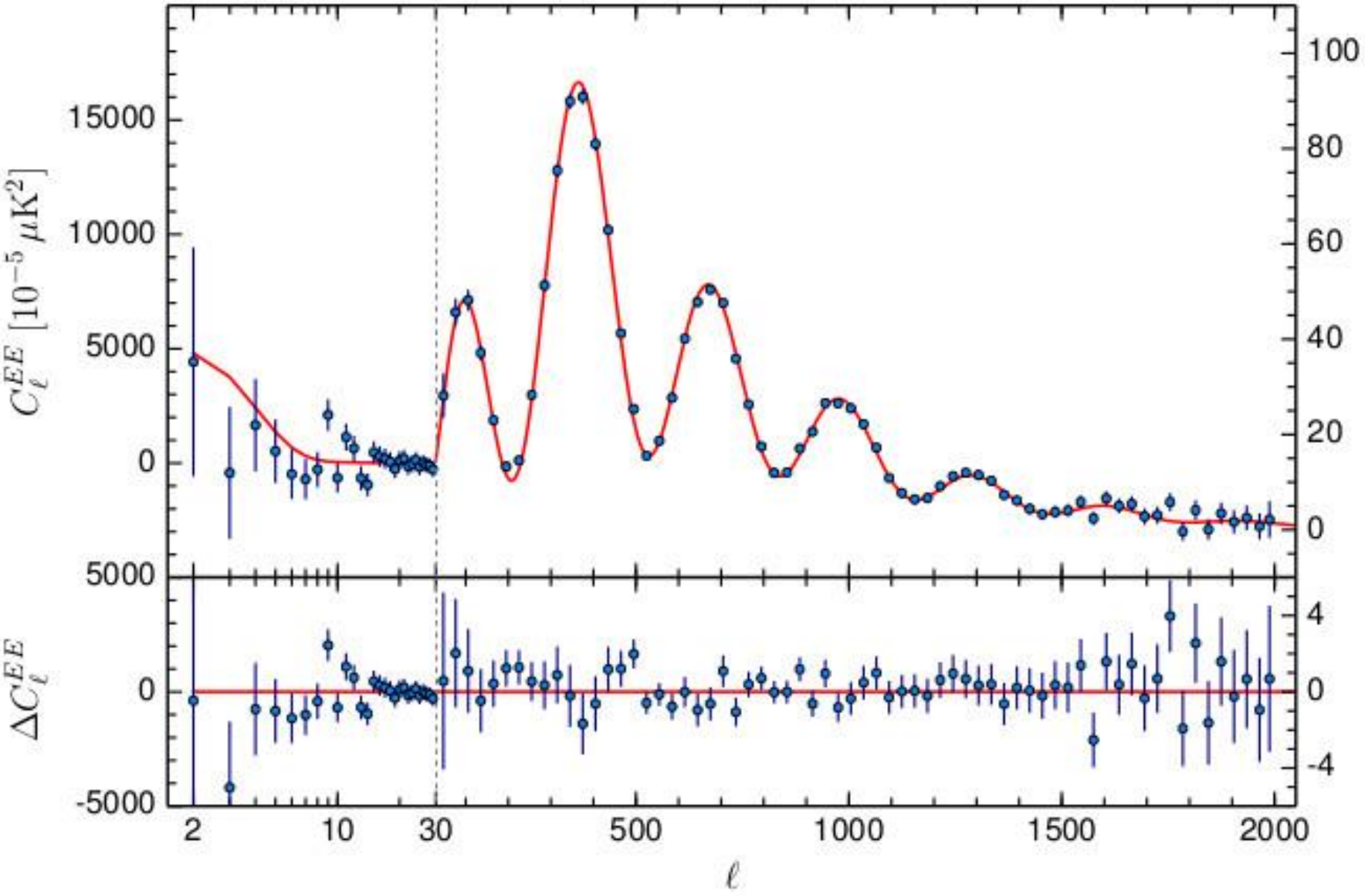

Planck Collaboration XI (2016)

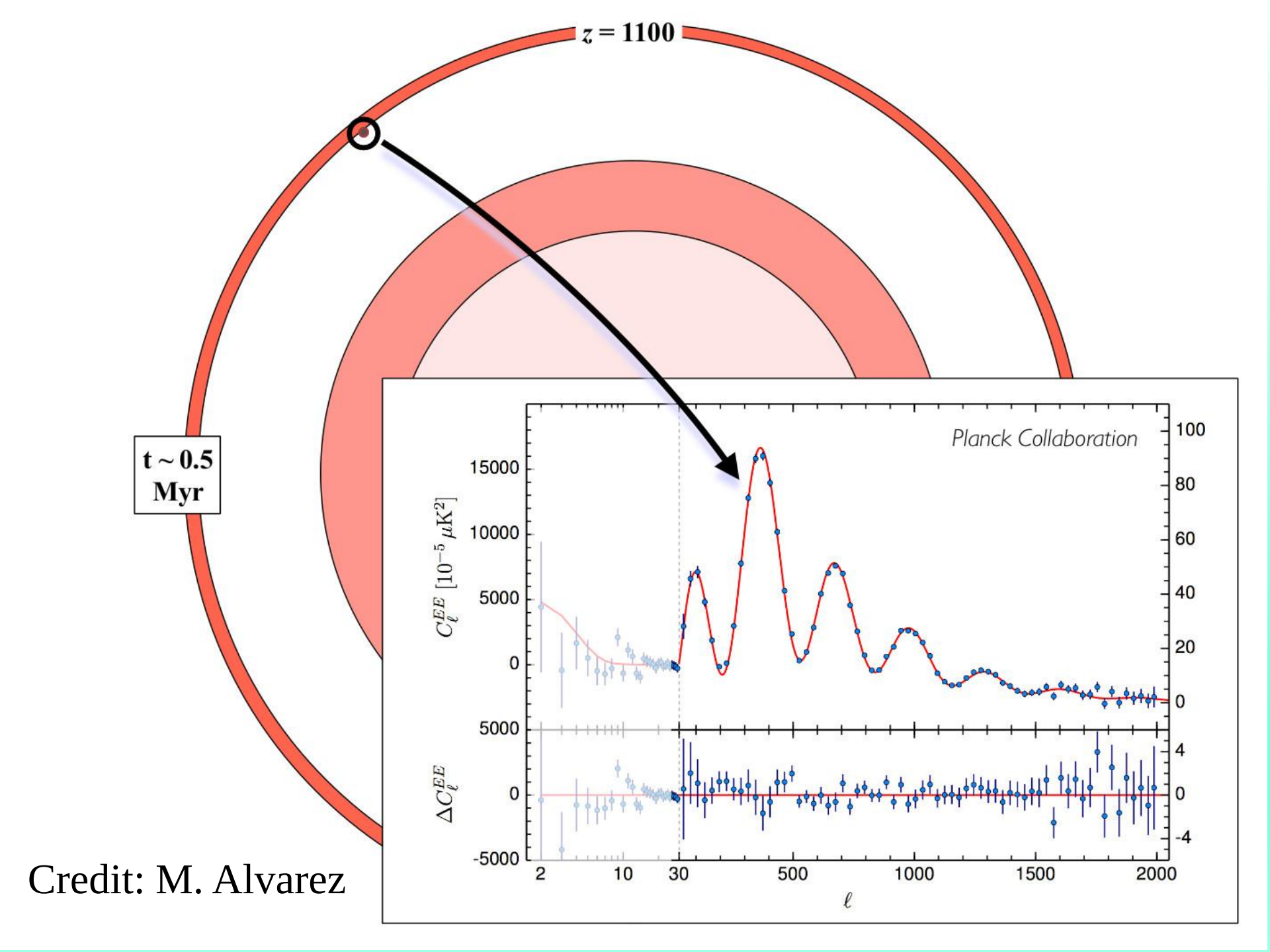

Credit: M. Alvarez

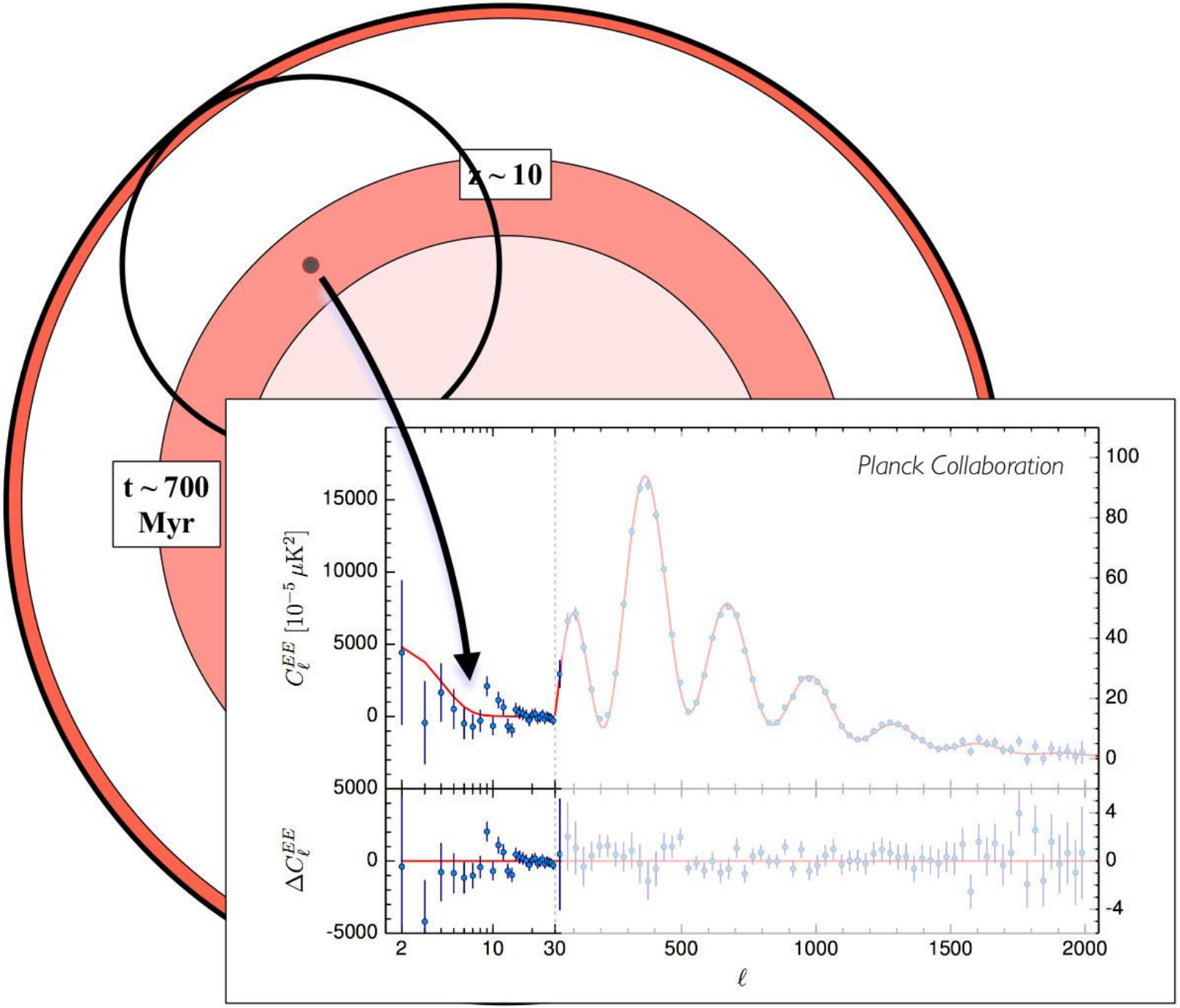
z ~ 10
t ~ 700 Myr
Planck Collaboration
C_ℓ^{EE} [10^{-5} μK^2]
ΔC_ℓ^{EE}
15000
10000
5000
0
5000
0
-5000
100
80
60
40
20
0
4
0
-4
2
10
30
500
1000
1500
2000
ℓ

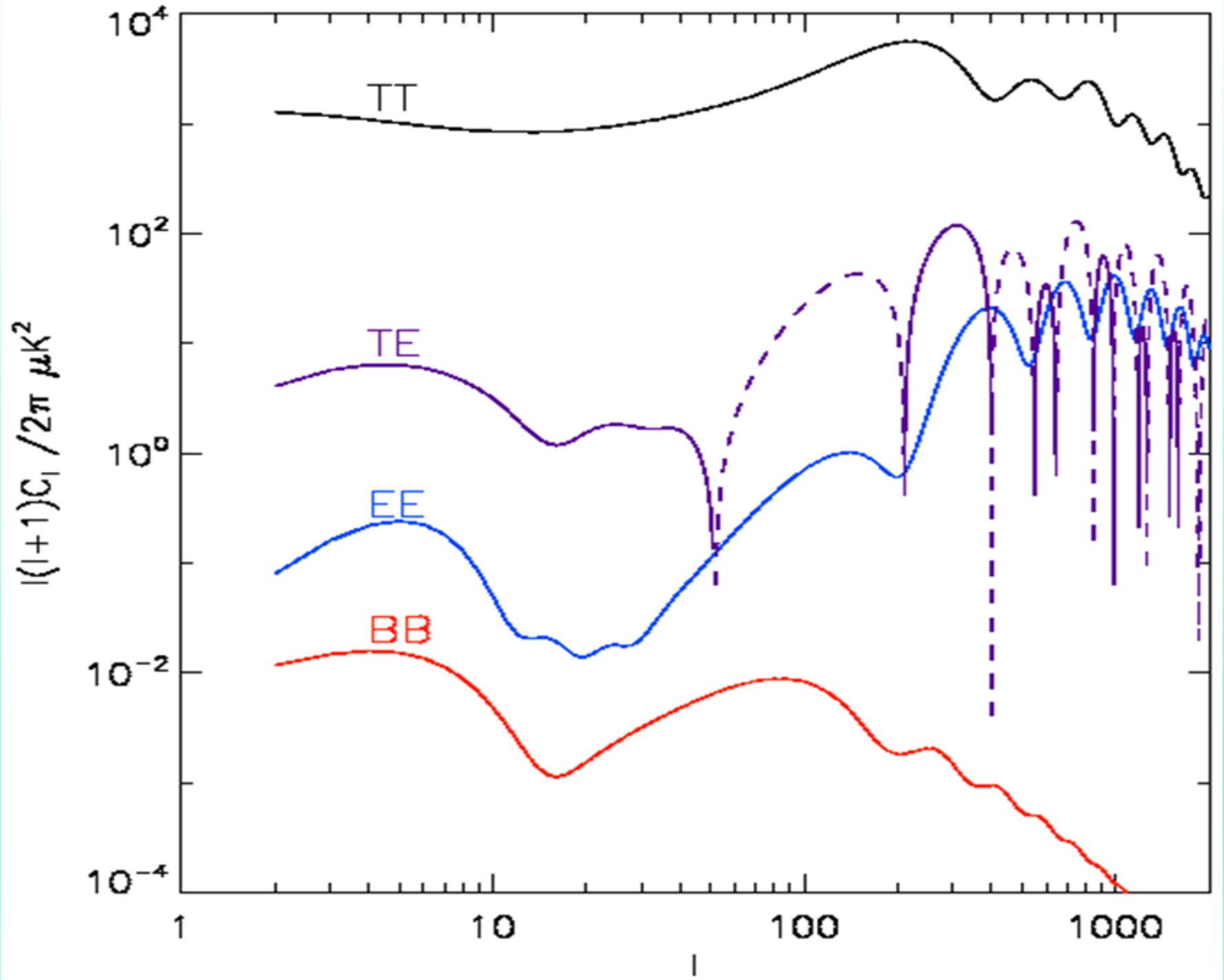
TT
TE
EE
BB
10^4
10^2
10^0
10^{-2}
10^{-4}
$l(l+1)C_l/2\pi\ \mu K^2$
1
10
100
1000
l

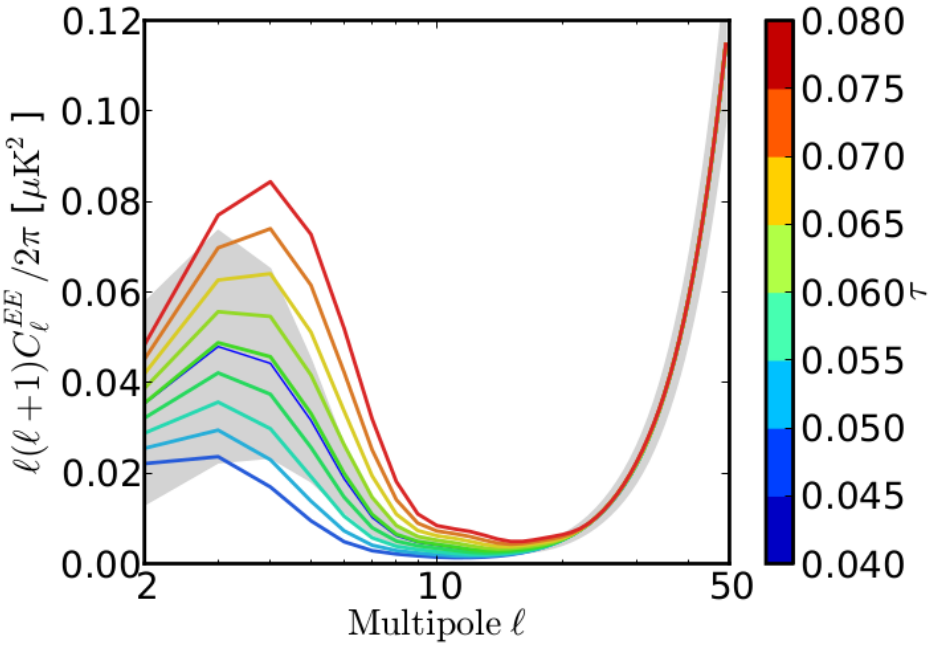

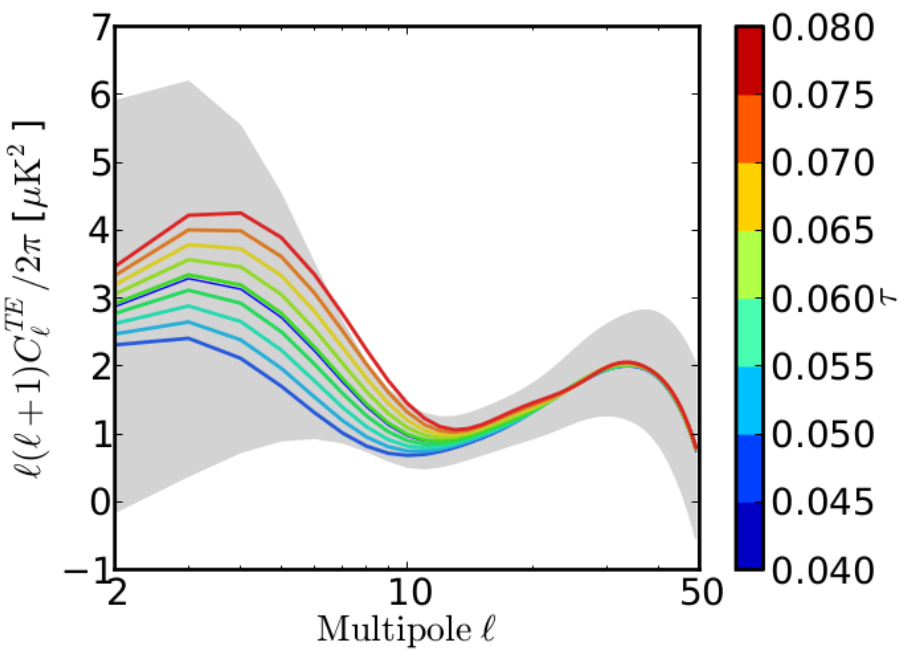

Zoom-in EE and TE power spectra for various τ values ranging from 0.04 to 0.08. Grey bands represent the cosmic variance (full-sky) associated with the $\tau = 0.06$ model. The low-l EE power spectrum dominate the constraints compared to the TE power spectrum. This is because of the relatively larger cosmic variance for TE (arising from the temperature term) and the intrinsically weaker dependence on τ ($\propto\tau$ compared with $\propto\tau^2$ for EE), as well as the fact that there is only partial correlation between T and E (Planck Int. XLVII 2016)

Cosmic variance - 1

If anisotropies are Gaussian, the estimates of C_ℓ have a χ^2 distribution with $2\ell + 1$ degrees of freedom and variance (Knox 1995)

$$(\Delta C_\ell)^2 = \frac{2}{2\ell + 1} C_\ell^2.$$

The factor $2\ell + 1$ follows from the fact that this is the number of m-samples of the power in each multipole moment, and the factor of 2 in the numerator is because the variance of a χ^2-distributed variable is twice the expectation number.

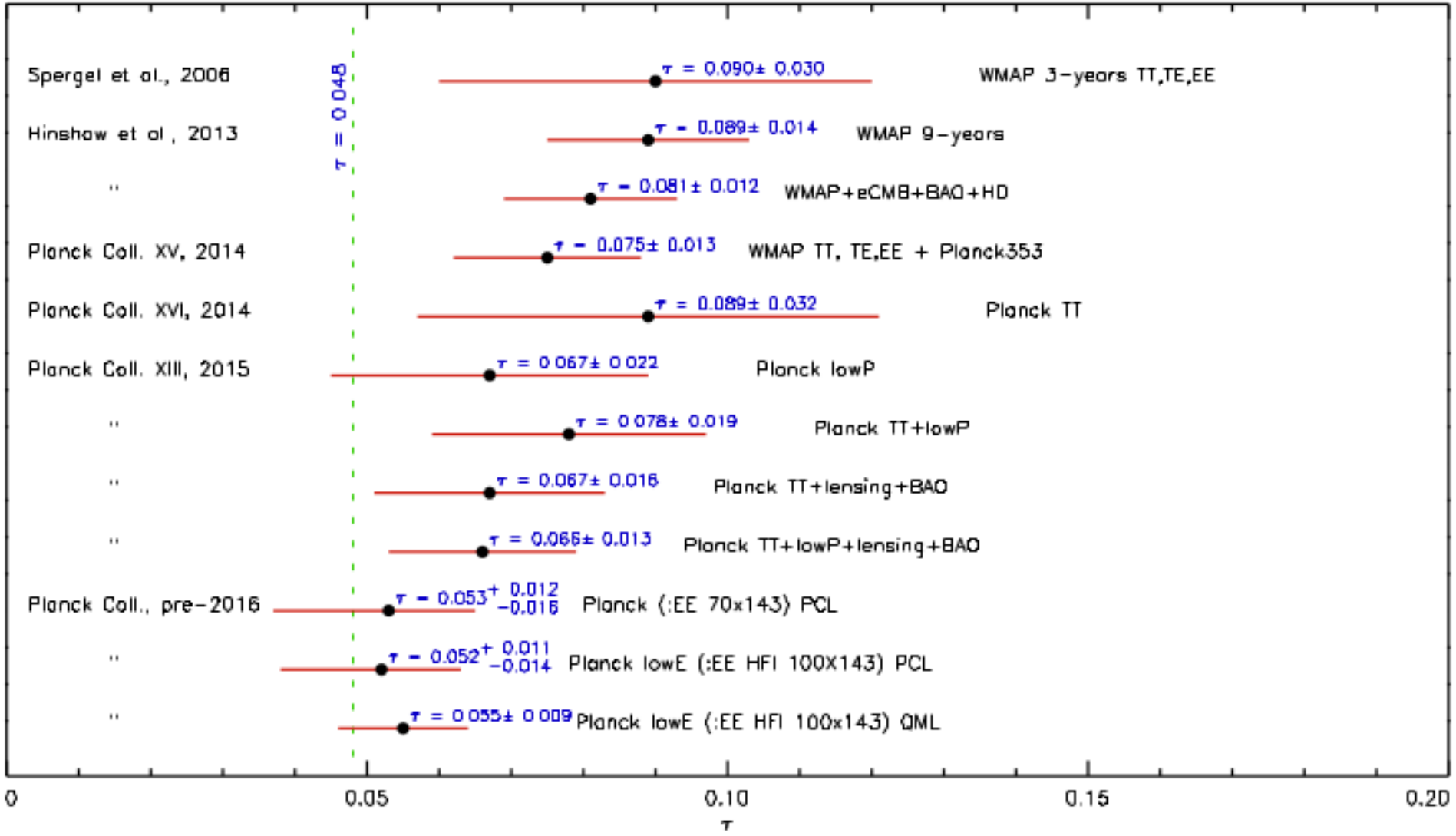

Fig. 41. History of τ determination with WMAP and *Planck*. We have omitted the first WMAP determination ($\tau = 0.17 \pm 0.04$, Bennett et al. 2003), which was based on TE alone.

Planck intermediate results. XLVI (2016). Latest Planck result: $\tau = 0.055 \pm 0.009$

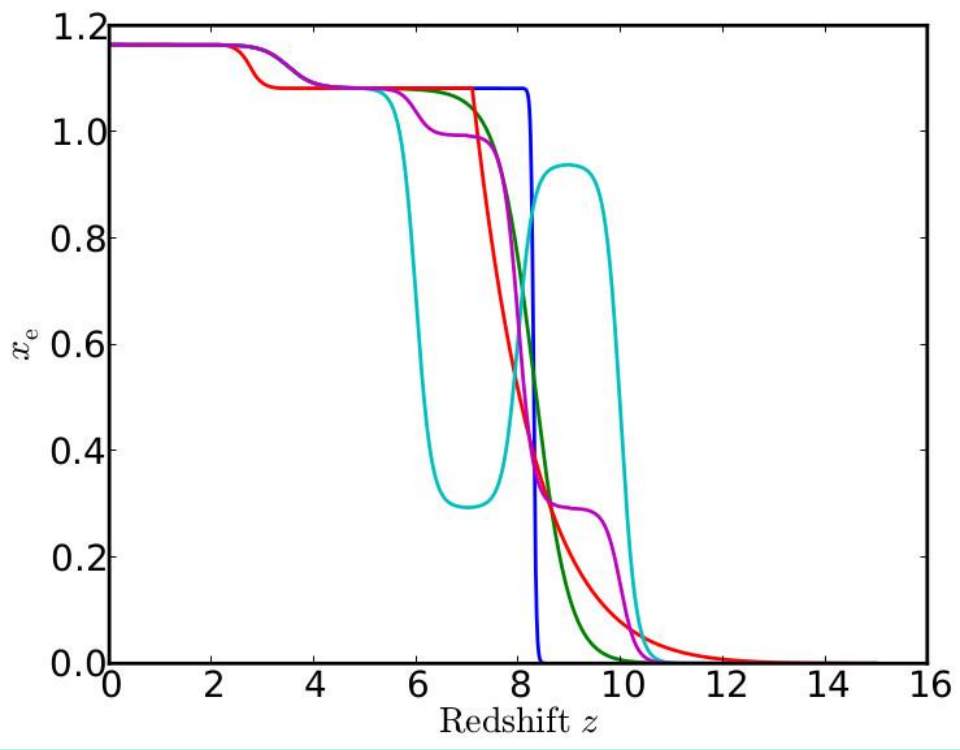

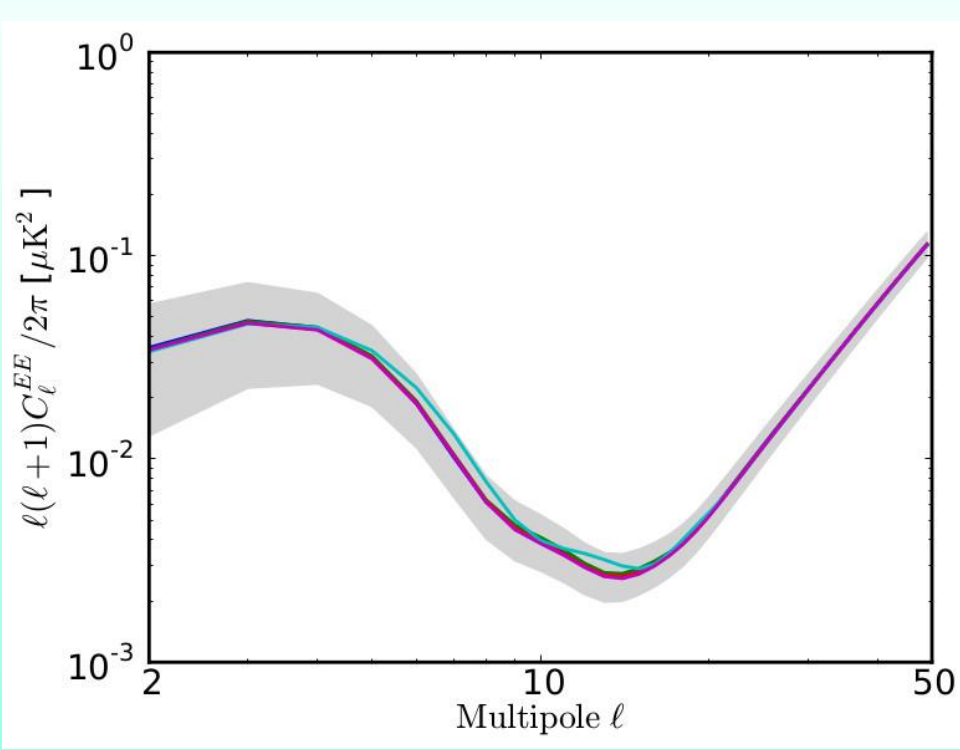

Left: Examples of evolution of the ionization fraction, all having the same optical depth, τ=0.06: green and blue are for redshift-symmetric instantaneous (δz = 0.05) and extended reionization (δz = 0.7), respectively; red is an example of a redshift asymmetric parameterization; and light blue and magenta are examples of an x_e defined in redshift bins. Right: corresponding EE power spectra with cosmic variance in grey. All models are essentially indistinguishable at the reionization bump scale. From`Planck Int. XLVII (2016).

Constraints on x_{HI} from the kinetic SZ effect - 1

- The “kinetic Sunyaev Zeldovich” or kSZ effect is due to Thomson scattering of CMB photons off free electrons moving with bulk velocity.
- It is common to distinguish between the “homogeneous” kSZ effect, arising when the reionization is complete (e.g., Ostriker & Vishniac 1986), and “patchy” (or inhomogeneous) reionization (e.g., Aghanim et al. 1996), which arises during the process of reionization, from the proper motion of ionized bubbles around emitting sources.
- These two components can be described by their power spectra, which can be computed analytically or derived from numerical simulations.

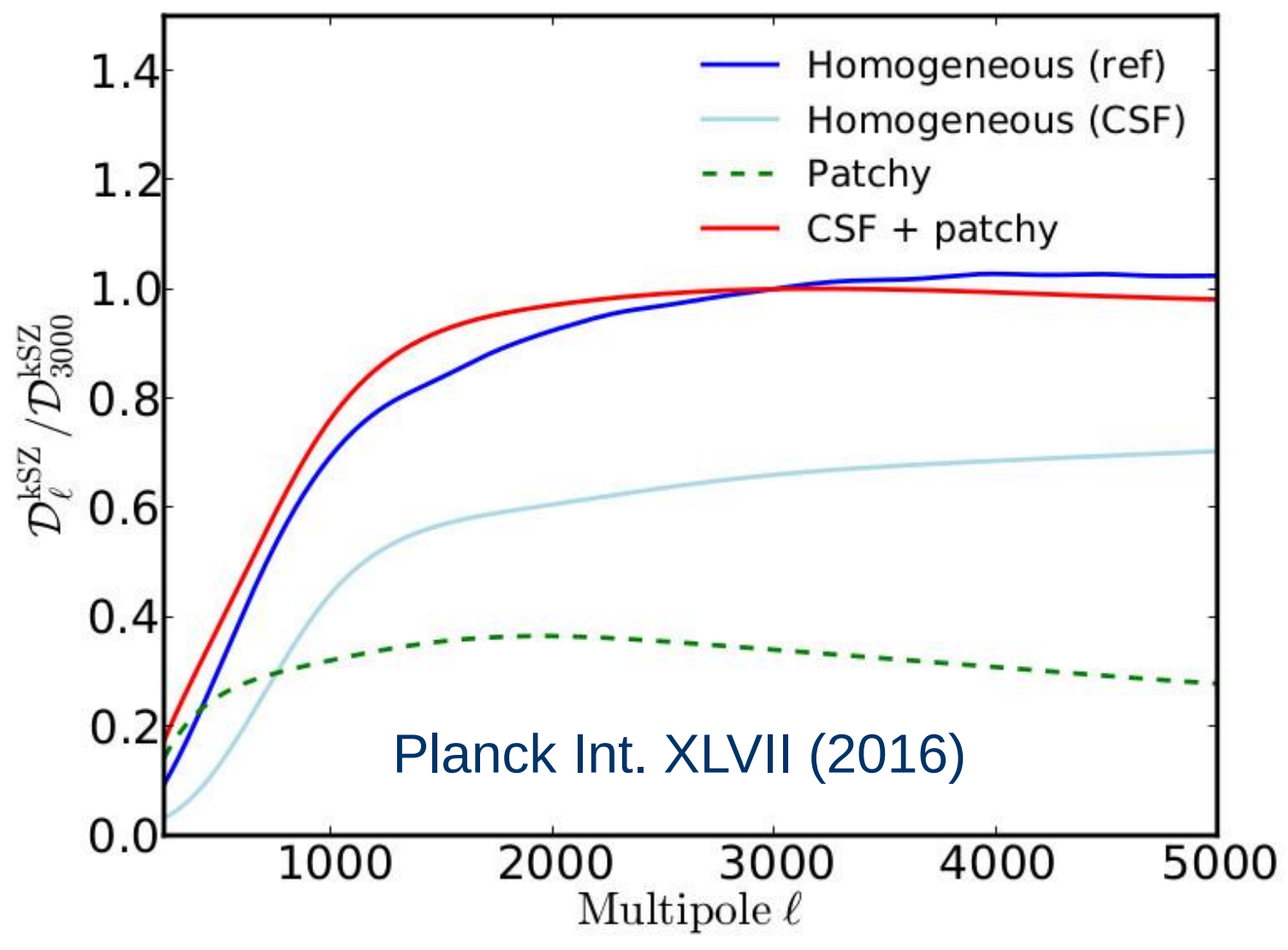

Power spectrum templates for the kSZ effect normalized to ℓ=3000. Homogeneous reionization based on Trac et al. (2011); model including the effects of cooling and star formation (CSF) from Shaw et al. (2012); patchy reionization model from Battaglia et al. (2013); and sum of CSF and patchy.

The simulations by Alvarez (2016) show that angular power spectrum generally exhibits two main features, a broad peak at $\ell \sim 20 - 30$ with an amplitude $\sim 10 - 30 \mu K^2$, and a small-scale plateau at $\ell \gtrsim 300$, with an amplitude of $\sim 1 - 5 \mu K^2$. The low–ℓ peak is caused by the so-called "Doppler-effect", arising from longitudinal modes in the velocity field $v_{\parallel} = (\mathbf{v} \cdot \hat{\mathbf{k}})$, while the broad plateau at higher multipoles is a superposition of transverse momentum correlations seeded by patchy ionization and density fluctuations, $x\mathbf{v}$ and $\delta\mathbf{v}$, respectively.

For reionization driven by UV sources located in relatively rare dark matter halos – the scenario favoured by existing data – the patchiness of reionization is 'seeded' by large scale velocity modes, and the amount of small scale power is dependent mainly on the duration and redshift of reionization, such that more extended reionization histories lead to larger fluctuations at $\ell \sim 3000$ at fixed τ.

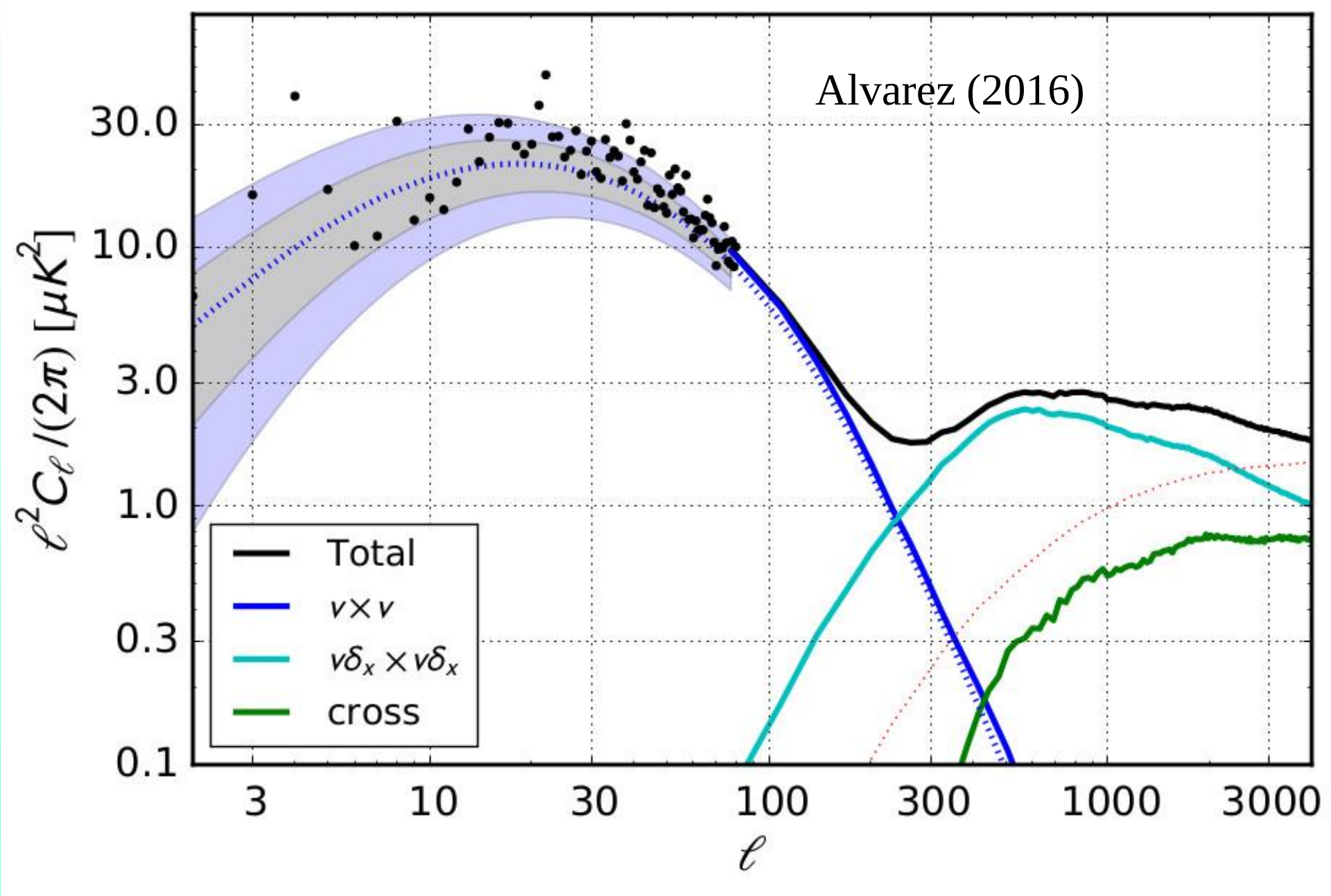
Alvarez (2016)
30.0
10.0
3.0
1.0
0.3
0.1
$\ell^2 C_\ell / (2\pi)\ [\mu K^2]$
Total
$v \times v$
$v\delta_x \times v\delta_x$
cross
3
10
30
100
300
1000
3000
ℓ

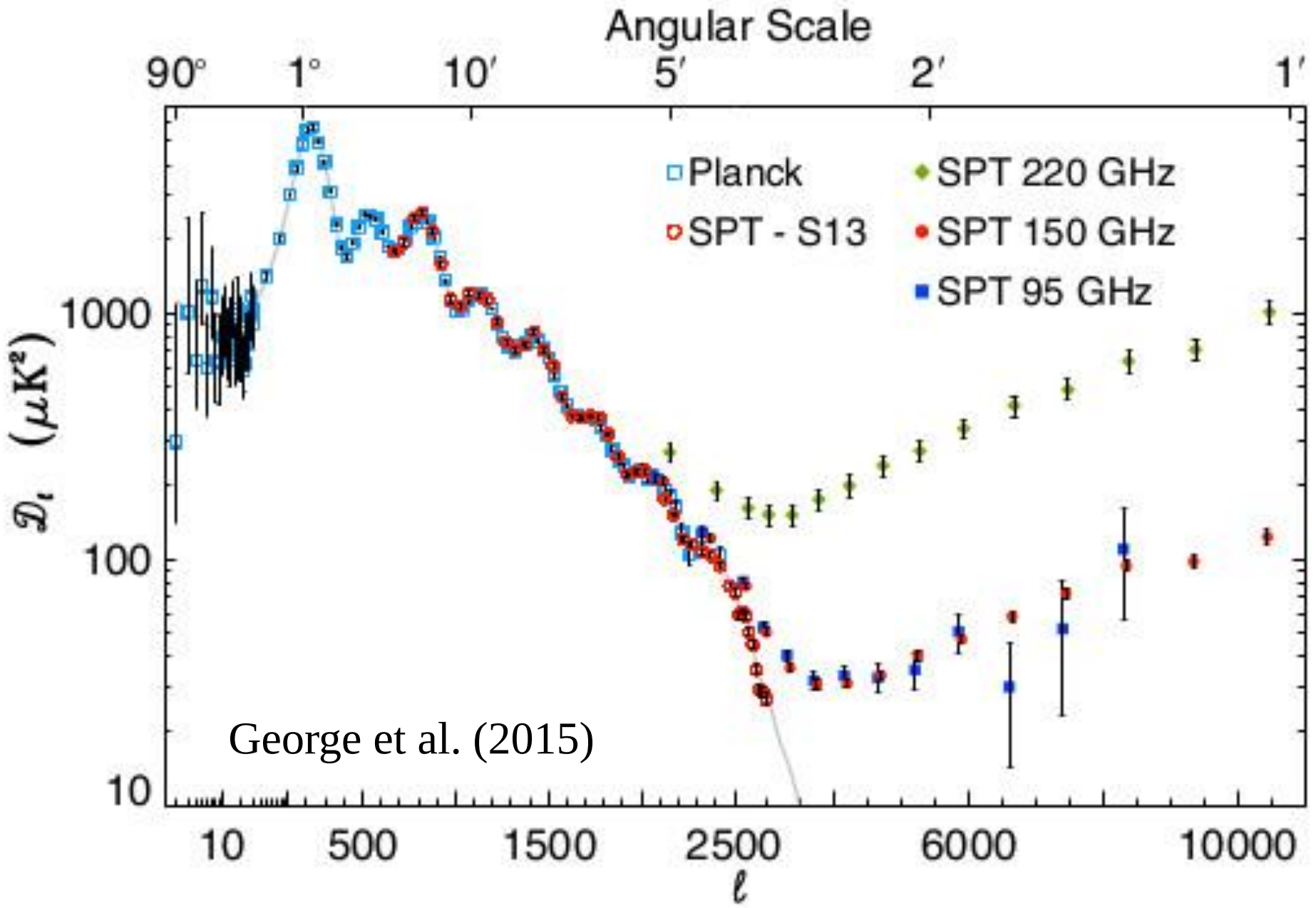

George et al. (2015)

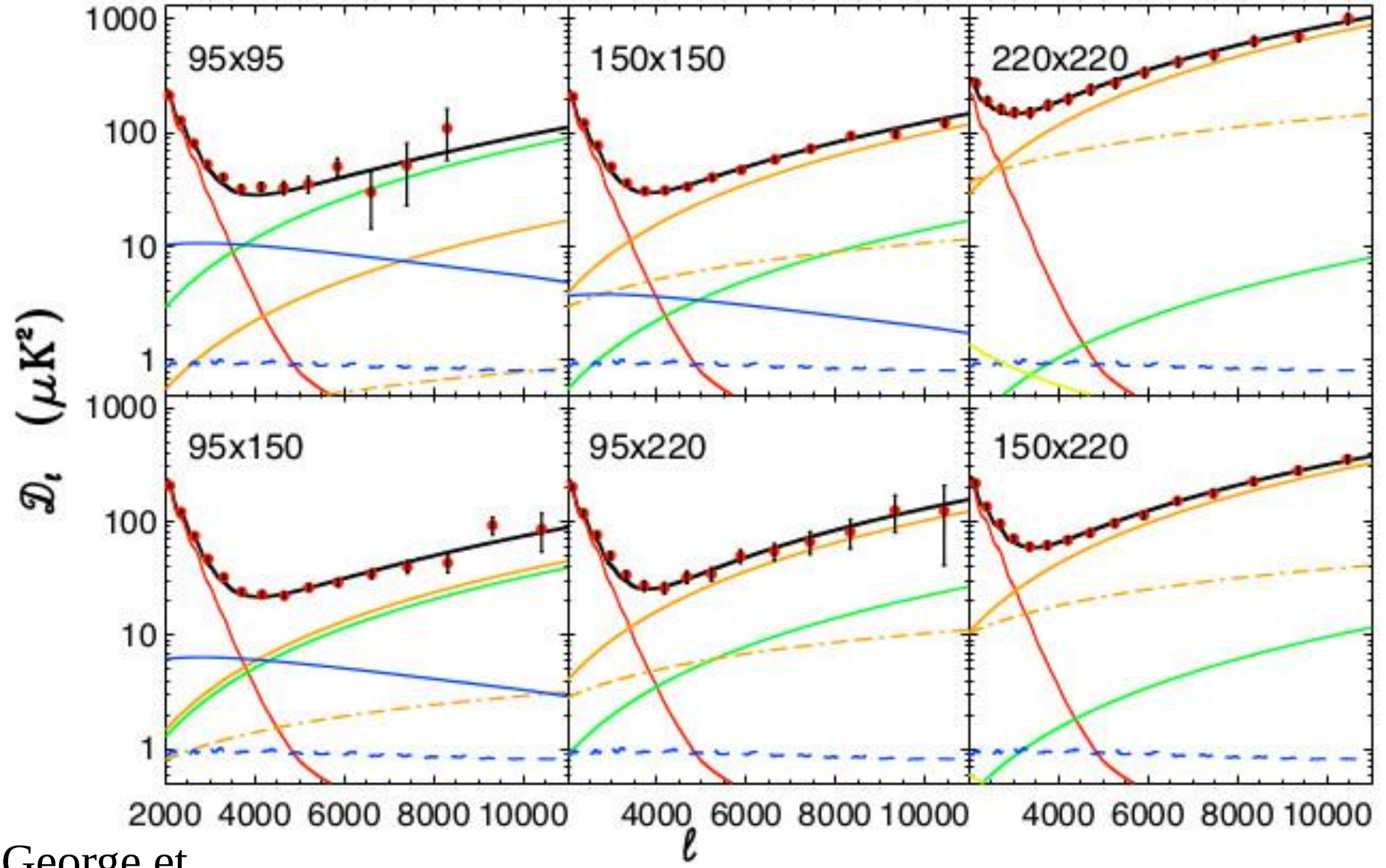

George et al. (2015)

$D^{kSZ}_{3000} = 2.9 \pm 1.3\,\mu K^2$, detection significant at the 98.1% confidence.

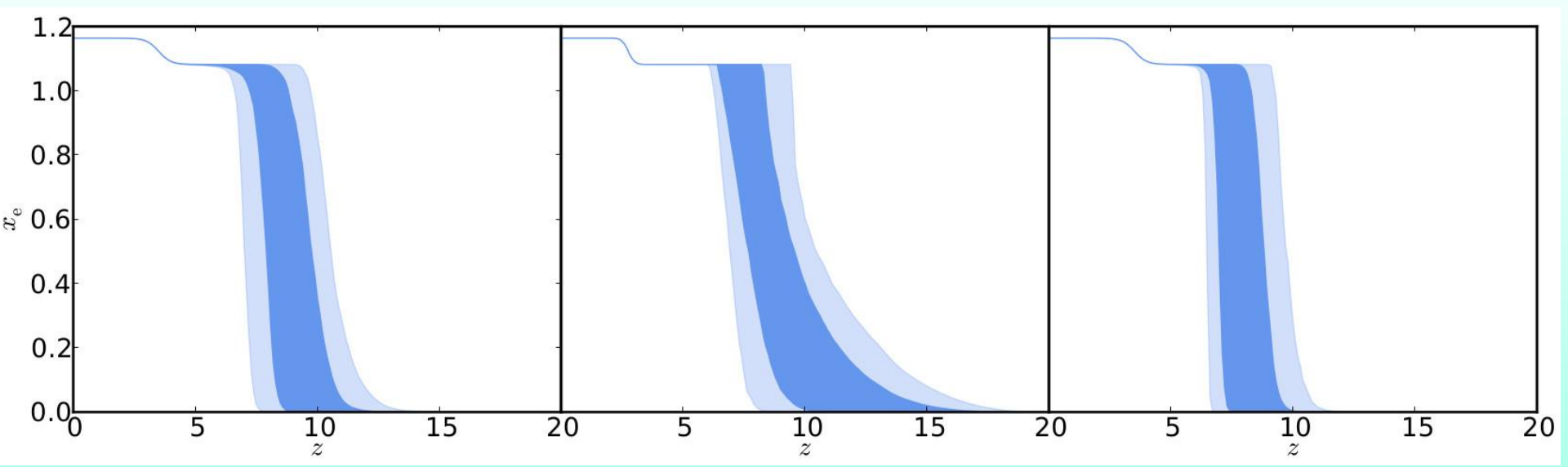

CMB constraints on ionization fraction during reionization. The allowed models, in terms of z_{re} and δz translate into an allowed region in $x_e(z)$ (68% and 95% in dark blue and light blue, respectively), including the $z_{end} > 6$ prior. Left: Constraints from CMB data using a redshift-symmetric function ($x_e(z)$ as a hyperbolic tangent with $\delta z=0.5$). Centre: Constraints from CMB data using a redshift-asymmetric parameterization ($x_e(z)$ as a power law). Right: Constraints from CMB data using a redshift-symmetric parameterization with additional constraints from the kSZ effect.

The step at z~3 corresponds to the He complete ionization.

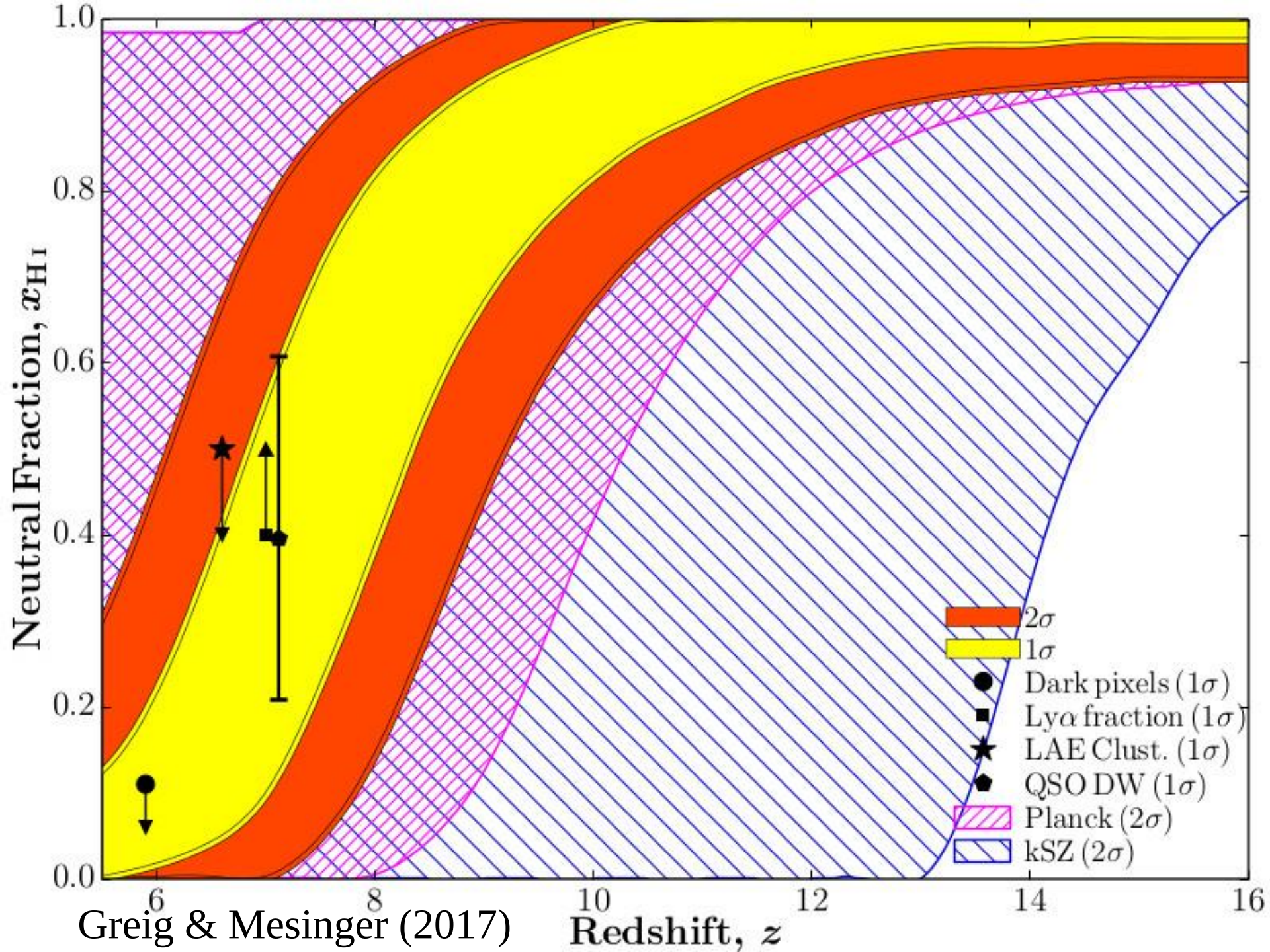

Greig & Mesinger (2017)

Reionization and 21cm HI line - 1

- A complementary view of the re-ionization history is provided by measurements of the 21 cm line, corresponding to the ground-state hyperfine transition of atomic H.
- In principle, the 21-cm signal provides a tomographic image of reionization because signals from different redshifts show up at different frequencies.

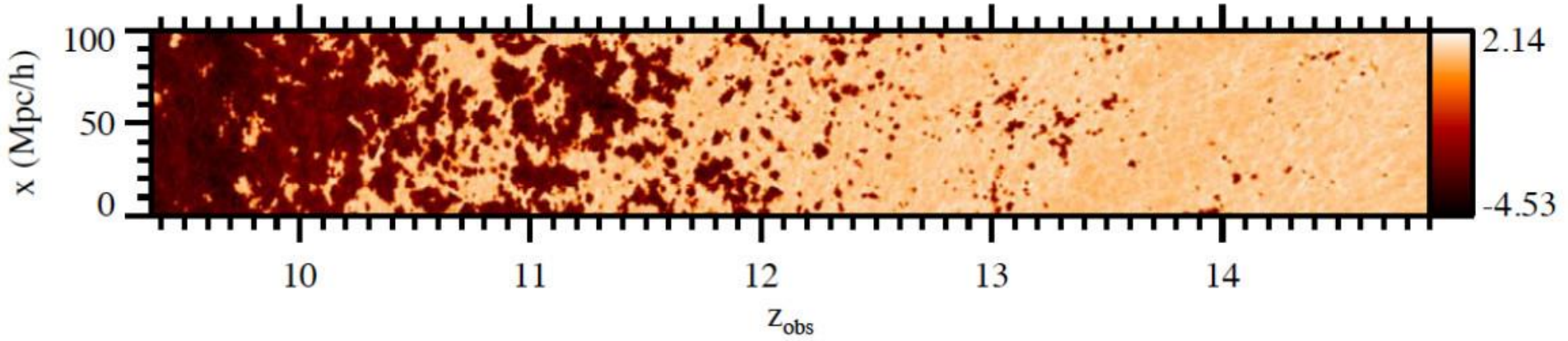

Image of a 100-Mpc h^{-1} radiative transfer simulation of reionization. Shown is a slice through the 21-cm emission signal on the light cone (showing $\log_{10}$ of the brightness temperature). Darker regions are ionized and brighter ones are neutral. From McQuinn (2016)

Reionization and 21cm HI line - 2

- However the current generation of instruments does not have the sensitivity to make images, and we must hope instead to achieve statistical detections of the signal.
- There is a worldwide effort to detect the 21-cm signal using both specialized and multipurpose interferometers, such as the Giant Metrewave Radio Telescope (GMRT) in India, the Mileura Widefield Array (MWA) in Australia, the Precision Array to Probe Epoch of Reionization (PAPER) in South Africa, the Low Frequency Array (LOFAR) primarily in the Netherlands, the Experiment to Detect the Global EoR Step (EDGES) and the 21-cm Array in China.
- Planning underway for the next-generation Hydrogen Epoch of Reionization Array (HERA) instrument and the Square Kilometre Array (SKA)-low.

Reionization and 21cm HI line - 3

The evolution of the ionized fraction $x_e(z)$ from zero to one should produce a soft (~20 mK) `step' in the spectrum as a function of frequency towards the end of the EoR. While the global step (e.g., Shaver et al 1999, Bowman et al. 2008) may provide a mean redshift of reionization and constrain the very high redshift spin temperature evolution (Pritchard & Loeb 2008), observations of the 21-cm fluctuations (which are comparable in amplitude to the mean signal) have the potential to unravel the processes behind the EoR.

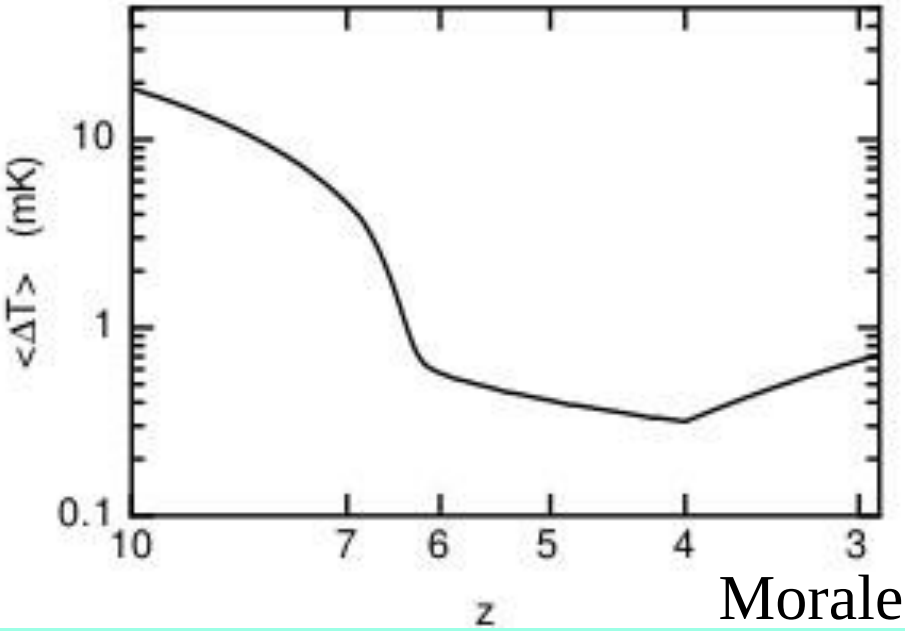

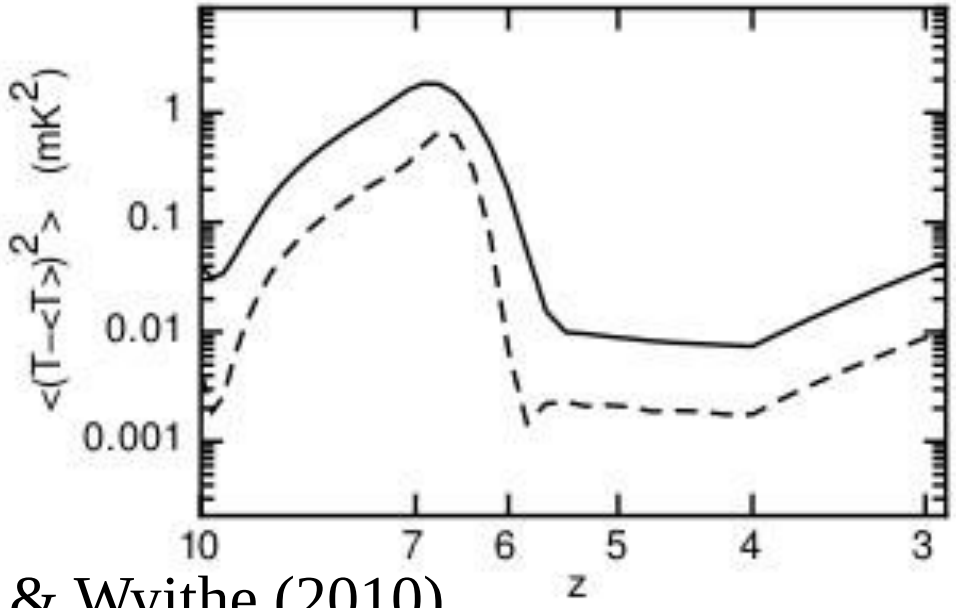
<(T−<T>)^2> (mK^2)
1
0.1
0.01
0.001
10
7
6
5
4
3
z

Morales & Wyithe (2010)

Reionization and 21cm HI line - 4

- The challenges associated with detecting the redshifted 21-cm signal are daunting. The foregrounds scale roughly in brightness temperature as $T_b \sim 500[(1 + z)/10]^{2.7}$ K (McQuinn 2016), i.e. are over 4 orders of magnitude brighter than the 21-cm signal.
- Fortunately, all appreciable foregrounds (synchrotron and bremsstrahlung) are smooth in frequency, in contrast to the 21-cm signal, allowing the foregrounds to be separated (Petrovic & Oh 2011).
- Realizing this separation with a real instrument is the largest challenge. Integration times of hundreds of hours are required to reach sensitivity to the signal in standard reionization models (Morales 2005, McQuinn et al. 2006, Parsons et al. 2012, Beardsley et al. 2013).

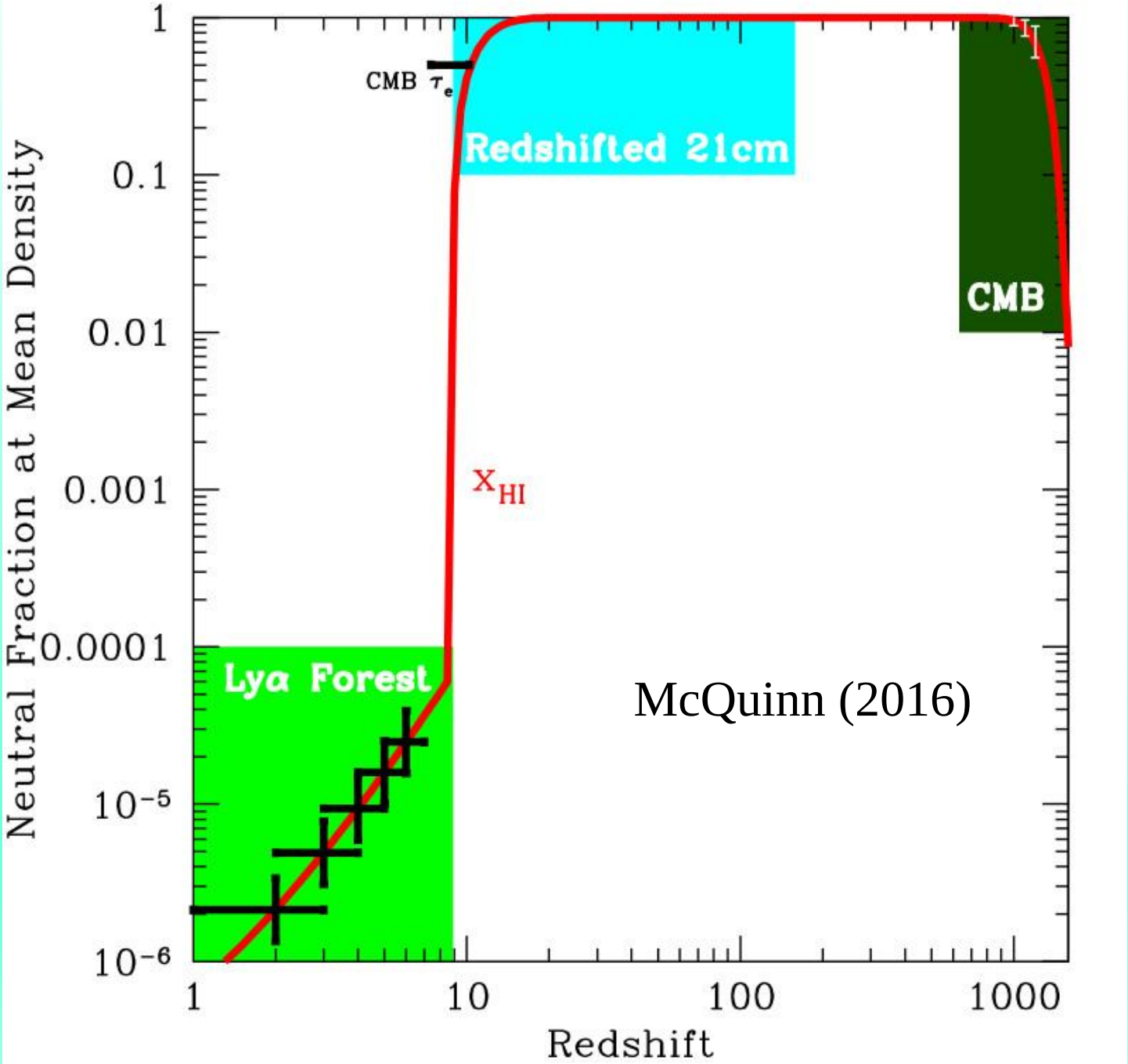

McQuinn (2016)

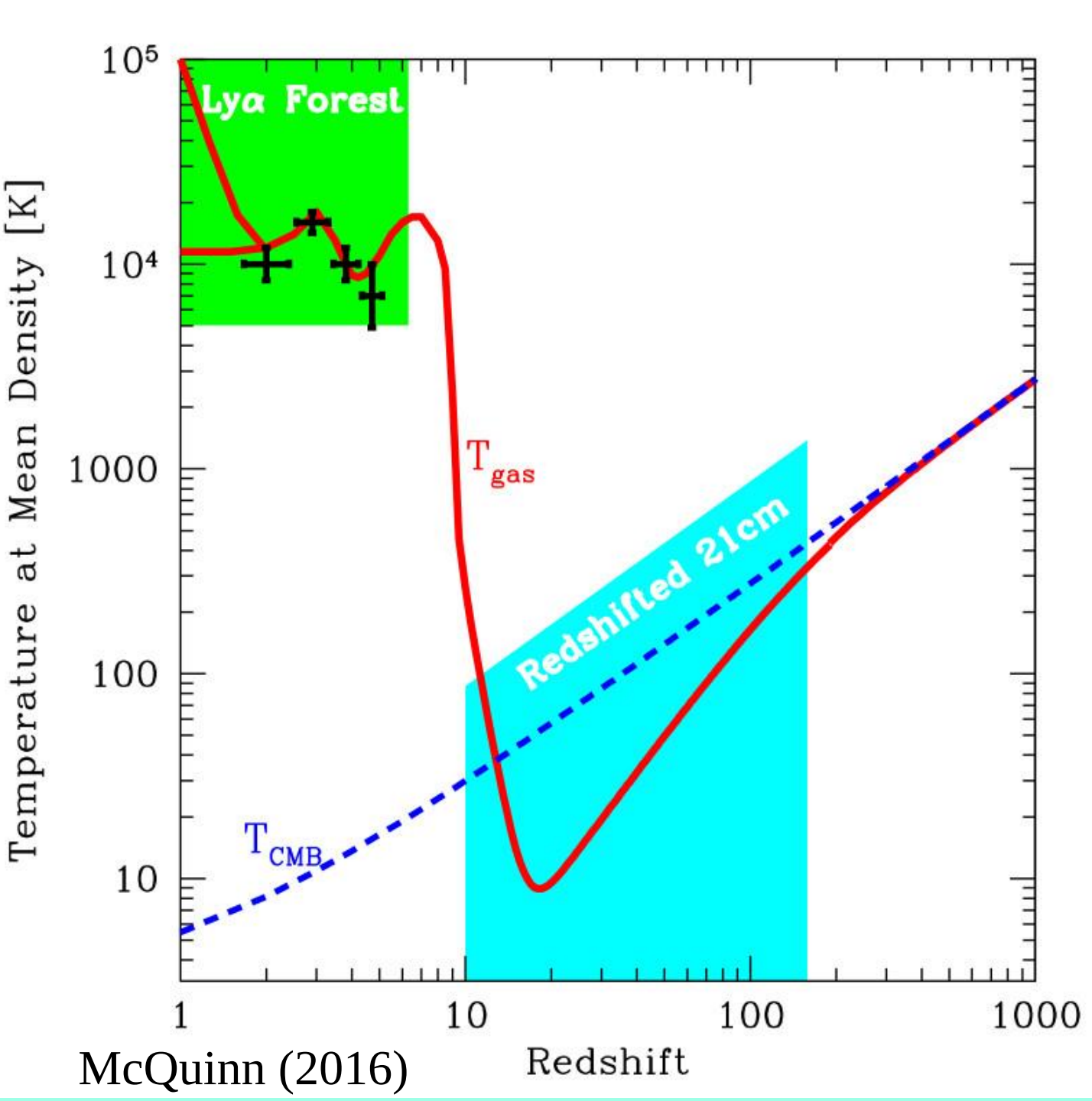

McQuinn (2016)

Thermal history of the IGM. The red curve show a model. The highlighted regions illustrate the potential purview of the named cosmological probe. The model curve bifurcates at low redshifts to indicate the IGM temperature becoming multiphase.

The EDGES detection (Bowman et al. 2018) - 1

- At redshifts z=20-30, before the epoch of cosmic dawn, i.e. before the appearance of the first stars and galaxies, the IGM was colder than the CMB, and the spin temperature of the 21 cm line of neutral hydrogen was coupled to the CMB temperature.
- Subsequently, the spin states were driven toward equilibrium with the thermal motion of the gas due to repeated scattering of Lyα photons from the first stars**.**
- This process lowers the spin temperature and leads to absorption of photons from the CMB, producing an absorption feature in the global radio background that should be observable today at radio frequencies of less than 200 MHz (Pritchard & Loeb 2012).
- Next, the emission from galaxies heats the gas leading to a 21 cm emission.

The EDGES detection - 2

- Recent results from EDGES suggest that the transition to equilibrium to the gas temperature happened at z~20 (Bowman et al. 2018).
- Surprisingly, the reported absorption profile is characterized by abrupt edges and a flattened bottom, which are not seen in any of the prior theoretical models (Cohen et al. 2017; Kaurov et al. 2018).
- The depth of the absorption feature, 0.5(+0.5, -0.2) K at 99% confidence level) is a factor of ~ 2.5 larger than the value in any of the standard models of the Cosmic Dawn.
- Attempts to explain the size of the signal include either new physics, such as interactions with dark matter (Barkana 2018; Muñoz & Loeb 2018; Fraser et al. 2018) or a low-frequency excess radio background (Feng & Holder 2018; Ewall-Wice et al. 2018).
- At the present time it is unclear whether the proposed explanations are physically possible and/or consistent with other measurements with many of the proposals already disfavored by more careful analysis.

Bowman et al. (2018)

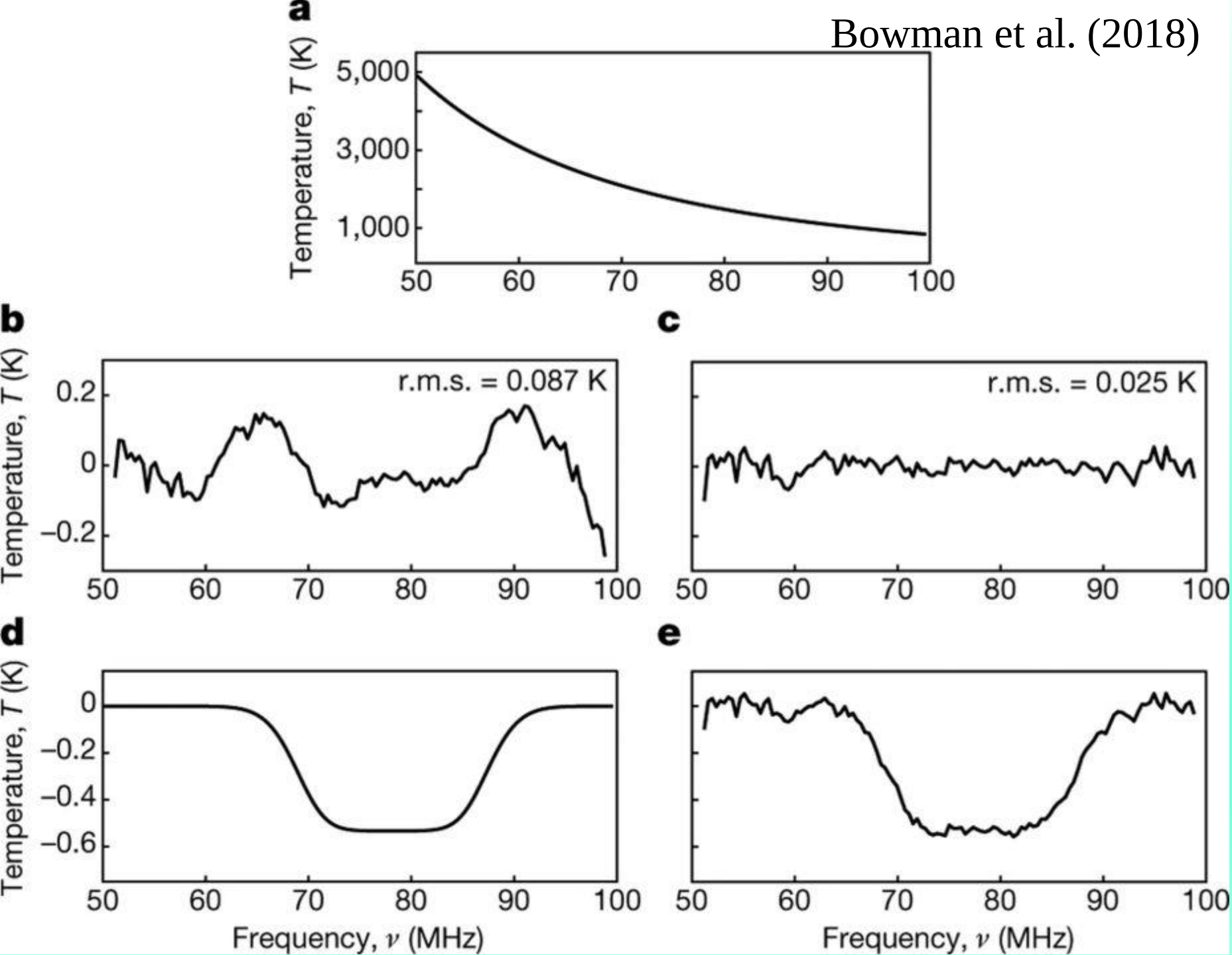

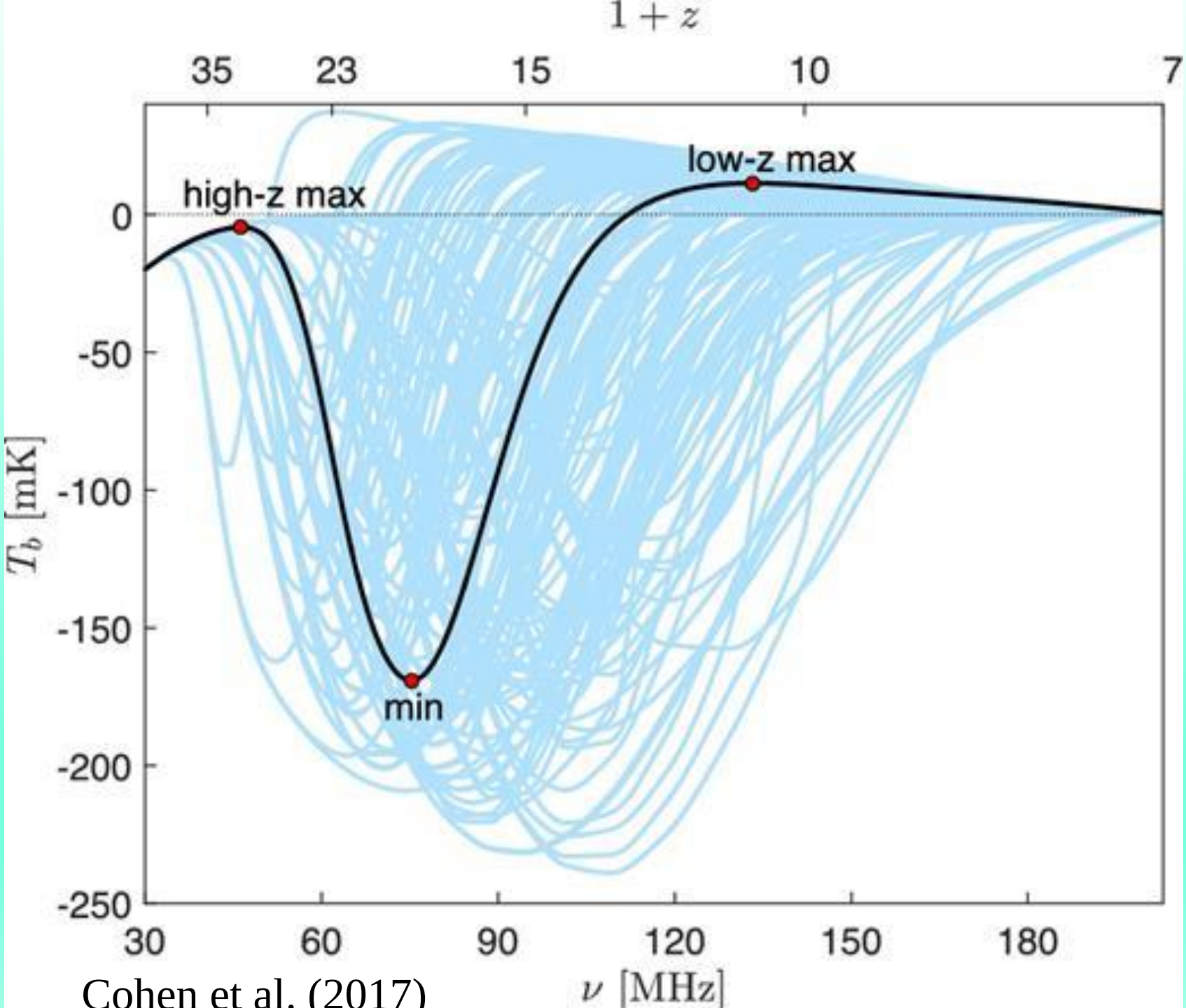

Cohen et al. (2017)

Evolution of the photo-ionization rate

The proximity (or inverse) effect - 1

- The prodigious number of absorption lines primarily due to Lyα absorption by intervening neutral hydrogen clouds along the line of sight to the QSO (Lynds, 1971; Sargent et al. 1980; Weymann et al. 1981) offer a way to investigate the intensity of the ionizing background (UVB) as a function of redshift.
- These Lyα systems appear to be in photoionization equilibrium with a background ultraviolet radiation field.
- The number of lines near the emission redshift of individual QSOs is observed to be lower than the mean value at that redshift (Carswell et al. 1982, Murdoch et al. 1986; Tytler 1987; Bajtlik et al. 1988; Lu et al. 1991; Bechtold 1994).
- This is known as the proximity or inverse effect.
- The UVB is a key probe of the sources of hydrogen ionizing photons ($E \geq 13.6$ eV) in the post-reionisation era at $z < 6$; its intensity and spectral shape provides a complete census of ionising photon production and its evolution with redshift.

The proximity (or inverse) effect - 2

- The simplest explanation for his “inverse” effect is enhanced ionization of HI in the vicinity of the QSO by ultraviolet photons from the QSO itself. Thus, the name “proximity effect” is also used. This interpretation, along with the assumptions about the spectrum of the background and the photoionization of the nearby intergalactic medium (IGM) by the QSOs, allows a measurement of the mean intensity of the ionizing background at the Lyman limit of hydrogen (Bajtlik et al. 1988), which can be compared to estimates of the integrated emission from QSOs.
- The determination of the ionizing background intensity is however not so easy.

The proximity (or inverse) effect - 4

- Analysis by Scott et al. (2000) for a sample of 99 quasars in the range $1.7 \leq z \leq 4.1$:
  - The proximity effect is present in the data, i.e. there exists a significant (5.5σ) deficit of lines at $z_{abs} \approx z_{em}$
  - Within 1.5 h^{-1} Mpc of the QSO emission redshift, the significance does depend on QSO luminosity, in accordance with the theory that this effect is caused by enhanced ionization of hydrogen in the vicinity of the QSO from UV photons from the QSO itself.

Evidence for the proximity effect (Scott et al. 2000)

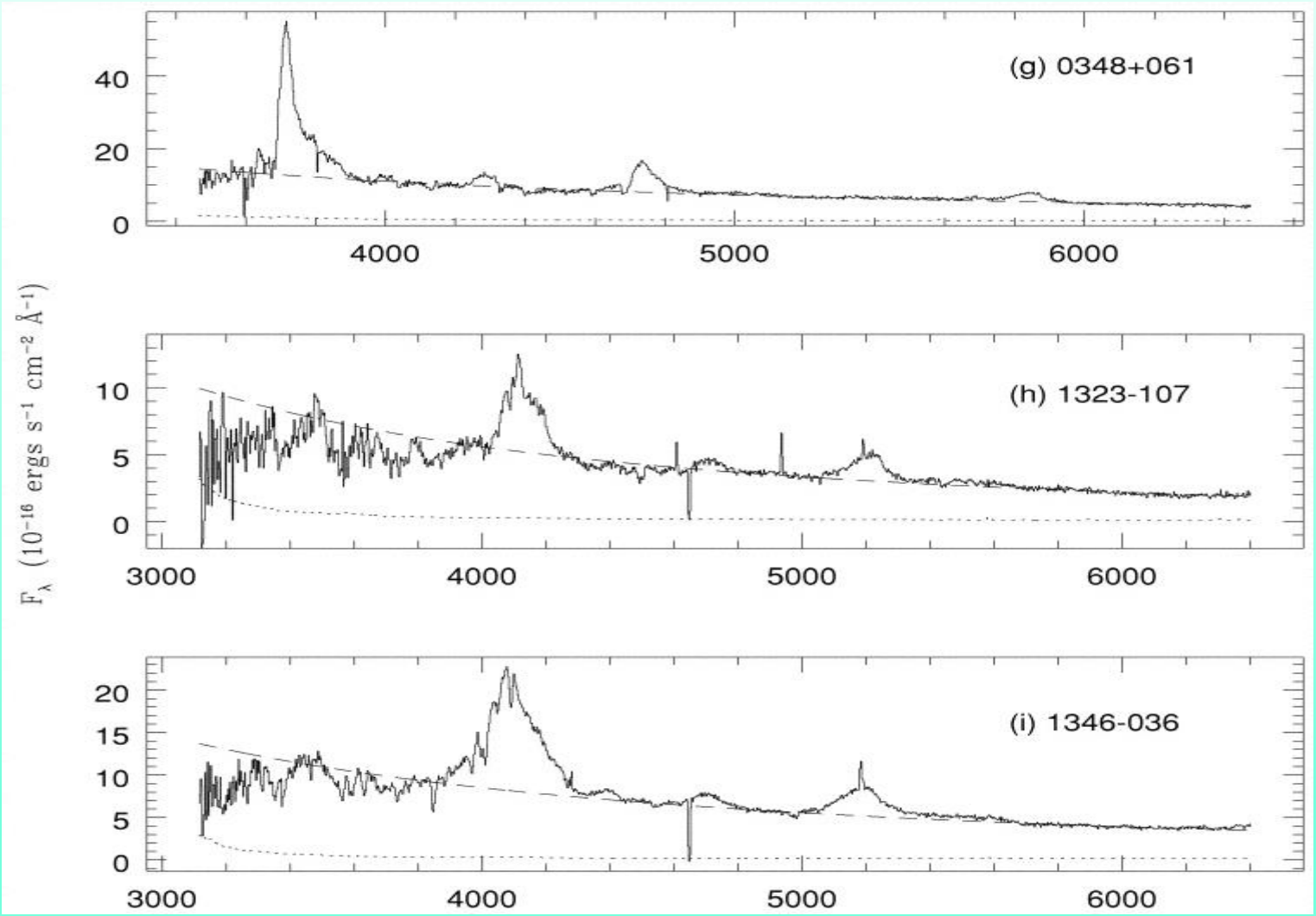

Spectrophotometry of $z \cong 2$ QSOs. Dashed line indicates the power-law continuum fit; dotted line indicates the 1σ errors.

Evidence for the proximity effect (Scott et al. 2000) -2

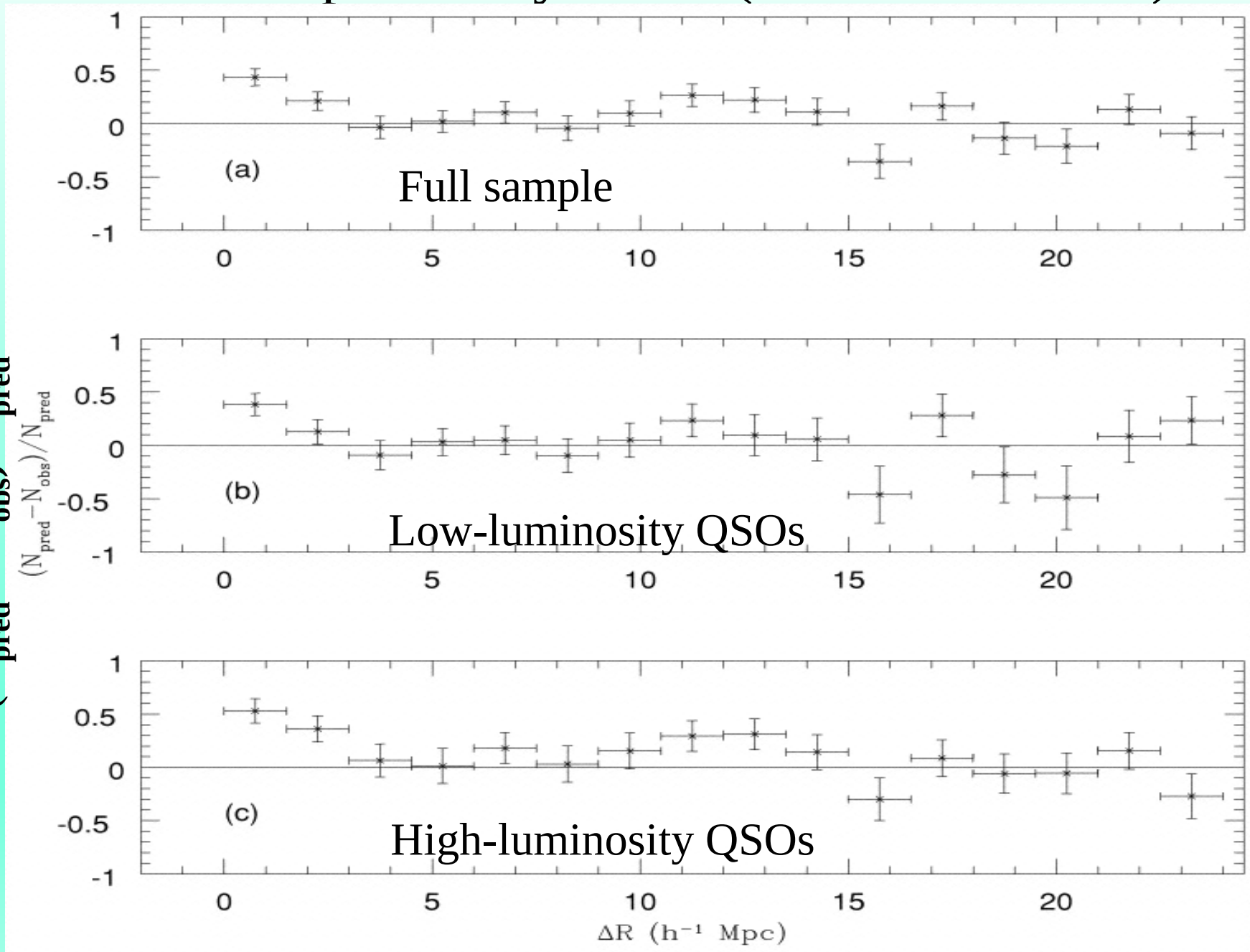

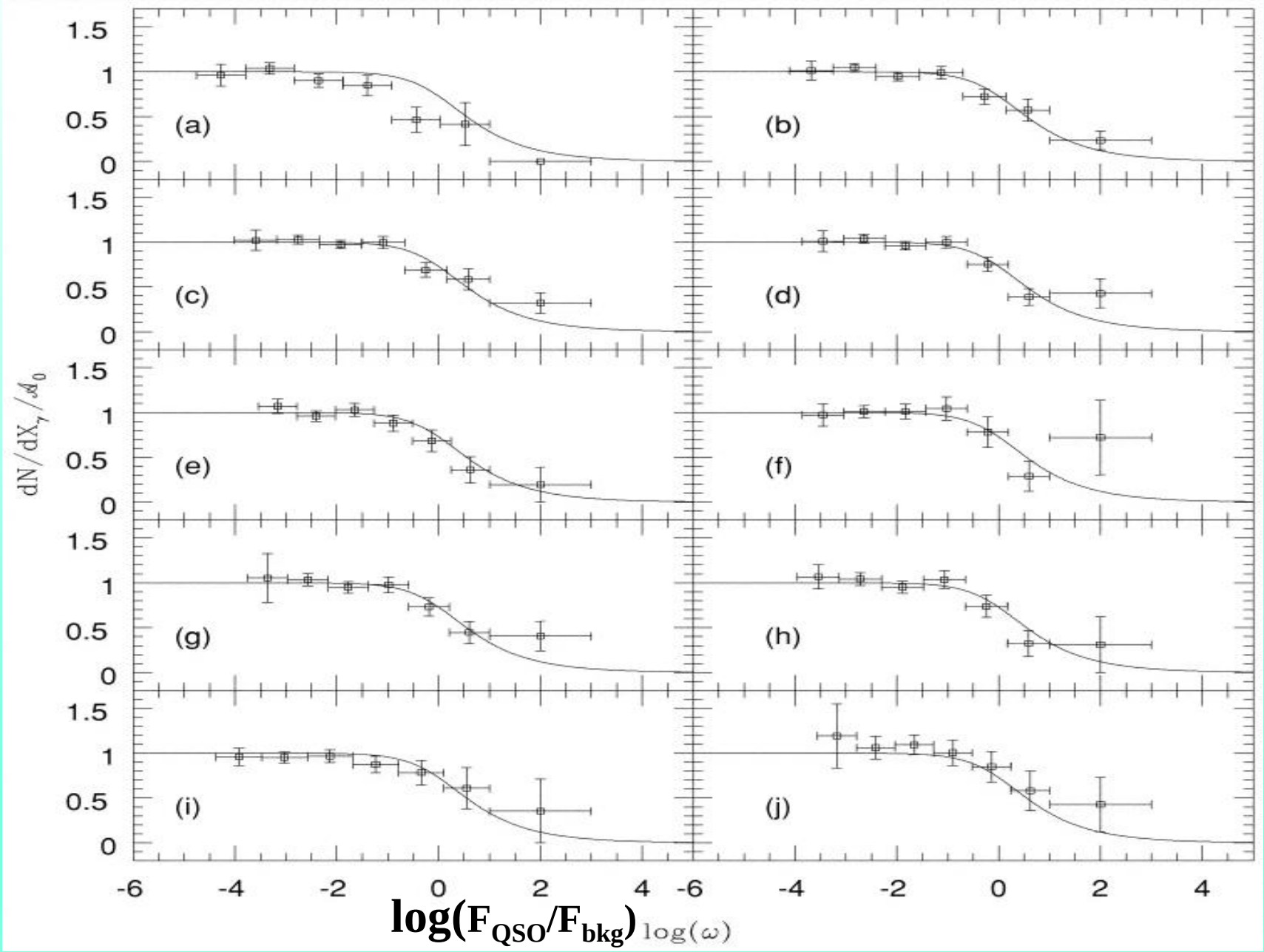

Amplitude of the proximity effect per coevolving redshift coordinate for the best-fit values of J_{-21} (BDO method); $\omega \approx F_{QSO}/F_{bkg}$

Mild evolution of ionizing background intensity confirmed by Dall'Aglio et al. (2008)

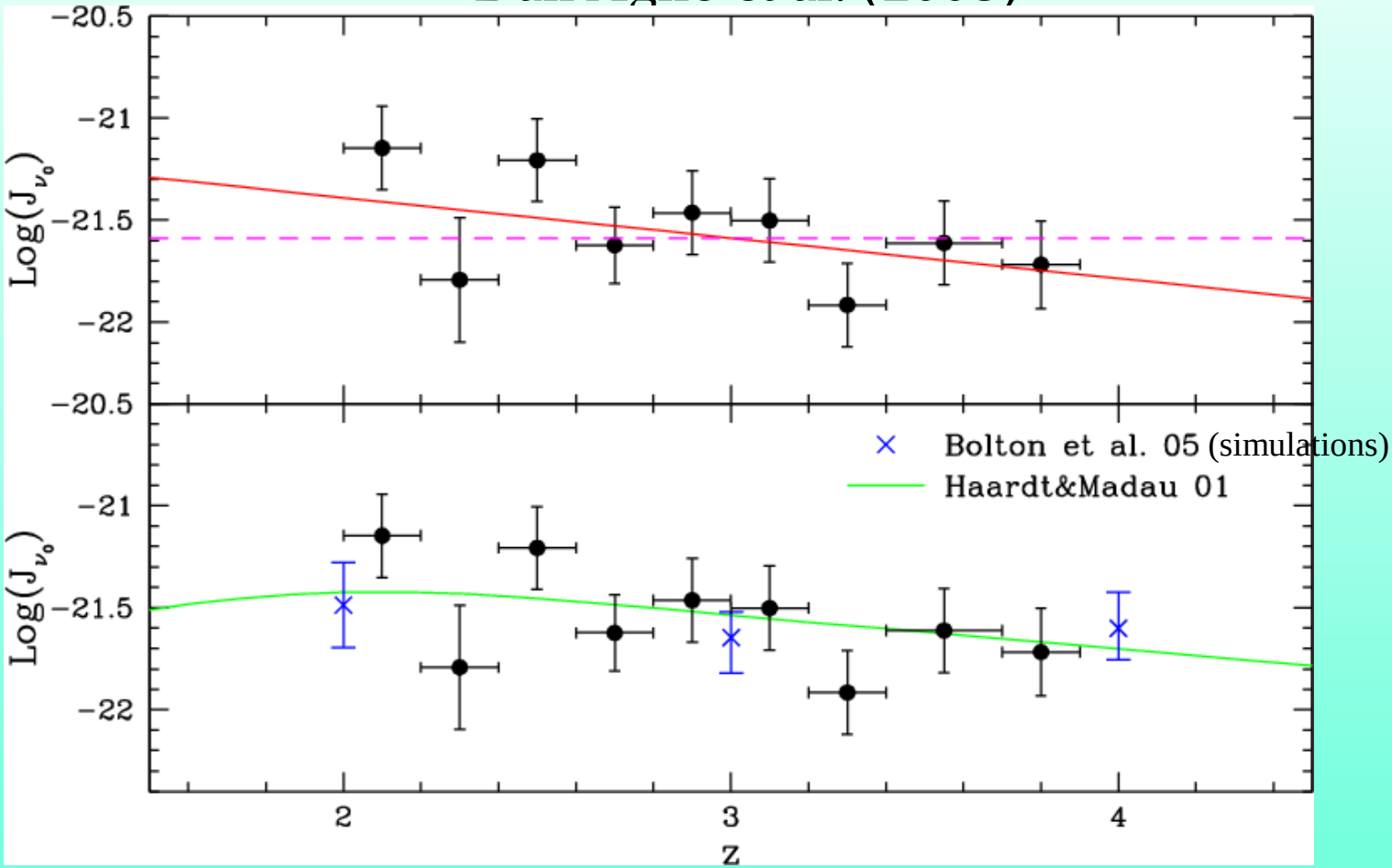

Top panel: constant value (dashed) and fit to the data (solid). Bottom panel: model (green line) including the contributions of the observed quasar and young star-forming galaxy populations, accounting also for intergalactic absorption and re-emission. Very good agreement may be partly fortuitous because predictions crucially depend on the poorly constrained escape fraction of Lyman continuum photons from galaxies

Evolution of the quasar luminosity density

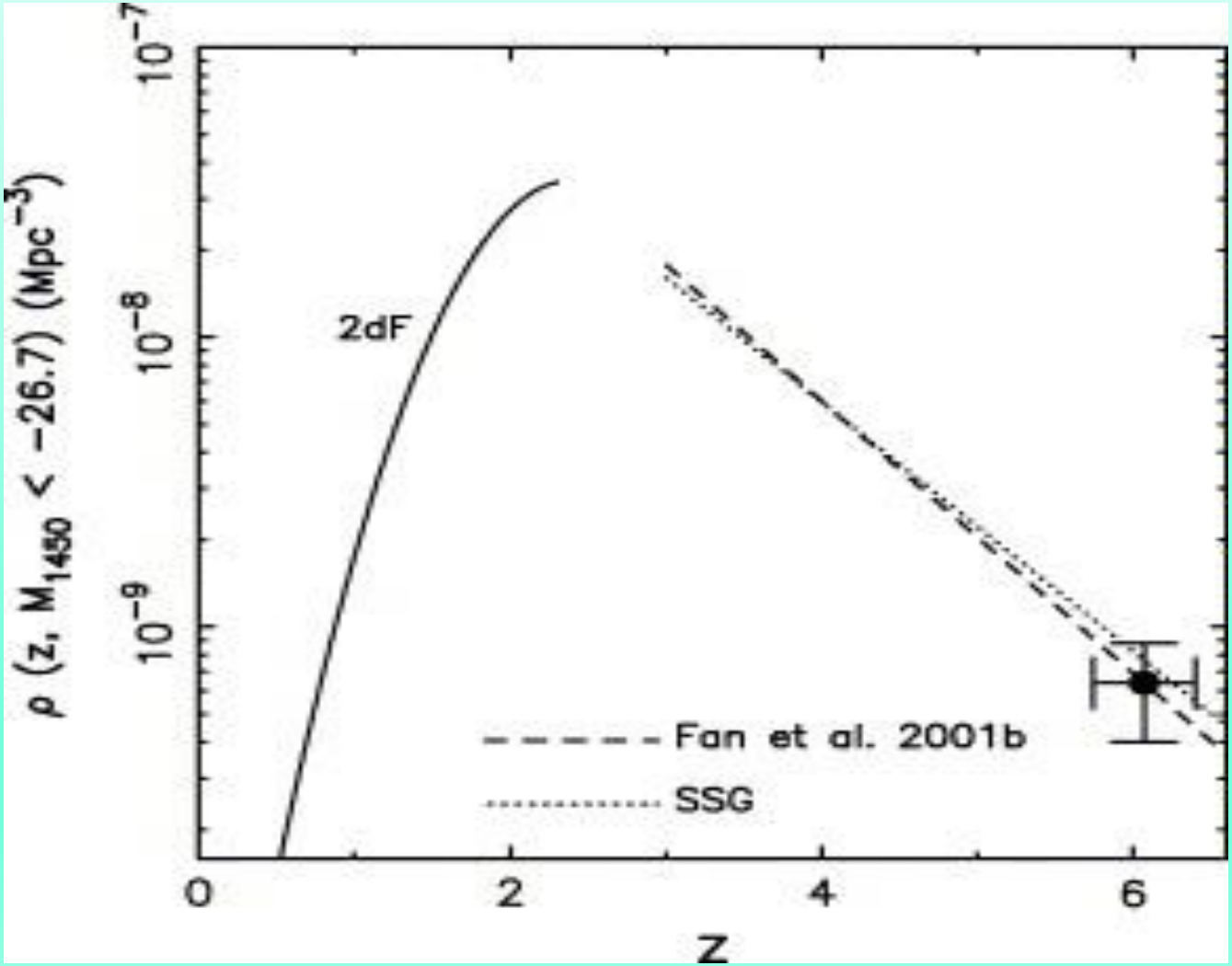

Ionizing background at z=5-6 from the proximity effect (Calverley et al. 2011) - 1

- The evolution of the UVB at $z\sim 6$ is of particular interest in connection with the understanding of the reionization history, to be discussed in the following.
- Since identifying individual lines becomes increasingly difficult at $z > 4$, Calverley et al. have carried out simulations of the global effect of the QSO ionizing radiation on the transmission of the QSO spectrum. The increased transmission is measured through the mean flux in the Lyα forest, rather than through line counting as in the classical measurements of the proximity effect.

Ionizing background at z=5-6 from the proximity effect - 2

- Calverley et al. (2011) measured the metagalactic hydrogen ionization rate, Γ_{bkg}, for 15 quasars covering the range $4.6 < z < 6.4$ by modelling the combined ionization field from the quasar and the UVB in the proximity zone.
- They define a characteristic length R_{eq} to be the distance from the quasar where the photoionisation rate from the UVB equals that from the quasar, i.e. $\Gamma_q(R_{eq}) = \Gamma_{bkg}$.

The photoionisation rate of HI (in units of s^{-1}) by a source of UV flux (the QSO in this case) is given by

$$\Gamma = \int_{\nu_0}^{\infty} \frac{4\pi J(\nu)\sigma_{HI}(\nu)}{h\nu} d\nu \ ,$$

where $J(\nu)$ is the intensity of the source, $\sigma_{HI}(\nu)$ is the ionisation cross-section of HI, and h is the Planck's constant. Assuming that the UV spectrum of the QSO is a power-law $J(\nu) \propto \nu^{-\alpha}$, using
$\sigma_{HI}(\nu) = 6.3 \times 10^{-18}(\nu_0/\nu)^{2.75}$ cm^2 (Kirkman & Tytler 2008; note that the exponent is often approximated as 3) and integrating we get, in units s^{-1},

$$\Gamma_{\rm bkg} = \frac{9.5 \times 10^8 F^{\rm Q}_{\nu_0}(R_{\rm eq})}{(\alpha + 2.75)}$$

Calverley et al. (2011) used $\alpha = 1.61 \pm 0.86$ (Telfer et al. 2002).

Evolution of the photoionization rate - 1

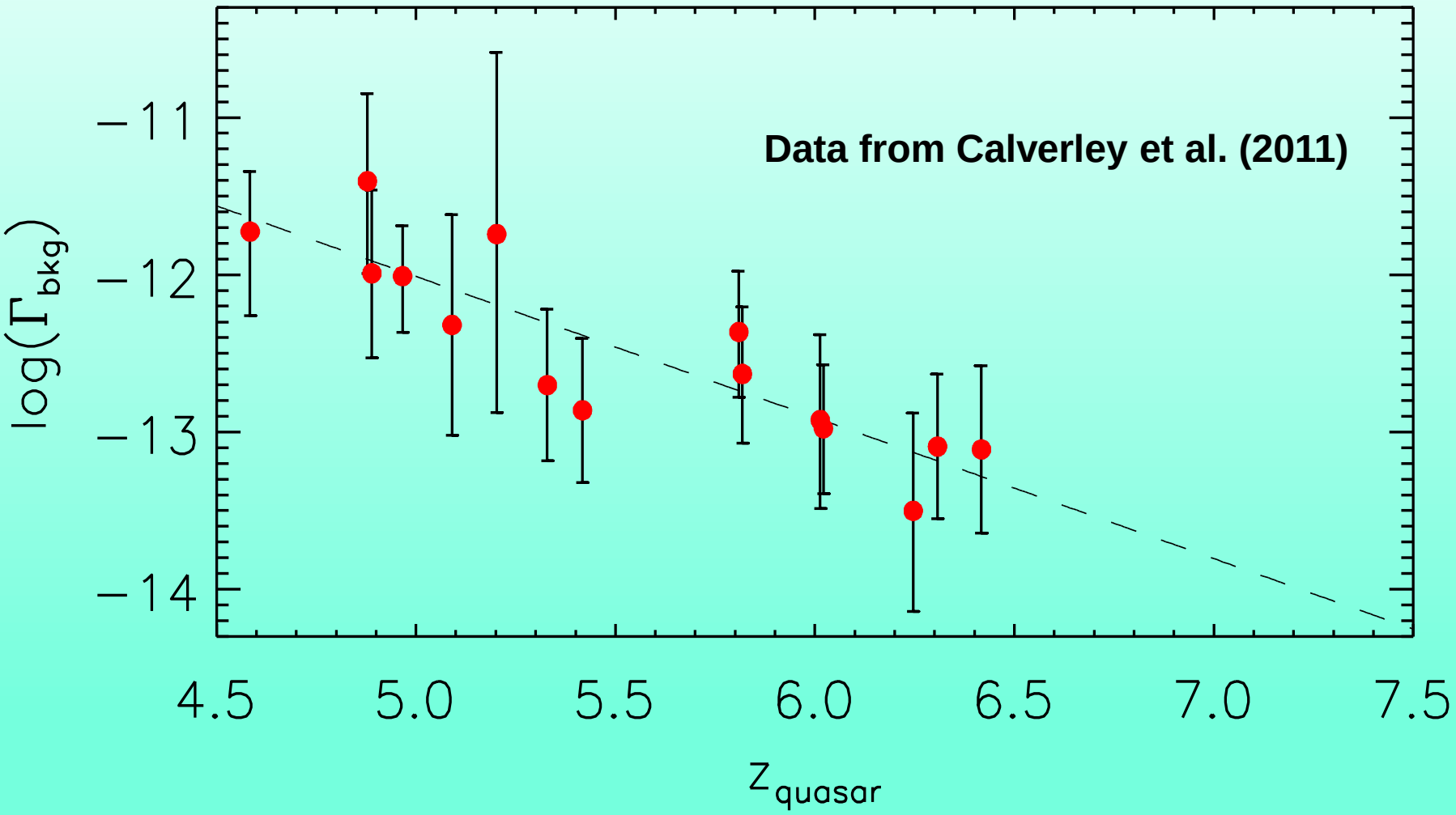

A smooth decline in Γ_{bkg} with redshift appears over this redshift range, with a formal correlation coefficient of −0.87.

Evolution of the photoionization rate

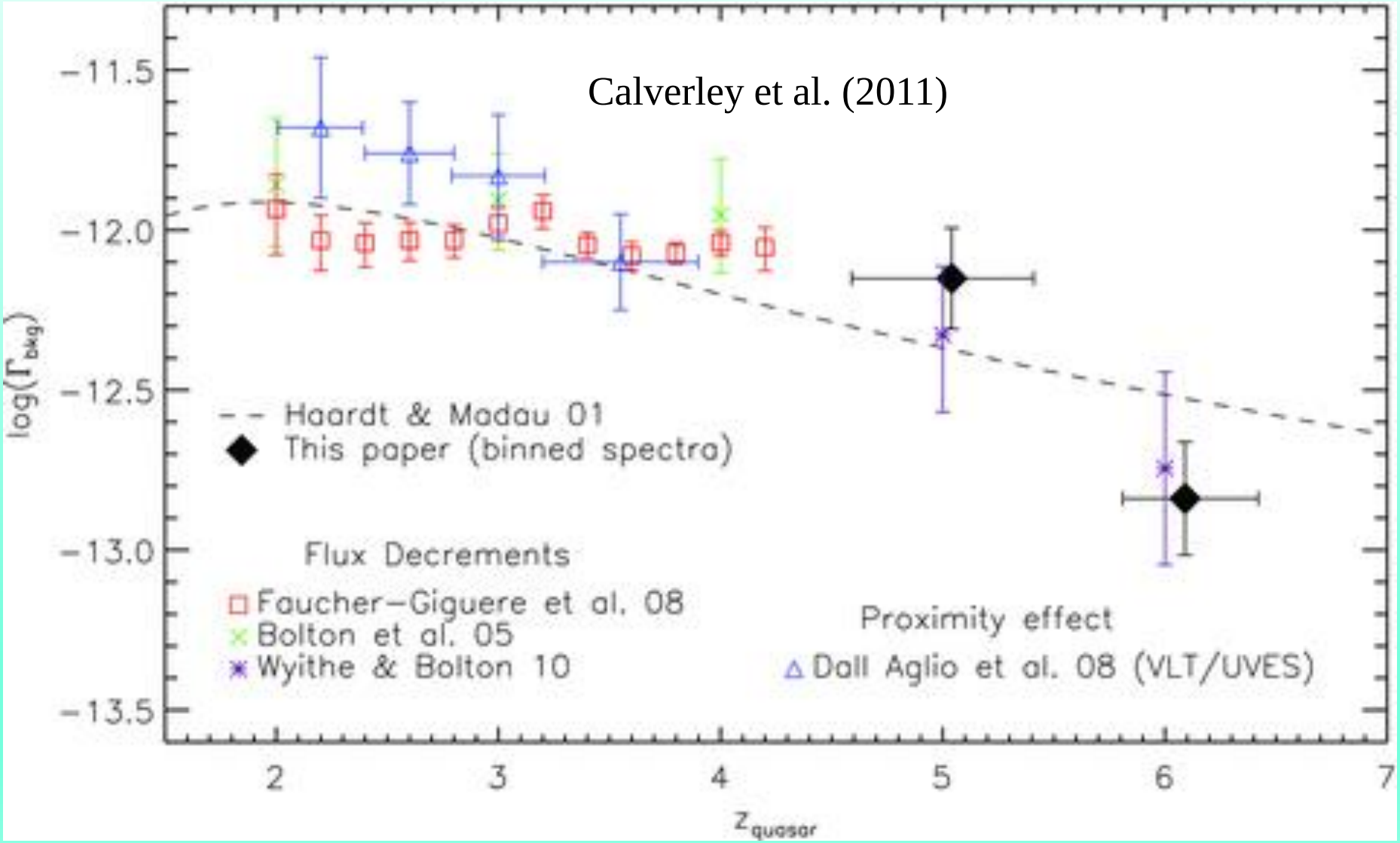

Evolution of the photoionization rate - 2

- The collection of data shown in the previous slide confirms a smooth decrease by an order of magnitude of the photo-ionization rate from $z\approx2$ to $z\approx6$.
- The smooth evolution of Γ_{bkg} suggests that the filling factor of ionized regions is still close to 1 over the z range probed by these data. In fact, $\Gamma_{bkg} \propto l(\nu_0,z)\ \varepsilon(\nu_0)$ where $l(\nu_0,z)$ is the mean free path of ionizing photons and $\varepsilon(\nu_0)$ is the ionizing emissivity. When the neutral fraction becomes significant, $l(\nu_0,z)$, hence Γ_{bkg}, should drop rapidly, but this is not observed. The increase of the number density of Lyα clouds implies that $l(\nu_0,z)$ decreases by a factor ~1.5–2.5 from z=5 to 6; then the emissivity should decrease by a factor < 5.

Evolution of the proximity region size - 2

- The ionizing emissivity is already quite low at z=6 (~1.5 ionizing photons per H atom). So, unless the trend of Γ_{bkg} changes at higher z, the end of re-ionization appears unlikely to occur much before z=6.4.

Ionizing photons from galaxies and AGNs

(Haardt & Madau 2012)

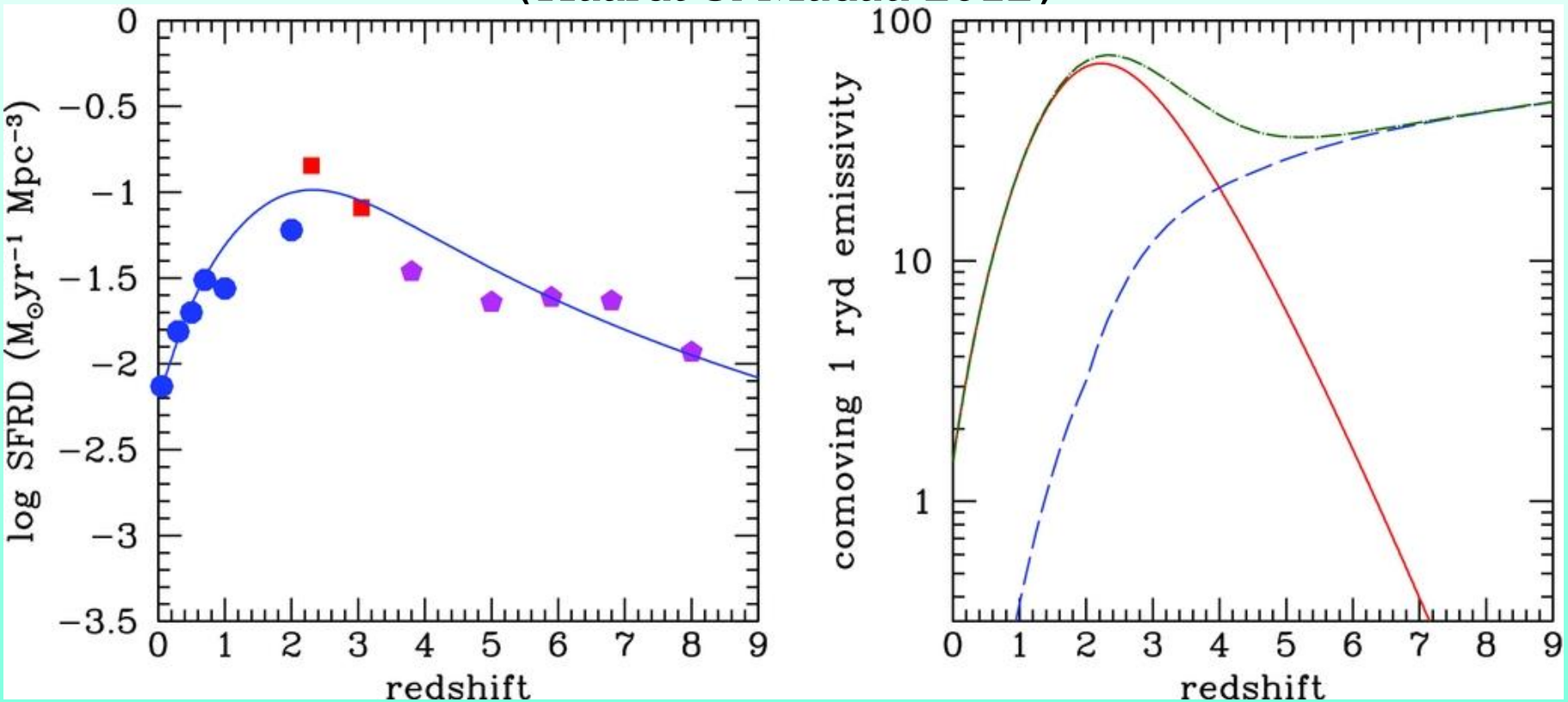

Left: the cosmic history of star formation. Data from Schiminovich et al. (2005, blue dots), Reddy & Steidel (2009, red squares), and Bouwens et al. (2011, magenta pentagons). The solid blue curve is a fit. Right: comoving galaxy emissivity (in units of 10^{23} erg s^{-1} Mpc^{-3} Hz^{-1}) of 1 Ryd photons escaping into the IGM (dashed line), for an escape fraction $\langle f_{esc} \rangle = 1.8 \times 10^{-4}(1 + z)^{3.4}$. Solid line: the best-fit QSO emissivity; blue dashed line: galaxy emissivity; green the dot-dashed line shows the total quasars + galaxies. See Puchwein et al. (2018) for an update.

AGNs contribution to re-ionization - 1

- The previous slide corresponds to the widely held view that, although QSOs are extremely bright UV sources, so they are natural candidates for producing large amounts of ionizing photons, they actually contribute little to HI re-ionization (Finkelstein et al. 2012), although they account for the He re-ionization.
- The reason is that their luminosity function peaks at $z \sim 2$ and falls off rapidly toward higher redshift. Measurements at $z \sim 6$ show that their ionizing flux is lower by more than a factor of 10 than needed to reionize the IGM (Willott et al. 2010).
- Also, if QSOs dominated the reionization of hydrogen, one would expect helium to be reionized in the same epoch, which is not the case (e.g., McQuinn 2012).

AGNs contribution to re-ionization - 2

- The idea that AGN can nevertheless provide an important contribution to the re-ionization has recently gained momentum since deep optical surveys at $z = 3 - 5$ with complete spectroscopic information (Glikman et al. 2011; Giallongo et al. 2015) showed the presence of a considerable number of faint AGNs producing a rather steep luminosity function (but see Parsa et al. 2018, Hassan et al. 2018, and Onoue et al. 2017 for different results).
- The presence of a faint ionizing population of AGNs could, if confirmed, strongly contribute to the ionizing UV background (Madau & Haardt 2015; Khaire et al. 2016, Puchwein et al, 2018), provided that a significant fraction of the produced LyC photons is free to escape from the AGN host galaxy even at faint luminosities.

AGNs contribution to re-ionization - 3

- Grazian et al. (2018) measured very high LyC escape fractions for a sample of AGNs at $z \sim 4$ down to an absolute magnitude of $M_{1450} \sim -23$: they found f_{esc} between 44 and 100% for all the observed faint AGNs, with a mean value of 74% at $3.6 < z < 4.2$ and $-25.1 \leq M_{1450} \leq -23.3$.
- Assuming that the LyC escape fraction remains close to ~ 75% down to $M_{1450} \sim -18$, they estimated that the AGN population can provide between 16 and 73% (depending on the adopted LF of the whole ionizing UV background at $z \sim 4$, measured through the Lyman forest.

AGNs contribution to re-ionization - 4

- Extrapolating these results to $z \sim 5 - 7$ Grazian et al. (2018) concluded that AGNs can provide a significant contribution to the reionization, depending on their poorly known LF at $z \geq 6$.
- Based on Spectroscopy of $5 < z < 7$ Galaxies in the QSO Field J1148+5251, Kakiichi et al. (2018) concluded that while faint galaxies are primarily driving reionisation, luminous galaxies and AGN may provide important contributions to the UV background or thermal fluctuations of the IGM at $z \approx 6$.
- Puchwein et al. (2018) argue that models with a large AGN contribution to the H reionization are disfavoured by the IGM temperature data, as well as by measurements of the HI and HeII Lyα forest opacities.

Early star-forming galaxies and the re-ionization of the universe - 1

- Observations of the GP effect demonstrate that the IGM was highly ionized since the universe was ~ 1 Gyr old.
- Re-ionization most likely caused by photons with E>13.6 eV (λ < 912 Å) generated by early star-formation in galaxies (the AGN luminosity density sinks down above z~3; no evidence for alternative sources of ionizing photons, like decaying elementary particles, but this remains an option).
- Need to verify if early star-forming galaxies produce and *let escape* enough ionizing photons.

Early star-forming galaxies and re-ionization - 2

- Star-forming galaxies are associated to collapsed dark matter halos. Initially these sources are rare and ionize only sparse `bubbles'. As the universe expands the mean IGM density decreases, more galaxies form with increasing mass and luminosity, and the ionized regions increase in number and extent allowing the volume fraction of ionized H, Q_{HII}, to increase rapidly until the IGM is fully ionized.
- The evolution of Q_{HII} from neutral (Q_{HII}=0) to fully ionized (Q_{HII}=1) is governed by the balance between the production rate of ionizing photons and the recombination rate:

$$\frac{dQ_{\rm HII}}{dt} \simeq \frac{1}{n_{\rm H}} \frac{dn_{\rm ion}}{dt} - \frac{Q_{\rm HII}}{t_{\rm rec}}$$

$$t_{\rm rec} \simeq 0.17 \left(\frac{1+z}{7}\right)^{-3} \left(\frac{C_{\rm HII}}{10}\right)^{-1} \ {\rm Gyr}$$

$C_{HII} = \langle n_H^2 \rangle / \langle n_H \rangle^2$

- The production rate, $dn_{ion}/dt = f_{esc}\,\xi_{ion}\,\rho_{UV}$, is the product of the comoving UV luminosity density, ρ_{UV}, the production rate of ionizing photons per unit UV luminosity, ξ_{ion} , and the fraction of photons that can escape a galaxy f_{esc} . Note that sometimes the above expression is written in terms of the SFR density instead of ρ_{UV}.
- The recombination rate depends on the IGM temperature and on the physical hydrogen density that decreases as $(1+z)^3$ and is enhanced in locally overdense regions by the `clumping factor' $C_{HII} = \langle n_H^2 \rangle / \langle n_H \rangle^2$. Recent analyses (Pawlik et al. 2009) show that photo-heating strongly reduces the clumping factor because the increased pressure support smooths out small-scale density fluctuations. Values of C_{HII} in the range 3 – 6 are found for $6 \leq z \leq 9$.

The high-z UV luminosity density - 1

- Great progress towards a census of high-z galaxies, i.e. towards the determination of ρ_{UV}, was made possible by the Wide Field Camera 3 on HST that undertook a series of deep images with the infrared detector (WFC3/IR) operating in the range 8500 Å – 1.7 μm of Hubble Ultra Deep Field (4.7 arcmin^2) reaching a 5σ point source sensitivity ~29th mag in 3 bands.
- These data have provided the reliable determinations of the galaxy UV luminosity function up to z≈9 and initial estimates up to z≈10 (Bouwens et al. 2008, 2016; Finkelstein et al. 2015; Bower et al. 2015; Ishigaki et al. 2018).

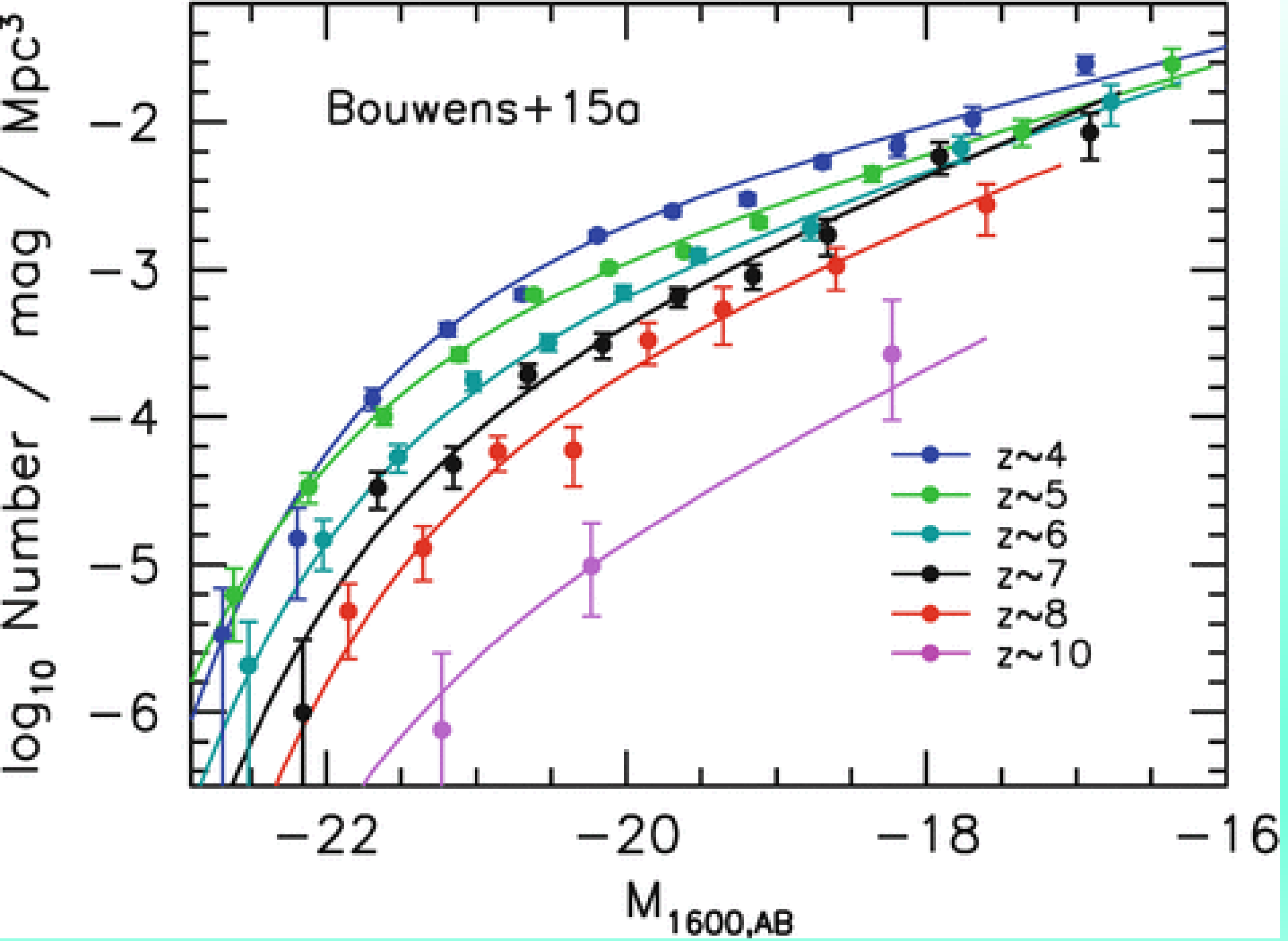
Bouwens+15a
z~4
z~5
z~6
z~7
z~8
z~10
log10 Number / mag / Mpc3
M1600,AB
−2
−3
−4
−5
−6
−22
−20
−18
−16

Ishigaki et al. (2018)

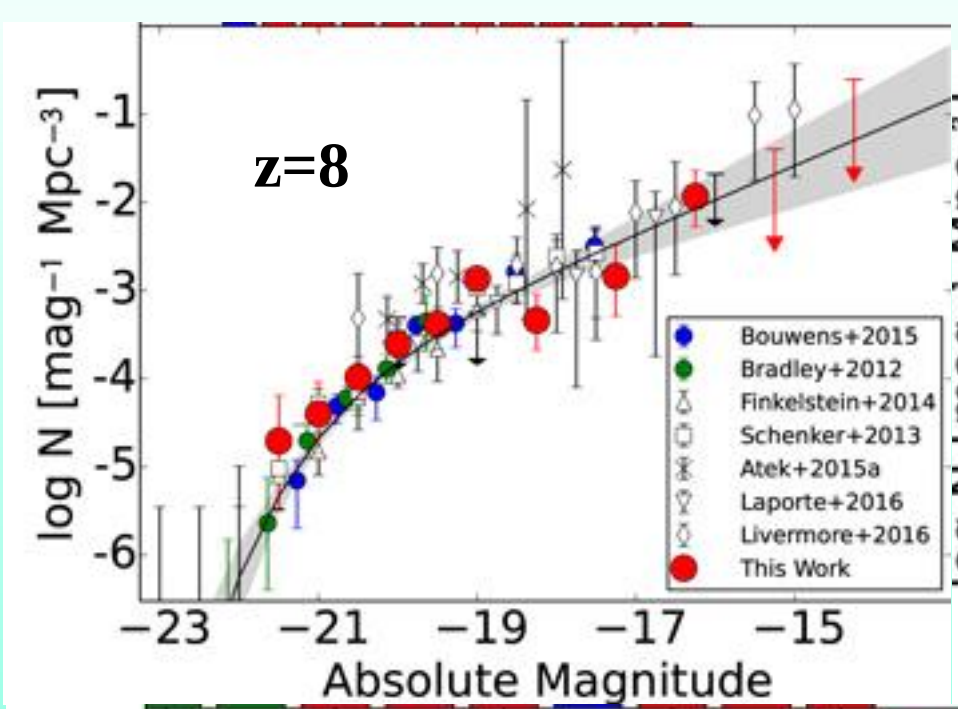

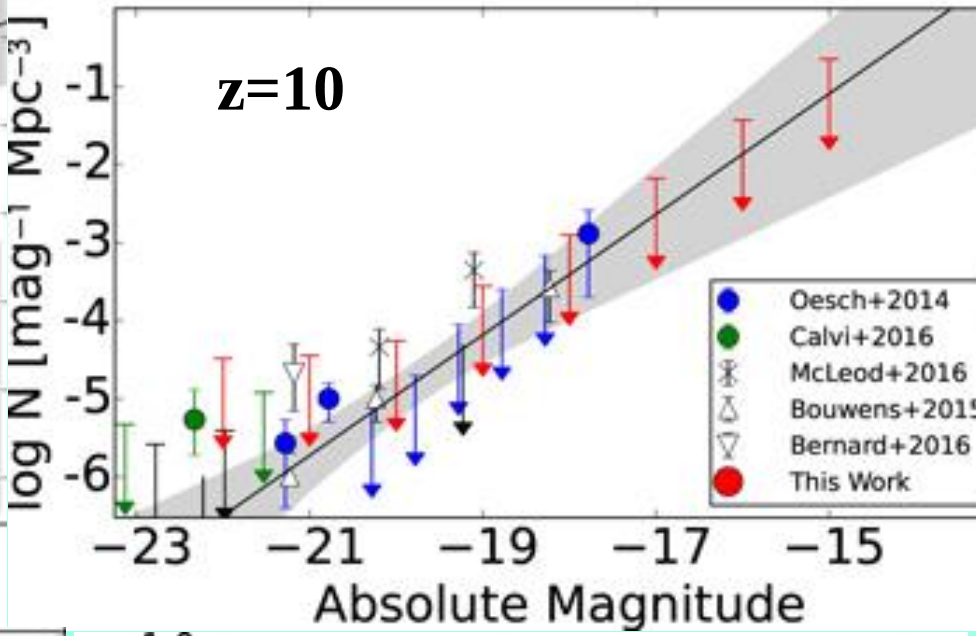

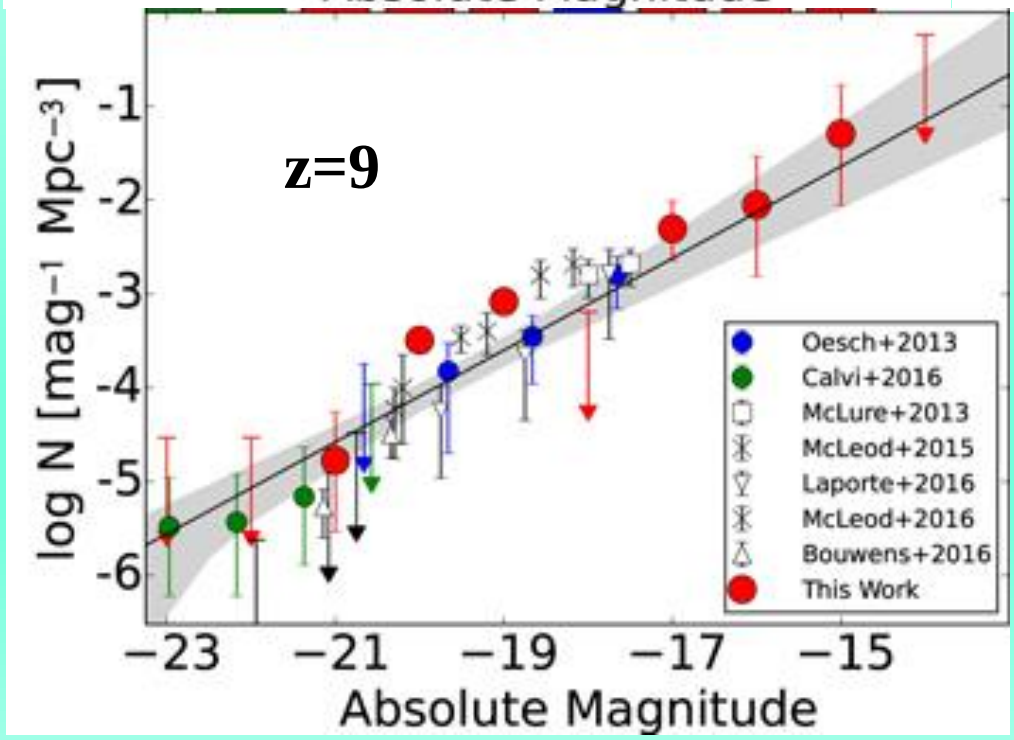

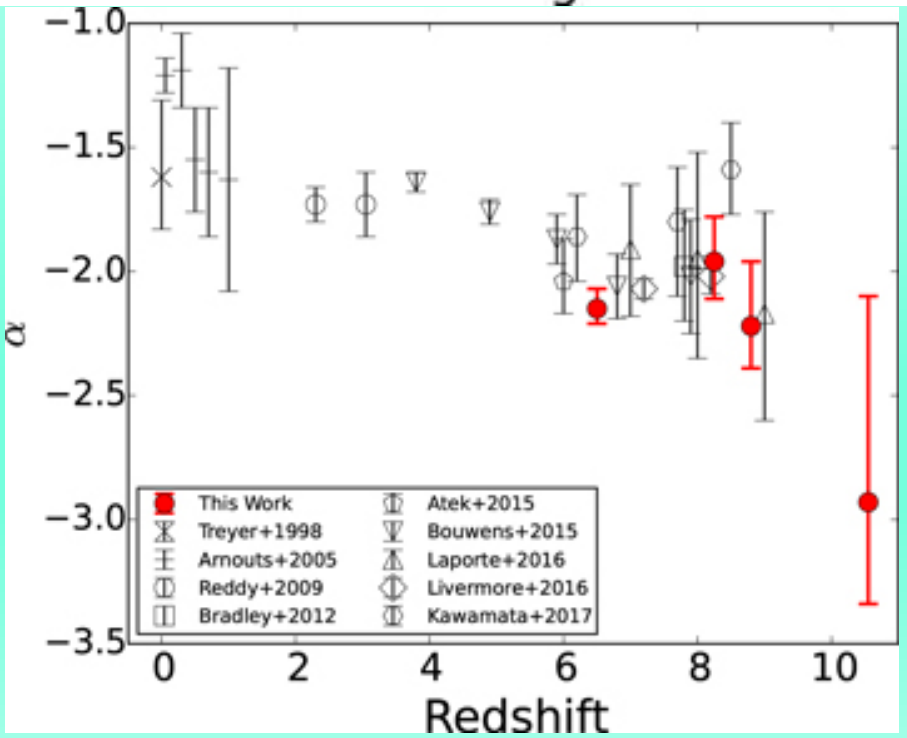

The high-z UV luminosity density - 2

- In principle, the UV luminosity density is straightfowradly obtained integrating the luminosity function:

$$\rho_{\rm UV}=\int_{L_{min}}^{L_{max}} \Phi(L) L \, dL$$

- In practice, however, there are large uncertainties. The observed slope of $\Phi(L)$ at high z is close to, and may be smaller than -2. But then, $\rho_{\rm UV}$ critically depends on the space density of galaxies fainter than we can readily probe with existing data sets.
- If the observed luminosity function can be extrapolated to lower luminosities (e.g., −10 mag) with constant slope, these ultra-faint (and largely individually undetectable) galaxies could produce ~ 7× as much light as the galaxies that we can probe directly with currently observable surveys (Bouwens 2016).
- Faint galaxies may then be expected to produce the vast majority of photons that reionized the universe.

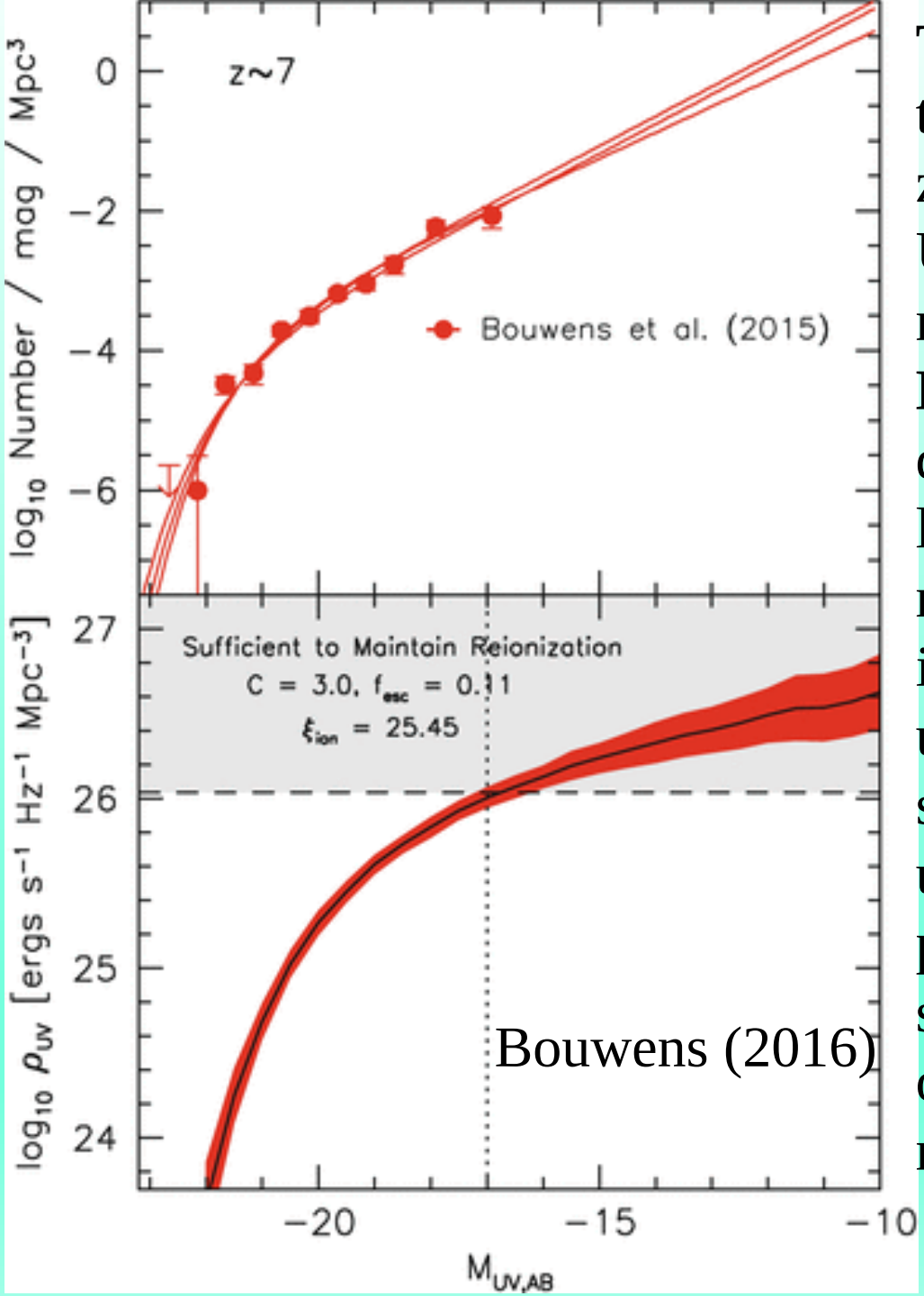

Top panel. Best-fit constraints on the galaxy luminosity function at z~7 in the rest-frame UV. Uncertainties in the fit are represented by the different lines. **Bottom panel**. UV luminosity density ρ_{UV} integrated to different lower luminosity limits presented relative to the luminosity density in the UV needed to reionize the universe. The red-shaded region shows the 68% confidence uncertainty. For the values of the parameters in the inset, only a slight extrapolation of the observed LF is enough to maintain ionization at z=7.

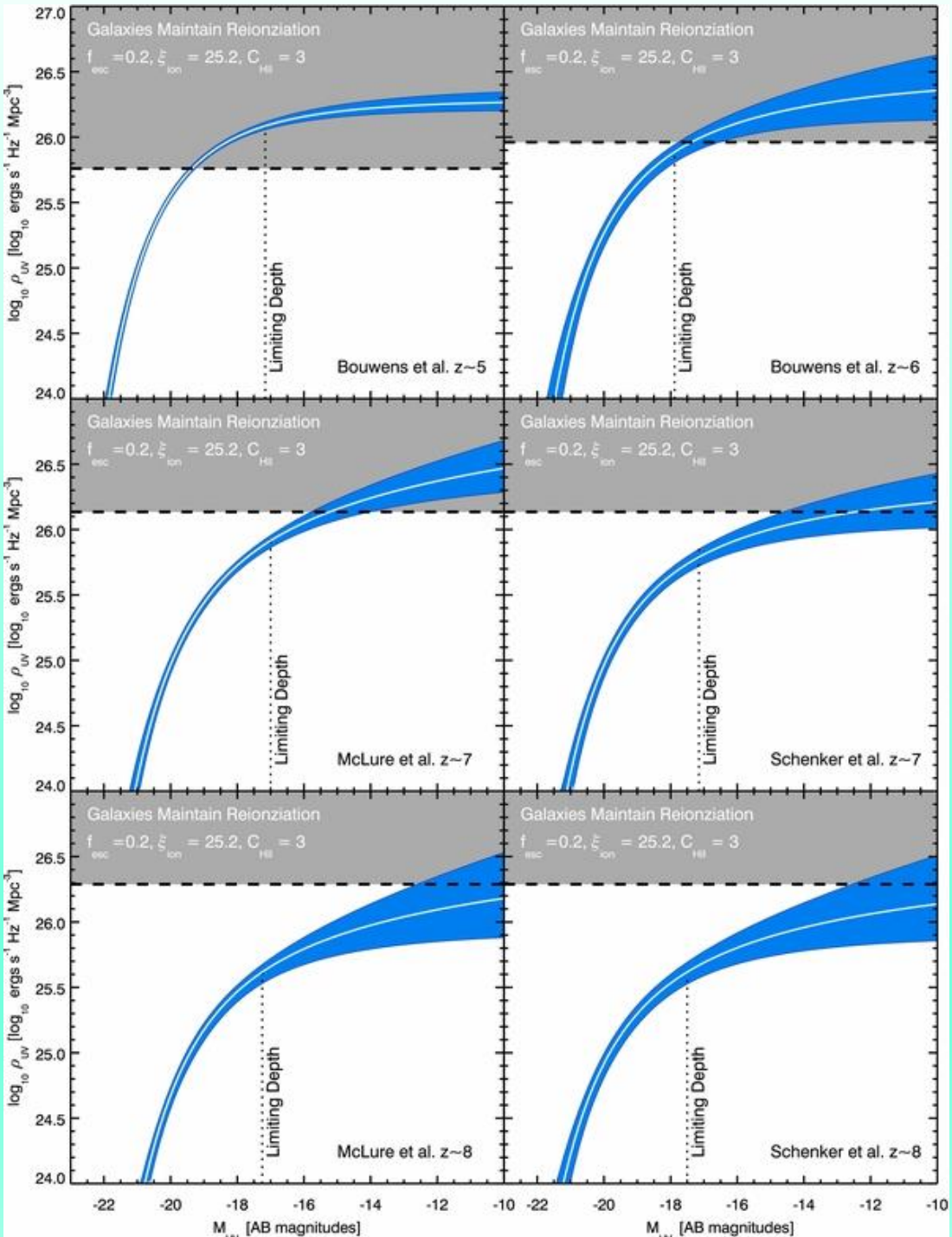

UV luminosity densities, ρ_{UV}, as a function of limiting magnitude M_{UV} and redshift z with the 68% credibility intervals. In each panel the dotted line shows the limiting depth of the luminosity function determinations. Also shown is the ρ_{UV} required for galaxies to maintain a fully ionized universe assuming $\log(\xi_{ion}/\ \mathrm{erg^{-1}\ Hz}) = 25.2$, $f_{esc} = 0.2$, $C_{HI} = 3$. From Robertson et al. (2013). An updated version of the figure at z=7 is in the next slide.

Faint End Cut-Off to the Luminosity Function - 1

- If the faint-end slope α of the UV LF is close to -2, then one could potentially expect a particularly significant contribution of galaxies at arbitrarily faint luminosities to the reionization of the universe. A faint-end slope of -2 is sufficiently steep for the total luminosity density to be technically divergent if the integral is extended all the way to zero.
- In reality, however, the galaxy LF cannot extend to arbitrarily low luminosities with such a steep faint-end slope and must eventually turn over at some luminosity. This is because several processes limit the possibility of low-mass collapsed halos to accrete or retain significant amounts of cool gas necessary for star formation:

- supernova winds can expel gas from small host halos, photo-ionization can heat gas sufficiently to prevent it from falling into low mass halos, and perhaps remove gas from existing galaxy-hosting halos, UV radiation can also impact the cooling rate of collapsing gas by dissociating molecules and photoionizing atomic gas.
- These processes are likely to contribute to suppressing significant star formation in very low-mass ($< 10^8$ $M_\odot$) halos.
- A warm dark matter component suppresses low mass halos. The available UV LFs already imply interesting upper limits on the mass of warm dark matter particle (Lapi & Danese 2015).
- Determining at which luminosity the UV LF cuts off is clearly important for assessing the total reservoir of ionizing radiation available to reionize the universe. However, if the faint end of the LF extends faintward of -13, it is unlikely that direct probes will be successful in revealing where the UV LF cuts off (Bouwens 2016).

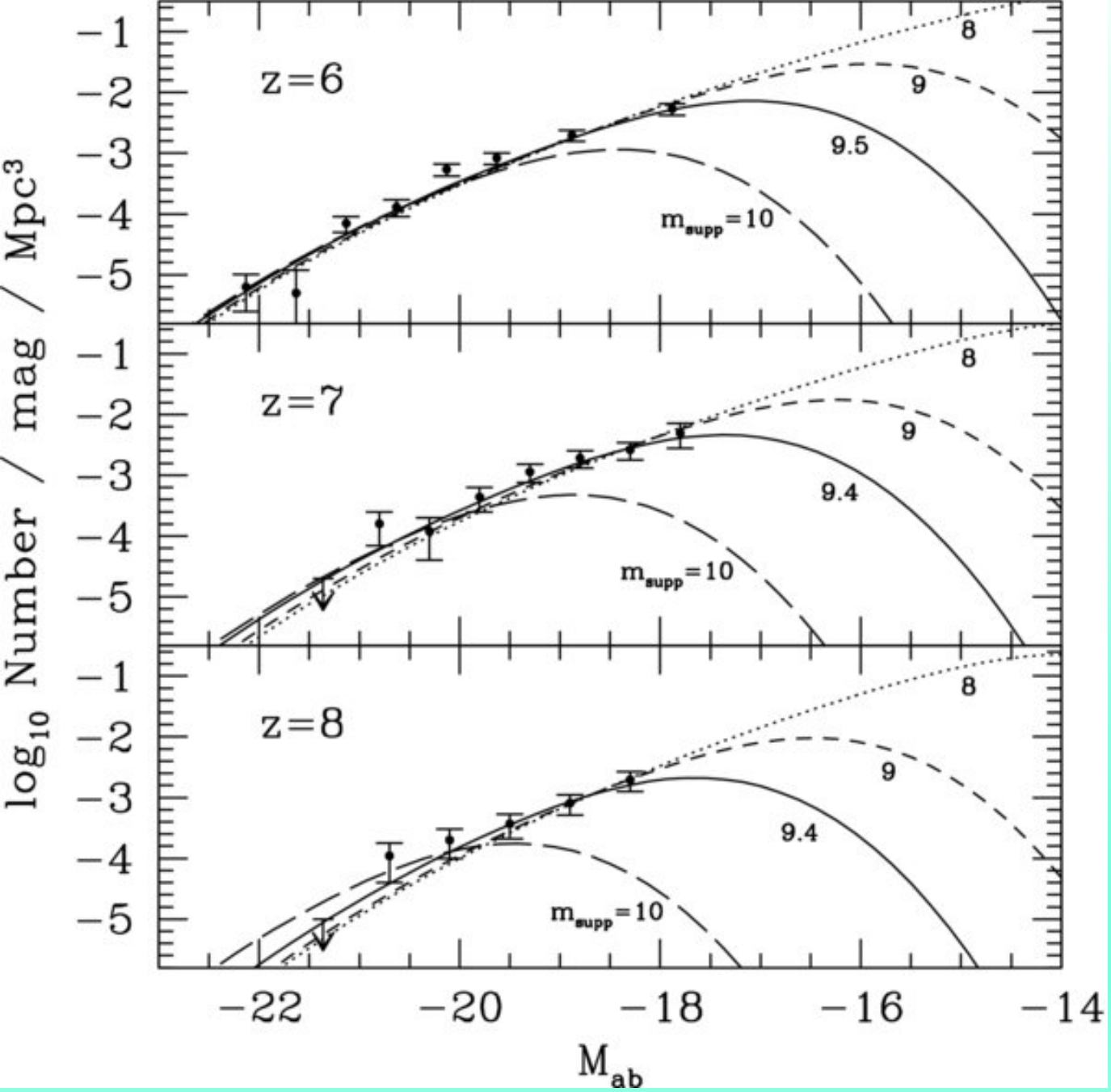

Fits of the observed UV LFs with a hierarchical galaxy formation model with starburst activity. The model provides a distribution of UV luminosities per dark matter halo of a given mass. A comparison with the data provides constraints on the minimum mass halo capable of hosting galaxies.

Muñoz & Loeb (2011)

Production Rate of Lyman-Continuum Photons -1

- To determine if the observed galaxy population can be successful in reionizing the universe, we must convert the overall luminosity density ρ_{UV} ($\sim$1600 Å) to the equivalent luminosity density in Lyman-continuum photons ($\leq$ 912 Å).
- It is conventional to model the spectrum of galaxies in the rest-frame UV as a power-law such that $f_\lambda \propto \lambda^\beta$ (or equivalently $f_\nu \propto \nu^{-(\beta+2)}$). While the spectrum of star-forming galaxies in the UV continuum cannot be perfectly described by a power-law, such a parameterization generally works for most of the spectral range to within ±20% (Bouwens 2016).
- In general, galaxies at z$\sim$4−8 have been found to have a mean β of $\sim-$ 1.6 at high luminosities and slowly trend towards bluer β's of $\sim-$ 2.2 at the lowest luminosities.

Production Rate of Lyman-Continuum Photons -2

- Since essentially all of the UV light produced by galaxies in the $z \sim 6-8$ universe derives from galaxies at very low luminosities, it is reasonable to use the β's measured for lower luminosity galaxies to convert the luminosity densities in the UV continuum into the equivalent density of ionizing photons.
- The conversion factor can be estimated using spectral synthesis models. It depends on the star-formation history, on ages and metallicities for the stars and on dust content, believed to be small in these faint high-z galaxies.

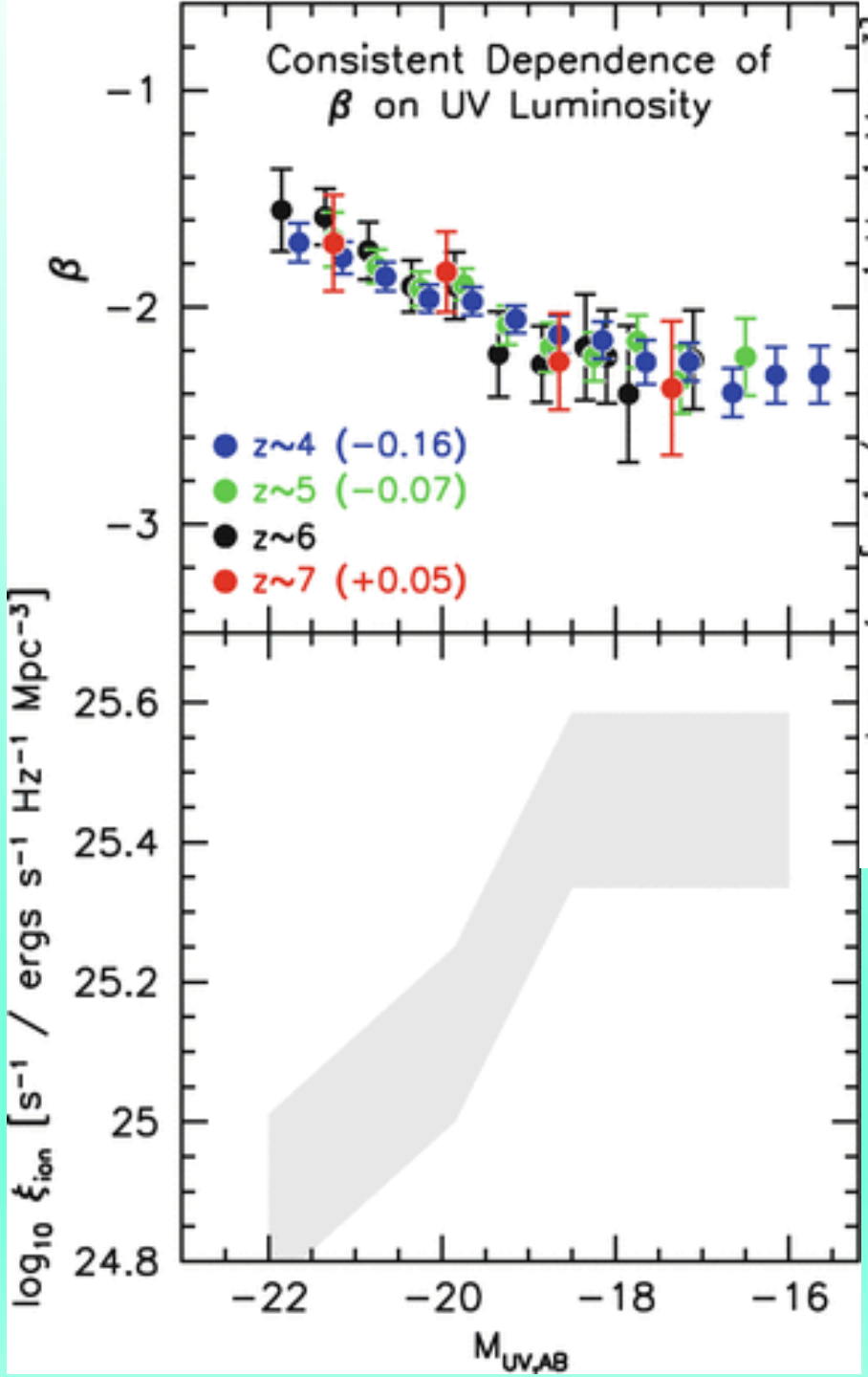

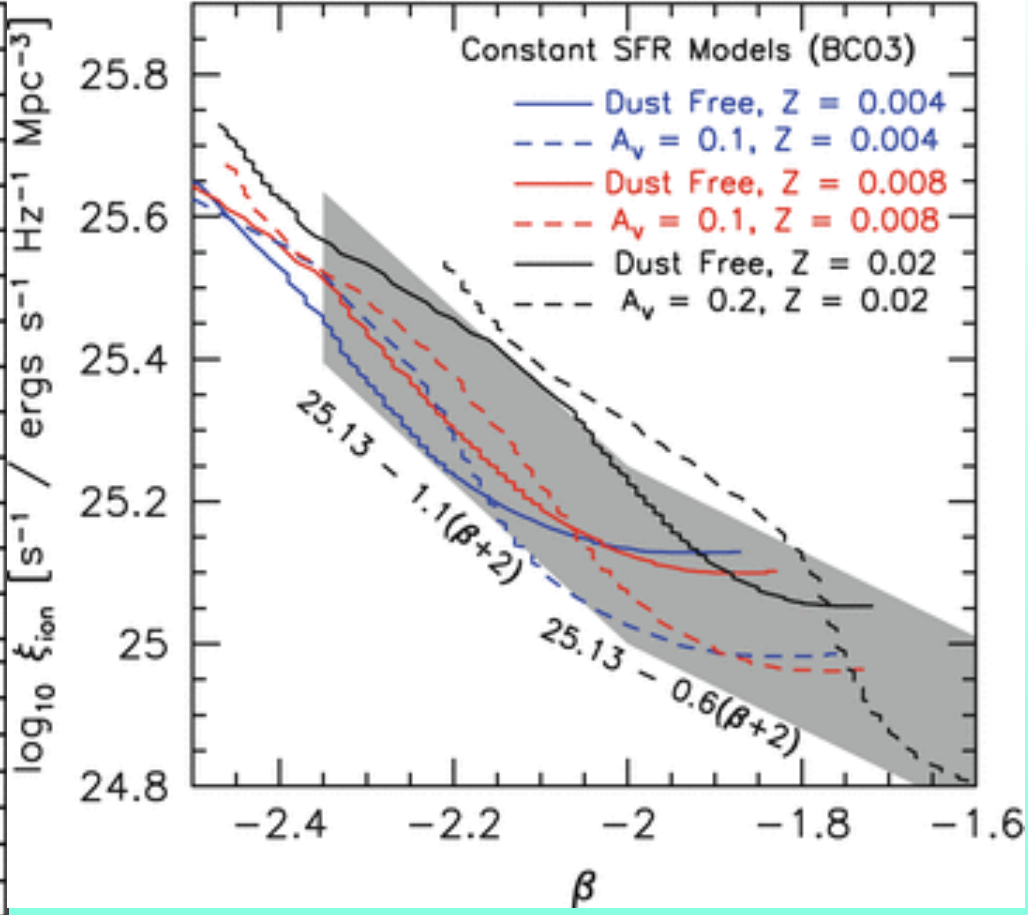

Right panel: ξ_{ion} vs β for different metallicities and stellar ages, without or with a small amount of dust. Bottom left: values of ξ_{ion} as a function of M_{UV} derived from the mean β in the upper left panel. From Bouwens (2016).

Lyman-Continuum Escape Fraction - 1

- For $z > 6$ galaxies to reionize the universe, a fraction ≥ 10 % of the ionizing radiation must escape into the intergalactic medium.
- Direct searches for such radiation from $z > 6$ are not really feasible, in that any escaping radiation from $z > 6$ galaxies to be detected would need to redshift through the thick Lyman-series forest. Observational efforts for direct detection are therefore limited to z of up to 3–4, low enough so that the average number of intervening absorption systems is not too great to hinder the detection of LyC emission.
- Searches for leaking ionizing radiation from galaxies at z of up to ~1 have given null results (Siana et al. 2010).

Lyman-Continuum Escape Fraction - 2

- Efforts to identify significant leaks of ionizing radiation from z∼2−4 galaxies have been more successful. The value of the escape fraction, f_{esc}, is however debated with reported values from 3–10% (Heckman et al. 2011) to 10–30% (Cooke et al. 2014; Fletcher et al. 2018), with strong variations from source to source, probably due to anisotropic LyC leakage.
- The available data suggests a sudden increase of f_{esc} with z at z ≈ 2 (Smith, B. et al. 2018).
- The large scatter in estimated values for f_{esc} is a consequence of the challenges inherent in accurately quantifying it. One issue is that foreground sources at lower redshift lying almost directly in front of star-forming galaxies are effectively mimicking the signature of Lyman-continuum emission of the background source (Siana et al. 2015).

Lyman-Continuum Escape Fraction - 3

- On the other hand, spectroscopic searches for LyC flux in high redshift galaxies have generally been performed on Lyman Break Galaxies (LBGs). But the standard LBG colour-selection criteria are designed to select galaxies based on the expectation of essentially zero detectable flux blueward of 912 Å. Therefore, this technique preferentially selects galaxies with little or no LyC.
- Another method to estimate f_{esc} exploits the effect of ionizing photons on the Lyα forest. As we have seen, the Lyα forest constrains the HI photo-ionization rate, which is related to the ionizing background intensity, J(ν). Comparing J(ν) with the non-ionizing background intensity derived from the UV luminosity function one can estimate the average escape fraction. The derived f_{esc} are in the range ~4-10% (Kuhlen & Faucher-Giguère 2012; Bouwens 2016).

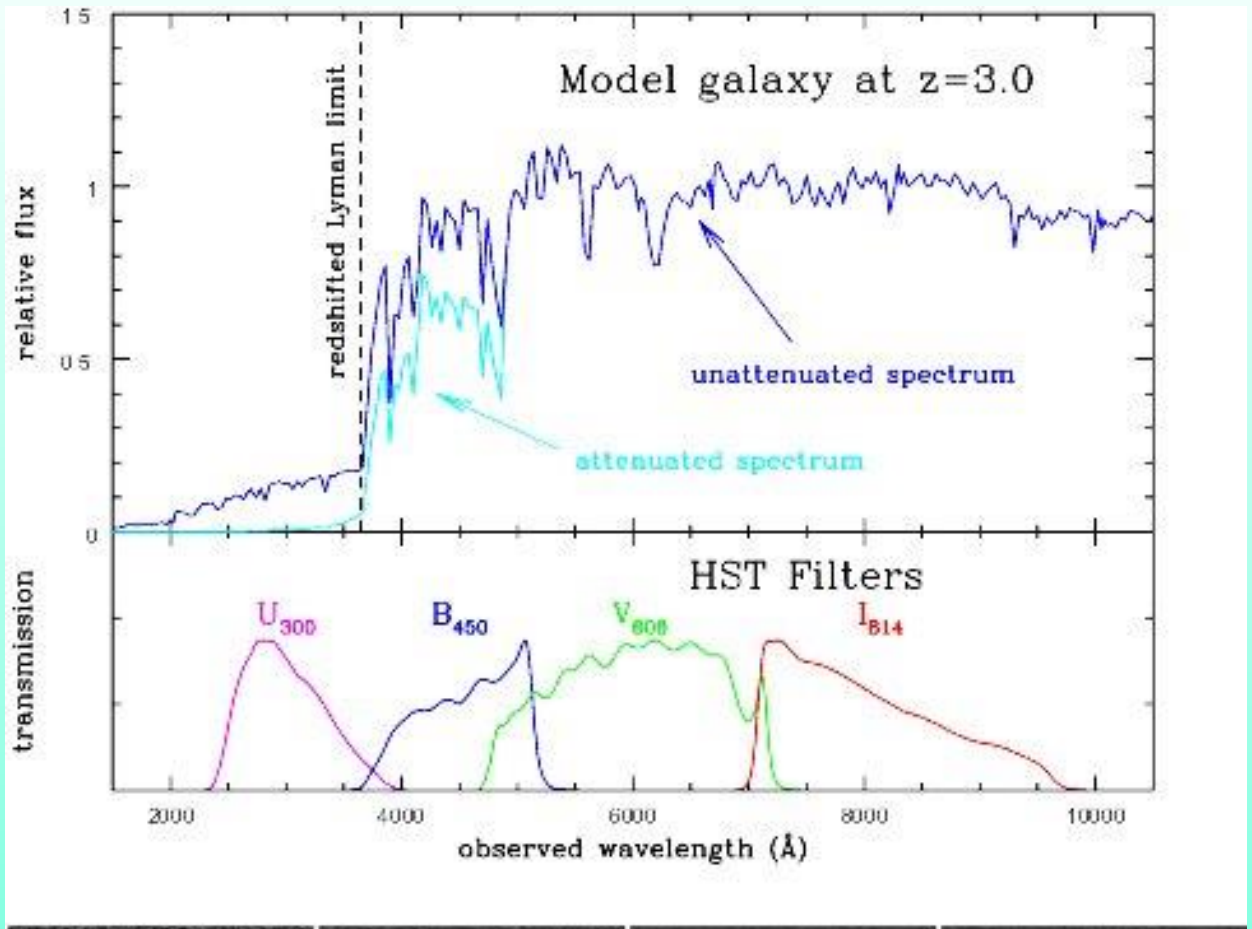

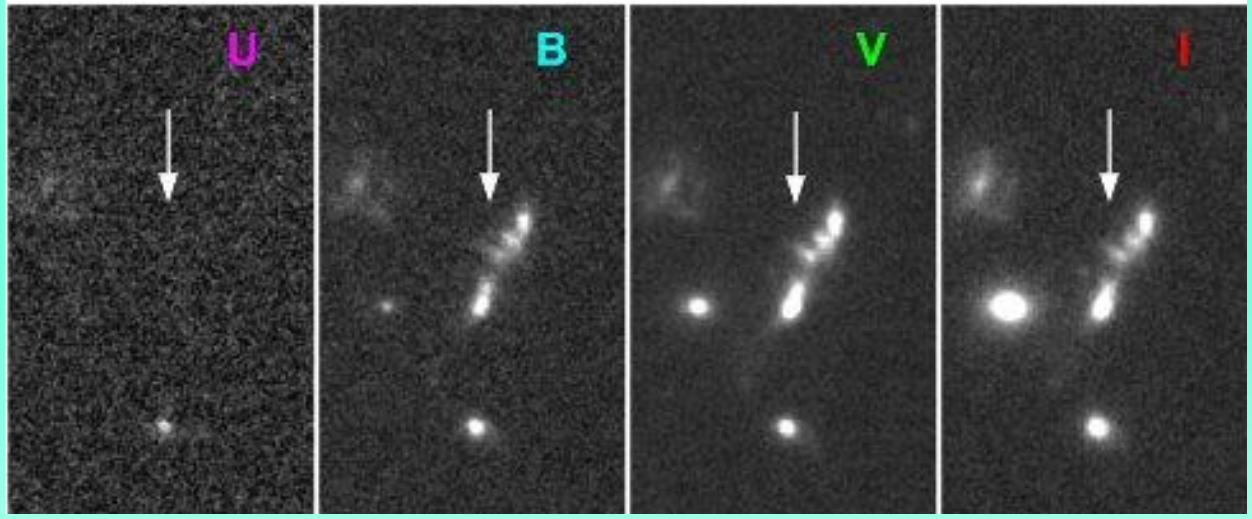

Lyman break galaxies and ‘drop-out’ technique (Dickinson 1998)

Lyman-Continuum Escape Fraction - 4

- Constraints on f_{esc} can also be inferred from the distribution of HI density observed in the afterglow spectra of long-duration γ-ray bursts, which may originate from the death of massive stars and therefore may have a similar spatial distribution in star-forming galaxies as the hot stars producing ionizing photons.
- From the HI column density one can derive the optical depth of neutral hydrogen absorption, hence the LyC transmission. The data by Chen H.-W. et al. (2007) give a *relative* $f_{esc} \approx 0.04 \pm 0.04$ (Bouwens 2016) at z=2-4.
- There is evidence, from $z \sim 2-3$ data, that galaxies at lower luminosities or with Lyα emission have $\sim 2-4\times$ higher values of the escape fraction than the highest luminosity galaxies (McLure et al. 2013; Nestor et al. 2013), supporting the view that faint galaxies dominate the ionizing photon budget at redshifts.

Conclusions - 1

- In spite of the fast progress achieved in recent years, we still know little about astrophysical processes that led to cosmological reionization.
- For many years, the QSO spectra, serving at distant lighthouses, did not show evidence of diffuse Lyα absorption, implying a highly ionized IGM up to z~5.
- A breakthough came when the Sloan Digital Sky Survey (SDSS) discovered bright quasars, already in place at $z \geq 6$, only a billion years following the Big Bang. Their spectra showed long stretches of zero flux, so-called Gunn-Peterson (GP) troughs.

Conclusions - 2

- Studies of resonant Lyα/β/γ absorption have shown that H reionization was still ongoing at z ~ 6 and fully completed by z~ 5.5.
- The next breakthrough came shortly afterwards, as the Wilkinson Microwave Anisotropy Probe (WMAP) satellite detected the optical depth to electron scattering for the CMB, τ, although the derived values of τ turned out to be overestimated.
- The latest analysis of Planck polarization data, yielding an electron scattering optical depth $\tau = 0.058 \pm 0.012$ (Planck Collaboration XLVII 2016), imply an average reionization redshift between z = 7.8 and 8.8.

Conclusions - 3

- The ionization state of the z=6–8 universe is being constrained by other tracers of reionization history, from the damping wing absorption profiles in the spectra of quasars, to the luminosity function and clustering properties of Lyα emitting galaxies.
- Such studies indicate that the IGM was significantly neutral at z between 6 and 7, in agreement with the Planck results.
- As we have seen, one can create a self-consistent model for the reionization of the universe using the observed galaxy population as a basis.

Conclusions - 4

- The most likely candidates for producing enough ionizing photons to account for the onset of reionization are early, low-luminosity star-forming galaxies.
- AGNs dominate the production of ionizing photons at $z \leq 3$-4. At higher z their contribution is probably minor, although its amplitude is still debated.
- Although there are in the literature a variety of self-consistent models for the reionization of the universe using the observed galaxy population as a basis, there are large uncertainties in the many factors that contribute to the calculation of the ionizing emissivity for galaxies. One can produce the required ionizing emissivity with a wide variety of different combinations of the key parameters (f_{esc} , ξ_{ion}, faint end of the luminosity function).

Conclusions - 5

- A much improved knowledge of the total photon output of faint high-z galaxies will be provided by the JWST.
- The next decade should also see a new paradigm for exploring the reionization epoch, in the form of 21 cm observations of HI at high redshifts (Furlanetto 2016). The Square Kilometre Array (SKA) and the various “pathfinder” projects will go a long way to providing a full empirical characterisation of H in the reionization epoch.